

AD-A241 651



2

NAVAL POSTGRADUATE SCHOOL Monterey, California



THESIS



DESIGN OPTIMIZATION OF BLADE STIFFENED
LAMINATED COMPOSITE
PLATES FOR MAXIMUM BUCKLING LOAD

by

Mark R. Achenbach

December, 1990

Thesis Advisor

Philip Y. Shin

Approved for public release; distribution is unlimited.

91-14067



91 10 24 132

Unclassified

security classification of this page

REPORT DOCUMENTATION PAGE

1a Report Security Classification Unclassified			1b Restrictive Markings		
2a Security Classification Authority			3 Distribution Availability of Report		
2b Declassification Downgrading Schedule			Approved for public release; distribution is unlimited		
4 Performing Organization Report Number(s)			5 Monitoring Organization Report Number(s)		
6a Name of Performing Organization Naval Postgraduate School		6b Office Symbol (if applicable) 34	7a Name of Monitoring Organization Naval Postgraduate School		
6c Address (city, state, and ZIP code) Monterey, CA 93943-5000			7b Address (city, state, and ZIP code) Monterey, CA 93943-5000		
8a Name of Funding Sponsoring Organization		8b Office Symbol (if applicable)	9 Procurement Instrument Identification Number		
8c Address (city, state, and ZIP code)			10 Source of Funding Numbers		
			Program Element No	Project No	Task No
			Work Unit Accession No		
11 Title (include security classification) DESIGN OPTIMIZATION OF BLADE STIFFENED LAMINATED COMPOSITE PLATES FOR MAXIMUM BUCKLING LOAD					
12 Personal Author(s) Mark R. Achenbach					
13a Type of Report Master's Thesis		13b Time Covered From To		14 Date of Report (year, month, day) December, 1990	15 Page Count 98
16 Supplementary Notation The views expressed in this thesis are those of the author and do not reflect the official policy or position of the Department of Defense or the U.S. Government.					
17 Cosati Codes			18 Subject Terms (continue on reverse if necessary and identify by block number)		
Field	Group	Subgroup	design optimization, blade stiffened plate, buckling		
19 Abstract (continue on reverse if necessary and identify by block number)					
<p>The buckling load of a blade stiffened laminated composite plate having midplane symmetry is maximized for a given total weight. The thicknesses of the layers and the width and height of the stiffener are taken as the design variables. Buckling analysis is carried out using a finite element method. The optimization problem is solved using commercially available optimization packages.</p> <p>Due to the highly nonlinear nature of the optimality equations, several local optimum solutions are found. To examine the relationship between the number of local optimums and their relative magnitudes, various combinations of fiber orientation for the laminate layers and the blade stiffener are investigated.</p>					
20 Distribution Availability of Abstract			21 Abstract Security Classification		
<input checked="" type="checkbox"/> unclassified unlimited <input type="checkbox"/> same as report <input type="checkbox"/> DTIC users			Unclassified		
22a Name of Responsible Individual Philip Y. Shin			22b Telephone (include Area code) (408) 646-2031		22c Office Symbol ME Sp

DD FORM 1473,84 MAR

83 APR edition may be used until exhausted
All other editions are obsolete

security classification of this page

Unclassified

Approved for public release; distribution is unlimited.

Design Optimization of Blade Stiffened Laminated Composite
Plates for Maximum Buckling Load

by

Mark R. Achenbach
Lieutenant, United States Navy
B.S., University of Illinois, 1983

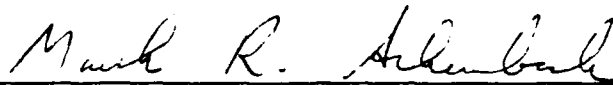
Submitted in partial fulfillment of the
requirements for the degree of

MASTER OF SCIENCE IN MECHANICAL ENGINEERING

from the

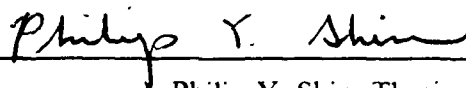
NAVAL POSTGRADUATE SCHOOL
December, 1990

Author:



Mark R. Achenbach

Approved by:



Philip Y. Shin, Thesis Advisor



Anthony J. Healey, Chairman,
Department of Mechanical Engineering

ABSTRACT

The buckling load of a blade stiffened laminated composite plate having midplane symmetry is maximized for a given total weight. The thicknesses of the layers and the width and height of the stiffener are taken as the design variables. Buckling analysis is carried out using a finite element method. The optimization problem is solved using commercially available optimization packages.

Due to the highly nonlinear nature of the optimality equations, several local optimum solutions are found. To examine the relationship between the number of local optimums and their relative magnitudes, various combinations of fiber orientation for the laminate layers and the blade stiffener are investigated.



Accession For	
NTIS GRA&I	<input checked="" type="checkbox"/>
DTIC TAB	<input type="checkbox"/>
Unannounced	<input type="checkbox"/>
Justification	
By	
Distribution/	
Availability Codes	
Dist	Avail and/or Special
A-1	

THESIS DISCLAIMER

The reader is cautioned that computer programs developed in this research may not have been exercised for all cases of interest. While every effort has been made, within the time available, to ensure that the programs are free of computational and logic errors, they cannot be considered validated. Any application of these programs without additional verification is at the risk of the user.

11/11

TABLE OF CONTENTS

I. INTRODUCTION	1
II. DESIGN APPROACH	3
A. GEOMETRY	3
B. STRESS ANALYSIS	3
C. BUCKLING ANALYSIS	8
1. Overall Plate Buckling Analysis	8
a. FEM Formulation	9
2. Stiffener Local Buckling Analysis	12
III. OPTIMIZATION PROBLEM	14
A. PROBLEM STATEMENT	14
B. OPTIMIZATION METHODS	15
1. IMSL Subroutine DNCONG	15
2. DOT using MFD	16
3. DOT using SLP	17
IV. RESULTS AND DISCUSSION	18
A. OPTIMUM SOLUTIONS	18
1. Case 1: $\Theta = 0.04$ and Ply Orientation $(0^\circ_{beam} / 90^\circ / 0^\circ)_{sym}$	19
2. Case 2: $\Theta = 0.04$ and Ply Orientation $(0^\circ_{beam} / 0^\circ / 90^\circ)_{sym}$	23
3. Case 3: $\Theta = 0.04$ and Ply Orientation $(90^\circ_{beam} / 90^\circ / 0^\circ)_{sym}$	25
4. Case 4: $\Theta = 0.04$ and Ply Orientation $(90^\circ_{beam} / 0^\circ / 90^\circ)_{sym}$	30
5. Case 5: $\Theta = 0.015$ and Ply Orientation $(0^\circ_{beam} / 90^\circ / 0^\circ)_{sym}$	36
6. Case 6: $\Theta = 0.015$ and Ply Orientation $(0^\circ_{beam} / 0^\circ / 90^\circ)_{sym}$	40
7. Case 7: $\Theta = 0.015$ and Ply Orientation $(90^\circ_{beam} / 90^\circ / 0^\circ)_{sym}$	42
8. Case 8: $\Theta = 0.015$ and Ply Orientation $(90^\circ_{beam} / 0^\circ / 90^\circ)_{sym}$	46
B. OPTIMIZATION EFFICIENCY	50
V. CONCLUSIONS	52

APPENDIX A. DESIGN ANALYSIS SUBROUTINES	54
APPENDIX B. OPTIMIZATION PROBLEM CODE LISTING USING IMSL .	73
APPENDIX C. OPTIMIZATION PROBLEM CODE LISTING USING DOT .	76
LIST OF REFERENCES	81
INITIAL DISTRIBUTION LIST	85

1111

LIST OF TABLES

Table 1. RESULTS: $\Theta = 0.04$, PLY ANGLE $(0^\circ_{BEAM} / 90^\circ / 0^\circ)_{SYM}$	19
Table 2. RESULTS: $\Theta = 0.04$, PLY ANGLE $(0^\circ_{BEAM} / 0^\circ / 90^\circ)_{SYM}$	23
Table 3. RESULTS: $\Theta = 0.04$, PLY ANGLE $(90^\circ_{BEAM} / 90^\circ / 0^\circ)_{SYM}$	25
Table 4. RESULTS: $\Theta = 0.04$, PLY ANGLE $(90^\circ_{BEAM} / 0^\circ / 90^\circ)_{SYM}$	30
Table 5. RESULTS: $\Theta = 0.015$, PLY ANGLE $(0^\circ_{BEAM} / 90^\circ / 0^\circ)_{SYM}$	36
Table 6. RESULTS: $\Theta = 0.015$, PLY ANGLE $(0^\circ_{BEAM} / 0^\circ / 90^\circ)_{SYM}$	40
Table 7. RESULTS: $\Theta = 0.015$, PLY ANGLE $(90^\circ_{BEAM} / 90^\circ / 0^\circ)_{SYM}$	42
Table 8. RESULTS: $\Theta = 0.015$, PLY ANGLE $(90^\circ_{BEAM} / 0^\circ / 90^\circ)_{SYM}$	46
Table 9. RUN TIMES: $\Theta = 0.04$, PLY ANGLE $(0^\circ_{BEAM} / 90^\circ / 0^\circ)_{SYM}$	50

111

LIST OF FIGURES

Figure 1.	Problem Geometry	4
Figure 2.	Half of Symmetric Laminate Plate	7
Figure 3.	Geometry for Case 1 with $p = 0.0002646$	19
Figure 4.	Buckling Shapes for Case 1 with $p = 0.0002646$	20
Figure 5.	Geometry for Case 1 with $p = 0.0002822$	21
Figure 6.	Buckling Shapes for Case 1 with $p = 0.0002822$	22
Figure 7.	Geometry for Case 2 with $p = 0.0003949$	23
Figure 8.	Buckling Shapes for Case 2 with $p = 0.0003949$	24
Figure 9.	Geometry for Case 3 with $p = 0.0000677$	25
Figure 10.	Buckling Shapes for Case 3 with $p = 0.0000677$	26
Figure 11.	Geometry for Case 3 with $p = 0.0001804$	27
Figure 12.	Buckling Shapes for Case 3 with $p = 0.0001804$	29
Figure 13.	Geometry for Case 4 with $p = 0.0000677$	30
Figure 14.	Buckling Shapes for Case 4 with $p = 0.0000677$	31
Figure 15.	Geometry for Case 4 with $p = 0.0001345$	32
Figure 16.	Buckling Shapes for Case 4 with $p = 0.0001345$	33
Figure 17.	Geometry for Case 4 with $p = 0.0001702$	34
Figure 18.	Buckling Shapes for Case 4 with $p = 0.0001702$	35
Figure 19.	Geometry for Case 5 with $p = 0.0000156$	36
Figure 20.	Buckling Shapes for Case 5 with $p = 0.0000156$	37
Figure 21.	Geometry for Case 5 with $p = 0.0000124$	38
Figure 22.	Buckling Shapes for Case 5 with $p = 0.0000124$	39
Figure 23.	Geometry for Case 6 with $p = 0.0000179$	40
Figure 24.	Buckling Shapes for Case 6 with $p = 0.0000179$	41
Figure 25.	Geometry for Case 7 with $p = 0.0000036$	42
Figure 26.	Buckling Shapes for Case 7 with $p = 0.0000036$	43
Figure 27.	Geometry for Case 7 with $p = 0.0000130$	44
Figure 28.	Buckling Shapes for Case 7 with $p = 0.0000130$	45
Figure 29.	Geometry for Case 8 with $p = 0.0000036$	46
Figure 30.	Buckling Shapes for Case 8 with $p = 0.0000036$	47
Figure 31.	Geometry for Case 8 with $p = 0.0000125$	48

Figure 32. Buckling Shapes for Case 8 with $p = 0.0000125$ 49

TABLE OF SYMBOLS

$[a]$	Nondimensionalized extensional stiffness matrix
$[A]$	Extensional stiffness matrix
b	Nondimensionalized width of stiffener
B	Width of stiffener
$[B]$	Coupling stiffness matrix
B'	Positive definite approximation of the Hessian matrix of the Lagrangian function on the q^{th} iteration of the optimization process
c	Ratio of the plate width to plate length
$[D]$	Bending stiffness matrix
e_b	Nondimensionalized beam elastic modulus
e_p	Nondimensionalized plate elastic modulus
E_{11_b}	Elastic modulus of the beam in the direction of the fiber orientation
E_{22_b}	Elastic modulus of the beam in the direction perpendicular to the fiber orientation
E_{11_i}	Elastic modulus of the i^{th} lamina in the direction of the fiber orientation
E_{22_i}	Elastic modulus of the i^{th} lamina in the direction perpendicular to the fiber orientation
f_i	Shape functions for the plate element
$F(X)$	Objective function for the optimization process
$g_j(X)$	Constraint functions for the optimization process
G_{12_b}	Shear modulus of the beam
G_{12_i}	Shear modulus of the i^{th} lamina
h	Nondimensionalized height of stiffener
H	Height of stiffener
i_b	Nondimensionalized moment of inertia for the stiffener
J	Critical constraints in the optimization process
$[k]$	Plate element stiffness matrix
$[K]$	Plate stiffness matrix
$[k]_b$	Beam element stiffness matrix
$[K]_b$	Beam stiffness matrix
$[K]_r$	Stiffness matrix of the plate and stiffener combination

$[k_G]$	Plate element geometric stiffness matrix
$[K_G]$	Plate geometric stiffness matrix
$[k_G]_b$	Beam element geometric stiffness matrix
$[K_G]_b$	Beam geometric stiffness matrix
$[K_G]_r$	Geometric stiffness matrix of the plate and stiffener combination
l_x	Nondimensionalized span length
L_x	Span length
l_y	Nondimensionalized span width
L_y	Span width
l_e	Element length for FEM formulation
$L(X, \lambda)$	Lagrangian function
$\{M\}$	Resultant inplane moment acting on the laminate plate
n	Half the number of layers for the symmetric plate (2n total layers)
$\{N\}$	Resultant inplane force acting on the laminate plate
n_x	Nondimensionalized load carried by the plate
p	Nondimensionalized load carried by the stiffened plate
p_1	Nondimensionalized first overall buckling load of the stiffened plate
p_2	Nondimensionalized second overall buckling load of the stiffened plate
p_3	Nondimensionalized third overall buckling load of the stiffened plate
p_b	Nondimensionalized load carried by the beam
p_s	Nondimensionalized local buckling load of the stiffener
q	Iteration number in the optimization process
$[Q]$	Reduced stiffness matrix
$[\bar{Q}]$	Reduced transformed stiffness matrix
\mathbb{R}^n	Design space
s_b	Nondimensionalized beam cross section
s_p	Nondimensionalized plate cross section
S^q	Search direction for the q^{th} iteration in the optimization process
t_i	Nondimensionalized thickness of the i^{th} lamina
t_T	Nondimensionalized thickness of the half plate
T_i	Thickness of the i^{th} lamina
$\{U\}$	Buckling shape

u_o	Midplane displacement in the x direction
v_o	Midplane displacement in the y direction
w_o	Midplane displacement in the z direction
X^o	Initial guess for the design variables in the optimization process
α^*	Step length for each iteration in the optimization process
β	Buckling load of the optimized stiffened plate
ε	Strain
ε^o	Midplane strain of plate
ζ	Search direction modification coefficient for the Fletcher-Reeves Conjugate Direction Method
η	Plate element local y direction coordinate for the FEM formulation
θ_i	Ply orientation angle of the i^{th} lamina
Θ	Nondimensionalized volume of the plate
κ	Midplane curvature of plate
$\{\lambda\}$	Vector of Lagrange multipliers
ν_{12}	Poisson's ratio for transverse strain in the 2 direction when stressed in the 1 direction
ν_{21}	Poisson's ratio for transverse strain in the 1 direction when stressed in the 2 direction
ξ	Plate element local x direction coordinate for the FEM formulation
σ	Stress
$\nabla F(X)$	Gradient of the objective function
$\nabla g_j(X)$	Gradient of the constraint functions

I. INTRODUCTION

Design optimization is not a new subject. Man has always strived to build the best, whether it be ancient man making a hunting bow or today's engineer designing a light-weight, high-strength wing for a high-performance aircraft. The goal for both is exactly the same, to make the best possible design subject to a set of design requirements. The difference between the two is not in the goal but in the technique. Ancient man used trial and error to improve on his previous designs and, over a period of time, he was able to produce an efficient weapon. Today, high-speed digital computers are used to analyze and improve designs by solving a large set of equations that have been formulated to mathematically model the design problem.

The design optimization problem of current interest is the maximization of the buckling load for a blade stiffened composite plate. This problem can be viewed from two different perspectives. On one hand, this is a design optimization problem which optimizes the shape of the plate and stiffener cross section to give the maximum load. On the other hand, this is a design optimization problem which optimizes the thickness and/or the ply angle of the composite laminae to give the maximum load. Previous works on the optimization of the plate and stiffener cross sectional shape have focused on the use of solid elastic materials [Refs. 1-4]. In the area of design optimization of composite plates, previous works have focused on plates without stiffeners. Optimization of the composite plate with respect to the lamina fiber orientations has been studied in [Refs. 5-17]. Of greater interest to this study are the previous works on the design optimization of composite plates where the laminae thickness and not the ply orientations are taken as the design variables [Refs. 18-21]. The current study combines the design optimization problems of cross section optimization and composite laminae thickness optimization into a single design optimization problem. This is done by optimizing a blade stiffened composite plate for the maximum buckling load by using the laminae thicknesses and the stiffener height and width as the design variables.

Composites are used as the structural material in this study because of their high strength-to-weight and stiffness-to-weight ratios. These properties are very important in many of today's engineered structures, especially in the aerospace industry where high strength is required but a severe penalty is incurred for added weight. Because of this, composites make an excellent choice for a structural material. However, the use of

composites greatly complicates the design analysis problem arising from the use of laminated materials with non-homogeneous properties. Now the analysis process must consider the orthotropic properties and the ply orientation of each individual lamina, the specific stacking order of the laminae, and the thickness of each individual lamina. One serious problem that arises is the coupling effect between extension and bending. Because a symmetric composite plate is chosen, the coupling between extension and bending is eliminated. This lack of coupling allows the use of linear buckling analysis up to the buckling load.

The formulation of a suitable design analysis technique is the first step in the design optimization. Since the optimum design can never be better than the design analysis that it is based on, the formulation is described in some detail. The buckling analysis of the stiffened plate is performed in two steps. First, a finite element method is used to determine the overall buckling load of the stiffened plate. This is done by treating the stiffener as a beam in forming the global stiffness matrix for the plate. Using FEM formulation, the first three buckling loads are solved numerically. The second part of the buckling analysis finds the local buckling load of the stiffener. By treating the stiffener as a plate with three sides simply supported and the fourth side as free, the local buckling problem can be solved analytically using a Levy's solution.

Once the design analysis technique has been formulated, the design variables, taken to be the laminae thickness and the stiffener height and width, are optimized using an optimization program. This study uses three different optimization programs which are all commercially available. They are: the IMSL Subroutine DNCONG; the Design Optimization Tools (DOT) program using Modified Feasible Direction; and the Design Optimization Tools (DOT) program using Sequential Linear Programming.

The specific problem investigated in this study is a symmetric blade stiffened composite plate that has two laminae and a stiffener on either side of the centerline. The fiber orientation of the laminae and the stiffener are allowed to be either 0° or 90° . Four different stacking orders of these fiber orientations are investigated. For each case, design optima are investigated. These optima are then compared to determine if there is a best stacking configuration. The study is completed for two different total volumes of material. Finally, the relative efficiencies of the three optimization routines are investigated to determine qualitatively which is the best suited for this specific problem.

II. DESIGN APPROACH

A. GEOMETRY

The geometry used in this study is a blade stiffened composite plate which is symmetric to the plate centerline as shown in Figure 1 on page 4. The plate is simply supported on all four sides and subject to a compressive inplane load in the stiffener direction. The blade stiffener is centered on the plate and spans the plate length, L_s .

Each lamina has a thickness of T_i and a ply orientation of angle θ_i . The stiffener is defined by a width of B and a height of H . The ply orientation of the stiffener can be either 0° or 90° . The independent engineering properties of each lamina and the stiffener are given by E_{11} , E_{22} , ν_{12} , G_{12} , and E_{11s} , E_{22s} , ν_{12s} , G_{12s} , respectively.

B. STRESS ANALYSIS

The analysis of a composite plate structure is based on classical lamination theory. From this theory, the stiffness of a composite structure can be determined from the material properties of the individual laminae [Ref. 22: p. 147]. The plate in this study is composed of individual layers which are made of orthotropic material. Also, the plate is thin with respect to its span length so it is assumed to be under plane stress conditions. From this, classical lamination theory can be applied to determine the composite's stiffness.

First, the stress strain relation for a orthotropic material under plane stress must be defined for the individual laminae. This relationship is given in Eq. (1) below.

$$\begin{Bmatrix} \sigma_1 \\ \sigma_2 \\ \sigma_{12} \end{Bmatrix} = \begin{bmatrix} Q_{11} & Q_{12} & Q_{16} \\ Q_{12} & Q_{22} & Q_{26} \\ Q_{16} & Q_{26} & Q_{66} \end{bmatrix} \begin{Bmatrix} \epsilon_1 \\ \epsilon_2 \\ \gamma_{12} \end{Bmatrix} \quad (1)$$

where the reduced stiffness matrix elements, Q_{ij} , are defined in terms of the elastic modulus in the 1-1 principal direction, E_{11} , the elastic modulus in the 2-2 principal direction, E_{22} , the shear modulus, G_{12} , and poisson's ratio relating transverse strain in the 1 direction when stressed in the 2 direction, ν_{12} , and poisson's ratio relating transverse strain in the 2 direction when stressed in the 1 direction, ν_{21} .

$$Q_{11} = \frac{E_{11}}{1 - \nu_{12}\nu_{21}}$$

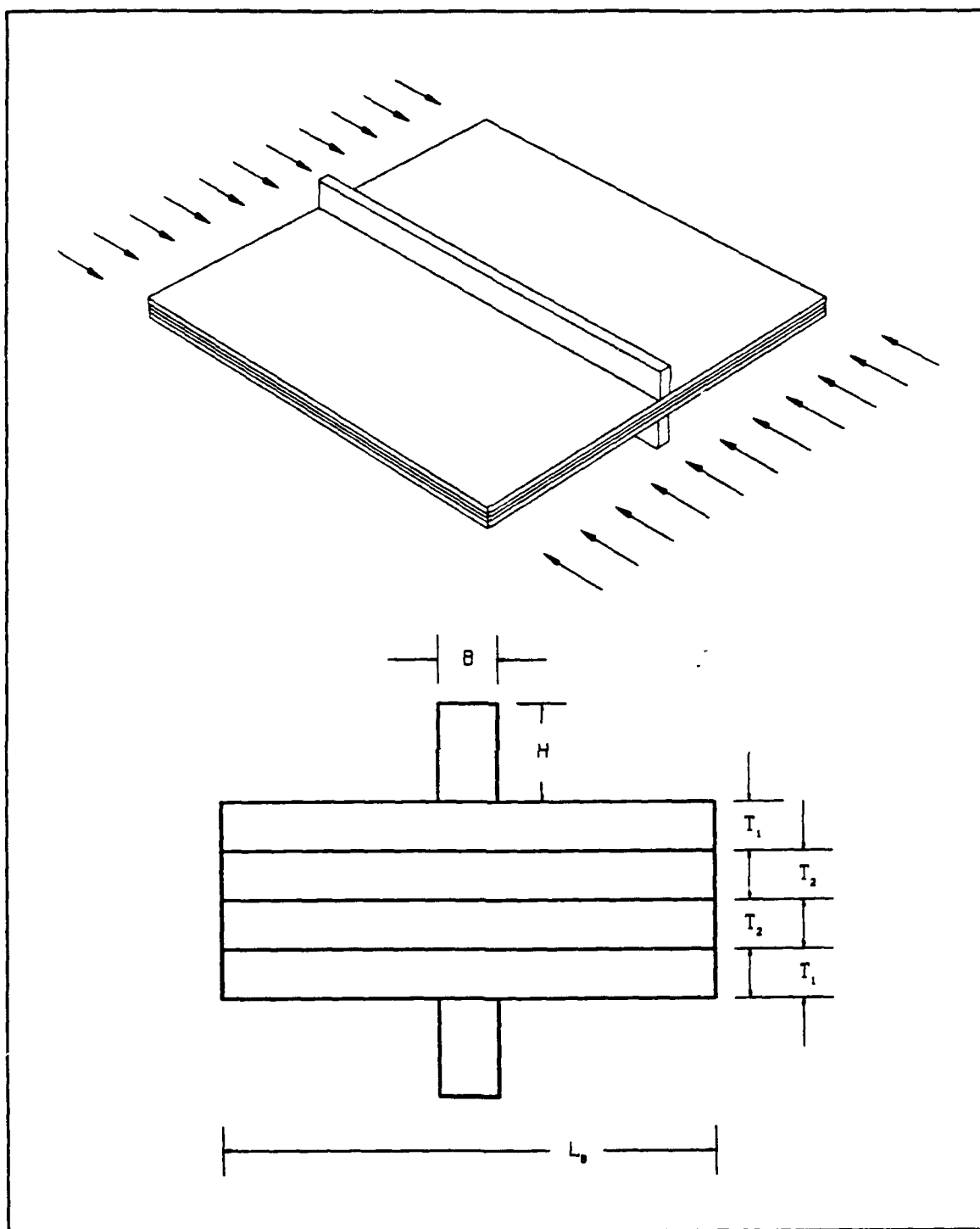


Figure 1. Problem Geometry: top) general view bottom) cross sectional view

$$Q_{12} = \frac{\nu_{12} E_{22}}{1 - \nu_{12} \nu_{21}}$$

$$Q_{22} = \frac{E_{22}}{1 - \nu_{12} \nu_{21}}$$

$$Q_{16} = 0$$

$$Q_{26} = 0$$

$$Q_{66} = G_{12}$$

For each lamina, the principal axes lie along the direction of the fiber orientation. Since the fiber orientation of each lamina is allowed to vary by an angle θ , Eq. (1) must be transformed to determine the stress strain relationship in the lamina geometric reference frame. This relationship is given in Eq. (2).

$$\begin{Bmatrix} \sigma_x \\ \sigma_y \\ \sigma_{xy} \end{Bmatrix} = \begin{bmatrix} \bar{Q}_{11} & \bar{Q}_{12} & \bar{Q}_{16} \\ \bar{Q}_{12} & \bar{Q}_{22} & \bar{Q}_{26} \\ \bar{Q}_{16} & \bar{Q}_{26} & \bar{Q}_{66} \end{bmatrix} \begin{Bmatrix} \epsilon_x \\ \epsilon_y \\ \epsilon_{xy} \end{Bmatrix} \quad (2)$$

where the elements of the reduced transformed stiffness matrix, \bar{Q}_i , are defined in terms of Q_i and θ as

$$\bar{Q}_{11} = Q_{11} \cos^4 \theta + 2(Q_{12} + 2Q_{66}) \sin^2 \theta \cos^2 \theta + Q_{22} \sin^4 \theta$$

$$\bar{Q}_{12} = (Q_{11} + Q_{22} - 4Q_{66}) \sin^2 \theta \cos^2 \theta + Q_{12}(\sin^4 \theta + \cos^4 \theta)$$

$$\bar{Q}_{22} = Q_{11} \sin^4 \theta + 2(Q_{12} + 2Q_{66}) \sin^2 \theta \cos^2 \theta + Q_{22} \cos^4 \theta$$

$$\bar{Q}_{16} = (Q_{11} - Q_{12} - 2Q_{66}) \sin \theta \cos^3 \theta + (Q_{12} - Q_{22} + 2Q_{66}) \sin^3 \theta \cos \theta$$

$$\bar{Q}_{26} = (Q_{11} - Q_{12} - 2Q_{66}) \sin^3 \theta \cos \theta + (Q_{12} - Q_{22} + 2Q_{66}) \sin \theta \cos^3 \theta$$

$$\bar{Q}_{66} = (Q_{11} + Q_{22} - 2Q_{12} - 2Q_{66}) \sin^3 \theta \cos \theta + Q_{66}(\sin^4 \theta + \cos^4 \theta)$$

Now Eq. (2) can be thought of as the stress strain relationship for the k^{th} layer of a multilayered laminate. Thus it is now written as Eq. (3).

$$\{\sigma\}_k = [\bar{Q}]_k \{\epsilon\}_k \quad (3)$$

The strain at any point through the depth of the laminate can be expressed in terms of the midplane strain, ϵ^o , the distance z from the centerline, and the midplane curvature, κ . See Figure 2 on page 7 for the definition of z .

The strain is now expressed as Eq. (4).

$$\begin{Bmatrix} \epsilon_x \\ \epsilon_y \\ \gamma_{xy} \end{Bmatrix} = \begin{Bmatrix} \epsilon_x^o \\ \epsilon_y^o \\ \gamma_{xy}^o \end{Bmatrix} + z \begin{Bmatrix} \kappa_x \\ \kappa_y \\ \kappa_{xy} \end{Bmatrix} \quad (4)$$

where

$$\{\epsilon_x^o \quad \epsilon_y^o \quad \gamma_{xy}^o\}^T = \left\{ \frac{\partial u_o}{\partial x} \quad \frac{\partial v_o}{\partial y} \quad \frac{\partial u_o}{\partial y} + \frac{\partial v_o}{\partial x} \right\}^T$$

and

$$\{\kappa_x \quad \kappa_y \quad \kappa_{xy}\}^T = \left\{ \frac{\partial^2 w_o}{\partial x^2} \quad \frac{\partial^2 w_o}{\partial y^2} \quad 2 \frac{\partial^2 w_o}{\partial x \partial y} \right\}^T$$

The resultant forces and moments acting on a laminate are obtained by integration of the stresses in each layer through the laminate thickness.

$$\begin{Bmatrix} N_x \\ N_y \\ N_{xy} \end{Bmatrix} = \int_{-t}^t \begin{Bmatrix} \sigma_x \\ \sigma_y \\ \tau_{xy} \end{Bmatrix} dz = 2 \sum_{k=1}^n \int_{z_{k-1}}^{z_k} \begin{Bmatrix} \sigma_x \\ \sigma_y \\ \tau_{xy} \end{Bmatrix} dz \quad (5a)$$

and

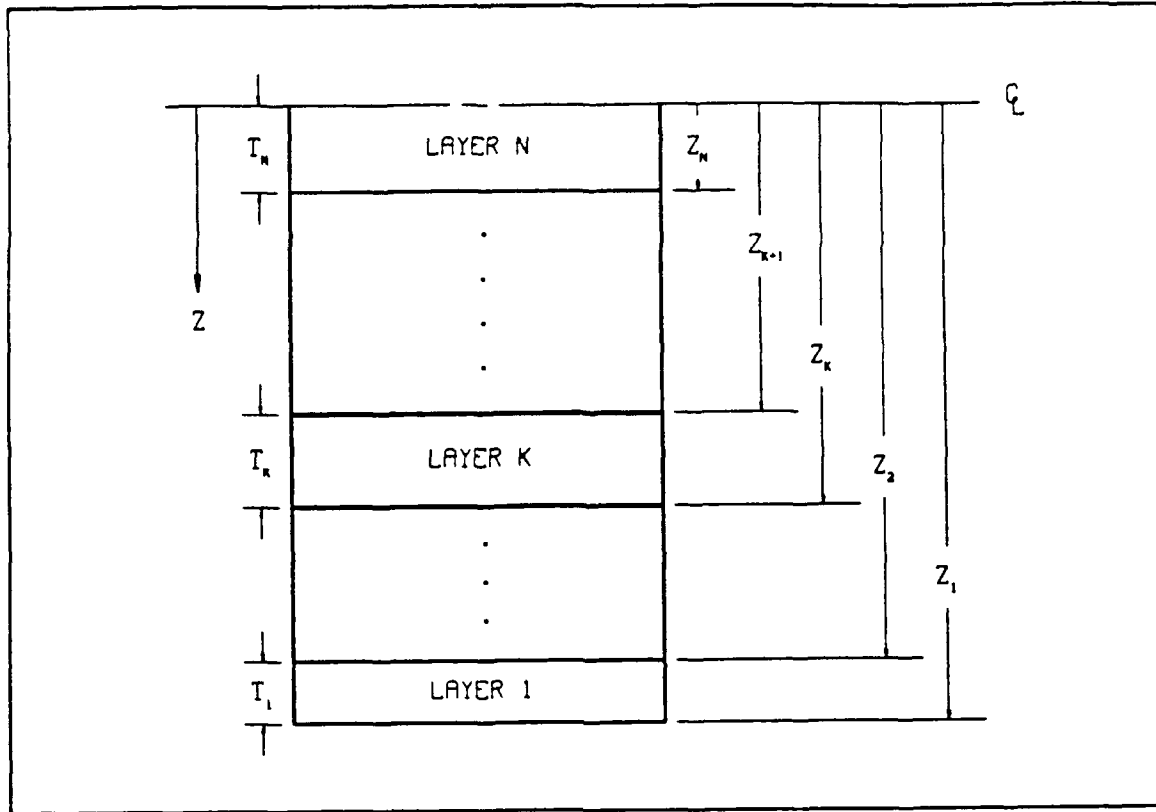


Figure 2. Half of Symmetric Laminate Plate

$$\begin{Bmatrix} M_x \\ M_y \\ M_{xy} \end{Bmatrix} = \int_{-t}^t \begin{Bmatrix} \sigma_x \\ \sigma_y \\ \tau_{xy} \end{Bmatrix} z dz = 2 \sum_{k=1}^n \int_{z_{k-1}}^{z_k} \begin{Bmatrix} \sigma_x \\ \sigma_y \\ \tau_{xy} \end{Bmatrix} z dz \quad (5b)$$

Substituting Eq. (4) into Eqs. (5a) and (5b) gives,

$$\begin{Bmatrix} N_x \\ N_y \\ N_{xy} \end{Bmatrix} = \begin{bmatrix} A_{11} & A_{12} & A_{16} \\ A_{12} & A_{22} & A_{26} \\ A_{16} & A_{26} & A_{66} \end{bmatrix} \begin{Bmatrix} \epsilon_x^o \\ \epsilon_y^o \\ \gamma_{xy}^o \end{Bmatrix} + \begin{bmatrix} B_{11} & B_{12} & B_{16} \\ B_{12} & B_{22} & B_{26} \\ B_{16} & B_{26} & B_{66} \end{bmatrix} \begin{Bmatrix} \kappa_x \\ \kappa_y \\ \kappa_{xy} \end{Bmatrix}$$

and

$$\begin{Bmatrix} M_x \\ M_y \\ M_{xy} \end{Bmatrix} = \begin{bmatrix} B_{11} & B_{12} & B_{16} \\ B_{12} & B_{22} & B_{26} \\ B_{16} & B_{26} & B_{66} \end{bmatrix} \begin{Bmatrix} \epsilon_x^o \\ \epsilon_y^o \\ \gamma_{xy}^o \end{Bmatrix} + \begin{bmatrix} D_{11} & D_{12} & D_{16} \\ D_{12} & D_{22} & D_{26} \\ D_{16} & D_{26} & D_{66} \end{bmatrix} \begin{Bmatrix} \kappa_x \\ \kappa_y \\ \kappa_{xy} \end{Bmatrix}$$

where

$$A_{ij} = 2 \sum_{k=1}^n (\bar{Q}_{ij})_k (z_k - z_{k-1})$$

$$B_{ij} = \sum_{k=1}^n (\bar{Q}_{ij})_k (z_k^2 - z_{k-1}^2) \quad (6)$$

$$D_{ij} = \frac{2}{3} \sum_{k=1}^n (\bar{Q}_{ij})_k (z_k^3 - z_{k-1}^3)$$

The A_{ij} terms are the extensional stiffness, the B_{ij} terms are the coupling stiffness, and the D_{ij} terms are the bending stiffness. Since the composite plate modeled in the study is symmetric about the middle surface, the terms B_{ij} all drop out [Ref. 22: p. 164]. Therefore, in this problem there is no coupling between extension and bending.

C. BUCKLING ANALYSIS

Buckling of the stiffened plate can occur in two ways. These are: the plate and stiffener can buckle as a unit into one of the global buckling modes; and the blade stiffener can experience local buckling. Because of this, the buckling analysis is performed in two steps. For the first case, the blade stiffener is treated as a beam and included in the formulation of the global stiffness matrix in the Finite Element Formulation. For the second case, the blade stiffener is treated as a plate subject to a inplane compressive load that has three sides simply supported and the fourth side free. [Ref. 23: pp. 2-3]

1. Overall Plate Buckling Analysis

From [Ref. 23: p. 4], the overall buckling equation in matrix form is

$$[K]\{U\} + [K]_b\{U\} - n_x[K_G]\{U\} - p_b[K_G]_b\{U\} = 0$$

where $[K]$ and $[K]_b$ are the plate and beam stiffness matrices, respectively, $[K_G]$ and $[K_G]_b$ are the plate and the beam geometric stiffness matrices, respectively, and $\{U\}$ is the

buckling shape. The amount of load carried by the beam and plate are p_b and n_x , respectively. The load share carried by the beam and by the plate is proportional to the relative stiffness of each. These relative loads are given by

$$n_x = \frac{e_p s_p}{e_p s_p + e_b s_b} p$$

$$p_b = \frac{e_b s_b}{e_p s_p + e_b s_b} p$$

where s_p and s_b are the nondimensional cross-sectional area of the plate and beam, respectively, and e_p and e_b are the nondimensional elastic moduli of the laminated plate and the beam, respectively. The nondimensional elastic modulus of the plate must be determined from the properties of the individual laminae. This value is calculated from the extensional stiffness matrix and is given by [Ref. 23: p. 4] as

$$e_p = \frac{|[a]|}{(a_{22}a_{66} - a_{26}^2)t_T}$$

Now the overall buckling equation can be written in the form,

$$[K]_T \{U\} - p[K_G]_T \{U\} = 0$$

where $[K]_T$ is the total stiffness of the plate and stiffener combination and $[K_G]_T$ is the total geometric stiffness of the plate and stiffener combination. This equation can easily be recognized as an eigenvalue problem with p representing the eigenvalues and $\{U\}$ representing the eigenvectors. This problem is solved using DNLASO, one of the subroutines from the package LASO2 [Ref. 24], which computes a few eigenvalues and the associated eigenvectors of a large (sparse) symmetric matrix using the Lanczos algorithm [Ref. 25]. The programming code used to calculate the first three buckling loads of the stiffened plate is Subroutine EIGEN contained in Appendix A.

a. FEM Formulation

In order to determine the stiffness matrices for the buckling equation, a finite element formulation is required. For this study, a 16 degree of freedom plate element is chosen for the plate and a 4 degree of freedom beam element is chosen for the stiffener. The plate is divided into four elements (2 X 2) and the stiffener is divided into two elements.

From [Ref. 26: p. 116] the beam element stiffness matrix, $[k]_b$, is defined as

$$[k]_b = \frac{e_b i_b}{l_e^3} \begin{bmatrix} 12 & -6l_e & -12 & -6l_e \\ -6l_e & 4l_e^2 & 6l_e & 2l_e^2 \\ -12 & 6l_e & 12 & 6l_e \\ -6l_e & 2l_e^2 & 6l_e & 4l_e^2 \end{bmatrix}$$

where the element length, l_e , is one half the nondimensionalized span length, l_s , and e_b is the nondimensionalized elastic modulus of the stiffener. The nondimensionalized moment of inertia of the stiffener, i_b , is defined as

$$i_b = \frac{2}{3} b[(h + t_T)^3 - t_T^3]$$

where t_T is one half the total plate thickness for the symmetric plate. From [Ref. 26: p. 388] the beam element geometric stiffness matrix, $[k_G]_b$, is defined as

$$[k_G]_b = \frac{p_b}{30l_e} \begin{bmatrix} 36 & -3l_e & -36 & -3l_e \\ -3l_e & 4l_e^2 & 3l_e & -l_e^2 \\ -36 & 3l_e & 36 & 3l_e \\ -3l_e & -l_e^2 & 3l_e & 4l_e^2 \end{bmatrix}$$

For the plate element, the geometric stiffness matrix elements, $k_{G_{ij}}$, are given by [Ref. 27: p. 432] as

$$k_{G_{ij}} = n_x \int_0^1 \int_0^1 \left(\frac{\partial f_i}{\partial \xi} \right) \left(\frac{\partial f_j}{\partial \xi} \right) d\xi d\eta \quad (7)$$

where f_i are the 16 shape functions for the element. The shape functions, f_i , are given below.

$$f_1 = (1 - 3\xi^2 + 2\xi^3)(1 - 3\eta^2 + 2\eta^3)$$

$$f_2 = (1 - 3\xi^2 + 2\xi^3)(\eta - 2\eta^2 + \eta^3)$$

$$f_3 = -(\xi - 2\xi^2 + \xi^3)(1 - 3\eta^2 + 2\eta^3)$$

$$f_4 = (\xi - 2\xi^2 + \xi^3)(\eta - 2\eta^2 + \eta^3)$$

$$f_5 = (3\xi^2 - 2\xi^3)(1 - 3\eta^2 + 2\eta^3)$$

$$f_6 = (3\xi^2 - 2\xi^3)(\eta - 2\eta^2 + \eta^3)$$

$$f_7 = (\xi^2 - \xi^3)(1 - 3\eta^2 + 2\eta^3)$$

$$f_8 = -(\xi^2 - \xi^3)(\eta - 2\eta^2 + \eta^3)$$

$$f_9 = (3\xi^2 - 2\xi^3)(3\eta^2 - 2\eta^3)$$

$$f_{10} = -(3\xi^2 - 2\xi^3)(\eta^2 - \eta^3)$$

$$f_{11} = (\xi^2 - \xi^3)(3\eta^2 - 2\eta^3)$$

$$f_{12} = (\xi^2 - \xi^3)(\eta^2 - \eta^3)$$

$$f_{13} = (1 - 3\xi^2 + 2\xi^3)(3\eta^2 - 2\eta^3)$$

$$f_{14} = -(1 - 3\xi^2 + 2\xi^3)(\eta^2 - \eta^3)$$

$$f_{15} = -(\xi - 2\xi^2 + \xi^3)(3\eta^2 - 2\eta^3)$$

$$f_{16} = -(\xi - 2\xi^2 + \xi^3)(\eta^2 - \eta^3)$$

The integral of Eq. (7) is solved numerically by using gauss quadrature.

For the plate element, the stiffness matrix elements, k_{ij} , are given by [Ref. 27: pp. 415-418] as

$$k_{ij} = \int_0^1 \int_0^1 \{ D_{11}C_1 + D_{12}C_2 + D_{16}C_3 + D_{22}C_4 + D_{26}C_5 + D_{66}C_6 \} d\xi d\eta$$

where

$$C_i = \left(\frac{\partial^2 f_i}{\partial \xi^2} \right) \left(\frac{\partial^2 f_j}{\partial \xi^2} \right)$$

$$C_2 = \left(\frac{\partial^2 f_i}{\partial \xi^2} \right) \left(\frac{\partial^2 f_j}{\partial \eta^2} \right) + \left(\frac{\partial^2 f_j}{\partial \xi^2} \right) \left(\frac{\partial^2 f_i}{\partial \eta^2} \right)$$

$$C_3 = 2 \left[\left(\frac{\partial^2 f_i}{\partial \xi^2} \right) \left(\frac{\partial^2 f_j}{\partial \xi \partial \eta} \right) + \left(\frac{\partial^2 f_j}{\partial \xi^2} \right) \left(\frac{\partial^2 f_i}{\partial \xi \partial \eta} \right) \right]$$

$$C_4 = \left(\frac{\partial^2 f_i}{\partial \eta^2} \right) \left(\frac{\partial^2 f_j}{\partial \eta^2} \right)$$

$$C_5 = 2 \left[\left(\frac{\partial^2 f_i}{\partial \eta^2} \right) \left(\frac{\partial^2 f_j}{\partial \xi \partial \eta} \right) + \left(\frac{\partial^2 f_j}{\partial \eta^2} \right) \left(\frac{\partial^2 f_i}{\partial \xi \partial \eta} \right) \right]$$

$$C_6 = 4 \left(\frac{\partial^2 f_i}{\partial \xi \partial \eta} \right) \left(\frac{\partial^2 f_j}{\partial \xi \partial \eta} \right)$$

Again, here the integration is done numerically by gauss quadrature. All of the elemental stiffness formulation is done in Subroutine ELESTF in Appendix A.

Now that all the elemental stiffness matrices (both stiffness and geometric) have been determined, the individual elemental matrices can be assembled into the global stiffness matrices. The geometric elemental stiffness matrices $[k_G]$ and $[k_G]_b$ are combined to form the total global geometric stiffness matrix $[K_G]_r$. The elemental stiffness matrices $[k]$ and $[k]_b$ are combined to form the total global stiffness matrix $[K]_r$. This global stiffness matrix assembling is done in Subroutine ASSEMB in Appendix A.

2. Stiffener Local Buckling Analysis

To calculate the local buckling load of the blade stiffener, it is treated as a separate plate buckling problem. Now the stiffener alone is treated as a plate with three sides ($x = 0$, $x = l_s$, $z = 0$) simply supported and the fourth side ($z = h$) free. It is subject to axial compressive load p_s . Because of the geometry and the fact that only the first buckling load is of interest, this problem can be solved analytically.

The general partial differential equation for the plate buckling problem is given from [Ref. 22: p. 260] as

$$D_{11} \frac{\partial^4 w}{\partial x^4} + 2(D_{12} + 2D_{66}) \frac{\partial^4 w}{\partial x^2 \partial z^2} + D_{22} \frac{\partial^4 w}{\partial z^4} - p \frac{\partial^2 w}{\partial x^2} = 0$$

where now the D_{ij} refer to the properties of the blade stiffener and p refers to the local buckling load p_o . By applying the boundary conditions and assuming a Levy's solution of the form

$$w = \sum_{m=1,3,5,\dots}^{\infty} Z_m \sin \frac{m\pi x}{l_a}$$

the buckling problem can be solved directly [Ref. 28: p. 208]. The calculation of p_o is carried out in Subroutine LEVYP contained in Appendix A.

III. OPTIMIZATION PROBLEM

A. PROBLEM STATEMENT

The optimization problem is to maximize the buckling load of the blade stiffened plate for a given total material volume (which is related to the total weight). The design variables are set as the nondimensionalized thickness of the individual lamina, t_i , and the nondimensionalized width and height of the stiffener. Here the nondimensionalized width, b , and the nondimensionalized height, h , of the stiffener are denoted as t_{n+1} and t_{n+2} , respectively. The nondimensional design variables, t_i , are subject to side constraints of

$$t_{i \min} \leq t_i \leq t_{i \max} \text{ for } i = 1, 2, \dots, (n+2)$$

where $t_{i \max}$ and $t_{i \min}$ are upper and lower bounds on the design variable dimensions, respectively, and n is half the number of layers for the symmetric plate.

The optimization problem for maximizing the buckling load is written as

$$\begin{aligned} & \max_{t_j} \beta \\ \text{subject to} \quad & 2 \sum_{i=1}^n c t_i + 2 t_{n+1} t_{n+2} - \Theta = 0 \\ & 1.000 p_1 \geq \beta \\ & 0.999 p_2 \geq \beta \\ & 0.998 p_3 \geq \beta \\ & p_i \geq \beta \end{aligned}$$

$$\text{and } t_{i \min} \leq t_i \leq t_{i \max} \text{ for } i = 1, 2, \dots, (n+2)$$

where p_1 , p_2 and p_3 are the first three overall buckling loads of the stiffened plate, p_b is the local buckling load of the stiffener, t_i are the design variables, Θ is the nondimensionalized total plate volume, and c is the relative width of the plate L_b/L_s . β is a parameter introduced to raise all the buckling loads during the optimization process, which finally converges to the buckling load (lowest eigenvalue) of the optimized design.

The first constraint represents the total volume constraint. Simply put, the total volume of the design cannot exceed the maximum available resource. The next four

constraints are minimum limits on the buckling loads. Here the buckling load of the stiffened plate must always be at least as large as the smallest value of p_1 , p_2 , p_3 or p_4 . The coefficients of 1.000, 0.999, and 0.998 in the second, third, and fourth constraints, respectively, are necessary to allow the calculation of the eigenvalues, p_1 , p_2 , and p_3 , when the buckling mode is bimodal or trimodal [Ref. 29: p. 355]. Finally, the side constraints place minimum and maximum limits on the size of each design variable.

B. OPTIMIZATION METHODS

The optimization problem above can be solved by a number of different methods. For this study three different commercially available programs are used to solve the optimization problem. Each of these methods uses a different optimization technique thereby providing three independent solutions of the optimization problem. The three methods used are: the IMSL library Subroutine DNCONG; Design Optimization Tools (DOT) using Modified Feasible Direction; and Design Optimization Tools (DOT) using Sequential Linear Programming. Each of these methods are variations on the general optimization routine. The general steps in the formulation of an optimization routine are listed below.

1. Start with initial guess X^0 for the 0th iteration, $q = 0$.
2. Update the iteration number, $q = q + 1$.
3. Evaluate the objective function, $F(X)$, and the constraint functions, $g_j(X)$, at the current value of X .
4. Identify the critical constraints, J .
5. Calculate the objective function gradient, $\nabla F(X)$, and the critical constraint function gradients, $\nabla g_j(X)$, for $j \in J$.
6. Determine the search direction, S^q .
7. Perform a one-dimensional search to find the step length, α^* .
8. Update the solution by adding the previous iterate solution to the product of the step length and search direction, $X^q = X^{q-1} + \alpha^* S^q$.
9. Check for convergence. YES: done; No: go to step 2.

For each of the optimization routines used in this study, a description of the variations from the standard optimization routine are given below.

1. IMSL Subroutine DNCONG

DNCONG is based on Subroutine NLPQL which is an optimization program developed by Schittkowski. This programming algorithm uses a successive quadratic programming method to solve the general nonlinear programming problem. In this

method, the search direction subproblem is formulated and solved by using a quadratic approximation of the Lagrangian function and by linearizing the constraints. The Lagrangian function, $L(X, \lambda)$, is given by

$$L(X, \lambda) = F(X) - \sum_{j=1}^{m'} \lambda_j g_j(X)$$

where λ is the vector of Lagrange multipliers and m' is the number of function constraints plus side constraints, $m' = m + 2n$. The search direction subproblem is formulated as

$$\min_{S \in \mathbb{R}^n} \quad \frac{1}{2} S^T B^q S + \nabla f(X^q)^T S$$

$$\begin{aligned} \text{subject to} \quad & \nabla g_j(X^q)^T S + g_j(X^q) = 0, \quad j = 1, \dots, m_e \\ & \nabla g_j(X^q)^T S + g_j(X^q) \geq 0, \quad j = m_e + 1, \dots, m \end{aligned}$$

$$\text{and} \quad X_{\min} - X^q \leq S \leq X_{\max} - X^q \quad \text{for} \quad k = 1, 2, \dots, n$$

where B^q is a positive definite approximation of the Hessian matrix of the Lagrangian function and X^q is the current iterate. The solution of the subproblem, S^q , is used as the search direction in the line search to find the new point X^{q+1} . [Ref. 30]

2. DOT using MFD

Design Optimization Tools (DOT) by VMA Engineering is a programming code designed to solve a variety of nonlinear constrained or unconstrained optimization problems. The version of DOT that uses a Modified Feasible Direction algorithm has a search direction, S^q , that is a modified form of the steepest descent direction. The actual modification to the search direction is done by using the Fletcher-Reeves conjugate direction method. With this method, the search direction is defined as

$$S^q = -\nabla F(X^{q-1}) + \zeta S^{q-1}$$

where

$$\zeta = \frac{|\nabla F(X^{q-1})|^2}{|\nabla F(X^{q-2})|^2}$$

This is a first order search direction which is extremely simple to calculate. The modification of the search direction gives dramatically improved results over the method of steepest descent. [Ref. 31: p. E-16]

3. DOT using SLP

Design Optimization Tools (DOT) using Sequential Linear Programming is a method that approximates a nonlinear problem as a linear problem and then optimizes. First, a first order Taylor Series approximation of the objective and constraint functions are calculated. Then, this approximation is optimized instead of the original nonlinear functions. Since the problem is now linear, the value of the objective and constraint functions are easily and inexpensively calculated. Also, now the gradients of the objective and constraint functions are available directly from the Taylor Series expression. The linear approximation problem is optimized using the method of Modified Feasible Direction. [Ref. 31: p. E-33]

151

IV. RESULTS AND DISCUSSION

The laminate plate chosen in this study has two layers with equal span length, L_x , and span width, L_y . The material selected for the laminae and the stiffener is a graphite epoxy composite. The material properties of this composite are:

$$E_{11} = 31.0 \times 10^6 \text{ psi}, \quad E_{22} = 3.4 \times 10^6 \text{ psi}$$

$$G_{12} = 0.75 \times 10^6 \text{ psi}, \quad \nu_{12} = 0.28$$

Design optimization results are obtained for two different total volume conditions ($\Theta = 0.04$ and 0.015) and four different fiber orientation stacking sequences:

$$(0^\circ_{\text{beam}} / 90^\circ / 0^\circ)_{\text{sym}}$$

$$(0^\circ_{\text{beam}} / 0^\circ / 90^\circ)_{\text{sym}}$$

$$(90^\circ_{\text{beam}} / 90^\circ / 0^\circ)_{\text{sym}}$$

$$(90^\circ_{\text{beam}} / 0^\circ / 90^\circ)_{\text{sym}}$$

The minimum and maximum thickness of each laminae are limited to $0.001L_x$ and $0.2L_x$, respectively. The same upper and lower limits are used for the stiffener width and height.

A. OPTIMUM SOLUTIONS

For each configuration, the known optimums and the values of the design variables at these optimums are given. Also listed are the active buckling modes and the number of the corresponding figure which presents the same information graphically. All of the results are presented in non-dimensional form.

1. **Case 1: $\Theta = 0.04$ and Ply Orientation $(0^\circ_{beam} / 90^\circ / 0^\circ)_{sym}$**

For this configuration, two different optimum solutions are identified. They are listed in Table 1 below. The same results are presented graphically in Figures 3-6.

Table 1. RESULTS: $\Theta = 0.04$, PLY ANGLE $(0^\circ_{beam} / 90^\circ / 0^\circ)_{sym}$

l_1	l_2	b	h	p	Buckling Modes
0.00738	0.01020	0.03801	0.06369	0.0002646	1,2,3,4
0.01521	0.00100	0.05794	0.06526	0.0002822	1,2,4

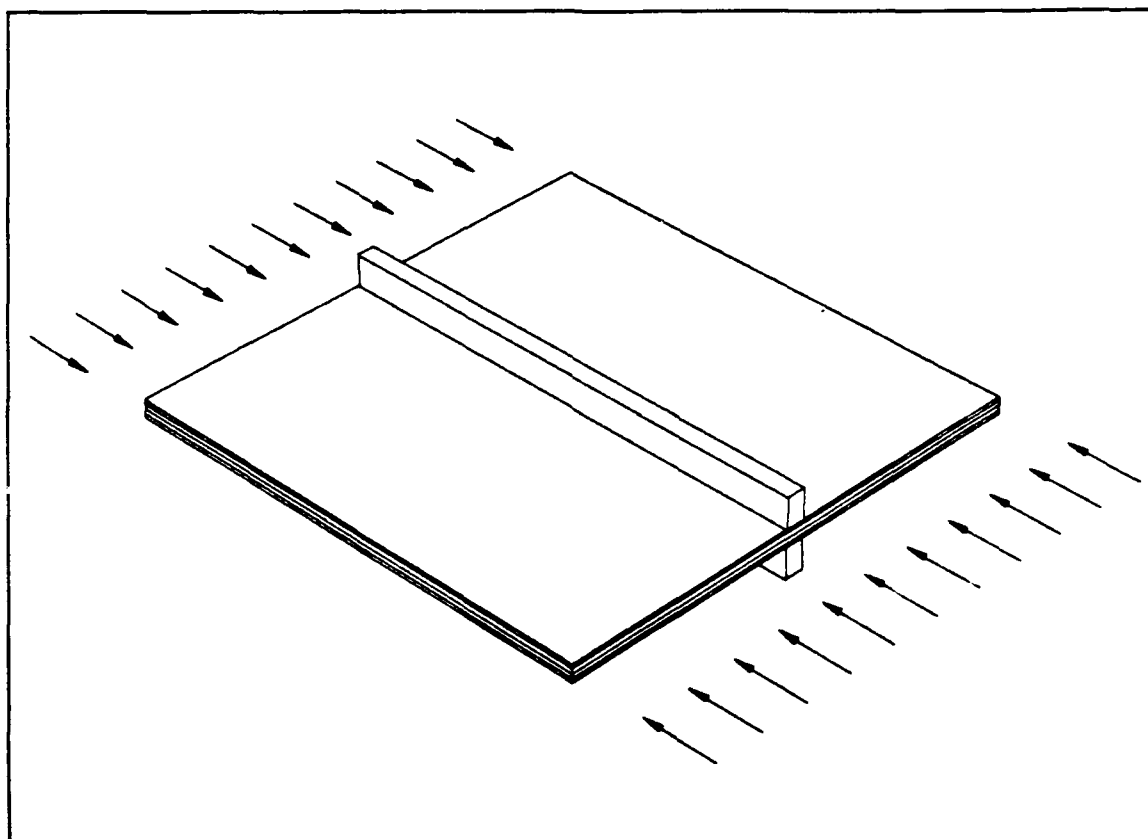


Figure 3. Geometry for Case 1 with $p = 0.0002646$: For Case 1, total volume $\Theta = 0.04$, with ply angle orientation $(0^\circ_{beam} / 90^\circ / 0^\circ)_{sym}$ (to scale)

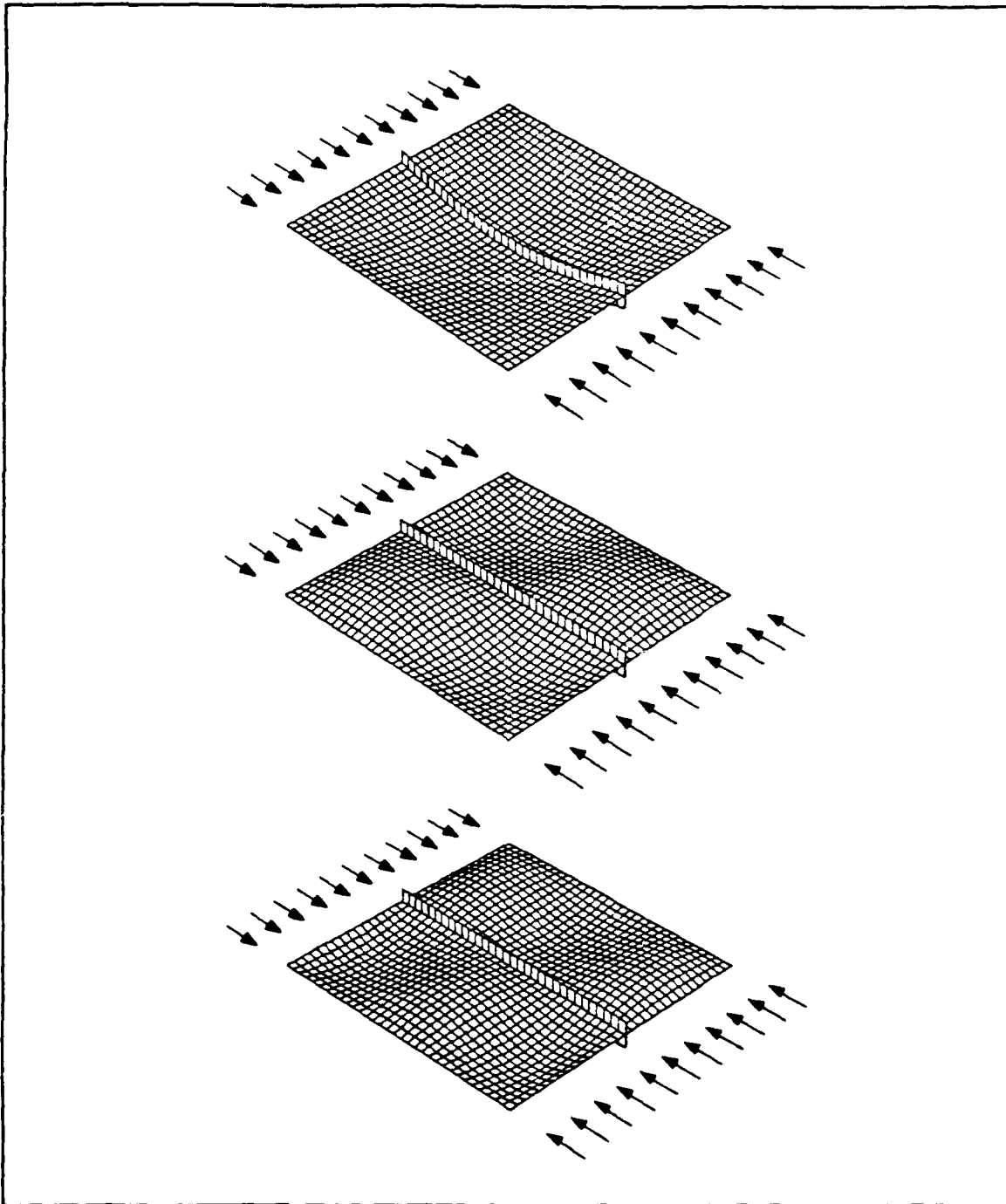


Figure 4. Buckling Shapes for Case 1 with $p = 0.0002646$: For Case 1, total volume $\Theta = 0.04$, with ply angle orientation of $(0^\circ_{\text{bottom}} / 90^\circ / 0^\circ)_{\text{sym}}$. Represented above are the buckling shapes of the simultaneous overall plate buckling modes.

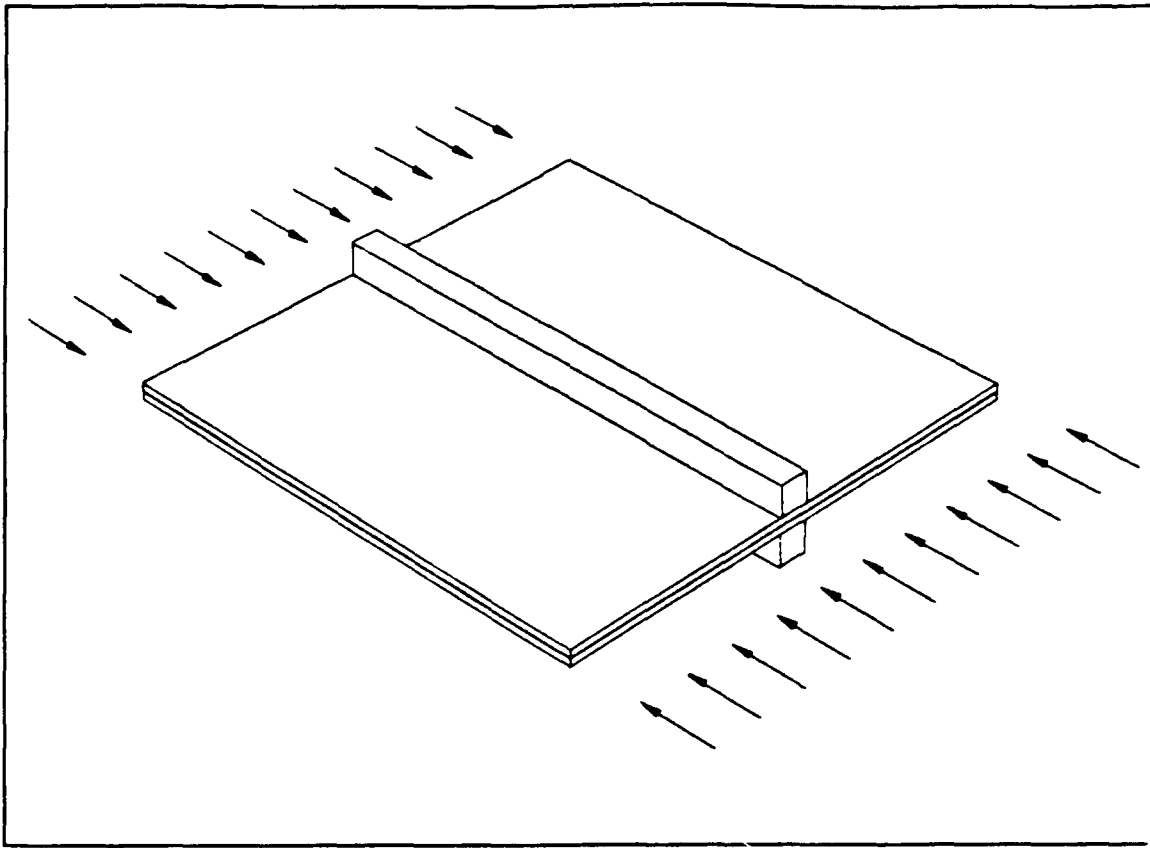


Figure 5. Geometry for Case 1 with $p = 0.0002822$: For Case 1, total volume $\Theta = 0.04$, with ply angle orientation $(0^\circ_{beam} / 90^\circ / 0^\circ)_{sym}$ (to scale)

Of the two optimum solutions found for Case 1, the global optimum occurs when modes 1, 2, and 4 are simultaneous. This is not the expected result in which all four buckling modes occur simultaneously. The increase in size of the stiffener for the global optimum result allows the τ_2 (0°) layer to decrease down to the lower limit. This causes the stiffener to be relatively rigid and the plate to be relatively weak in the loading direction. Therefore, for the global optimum case, a much greater portion of the load is carried by the stiffener.

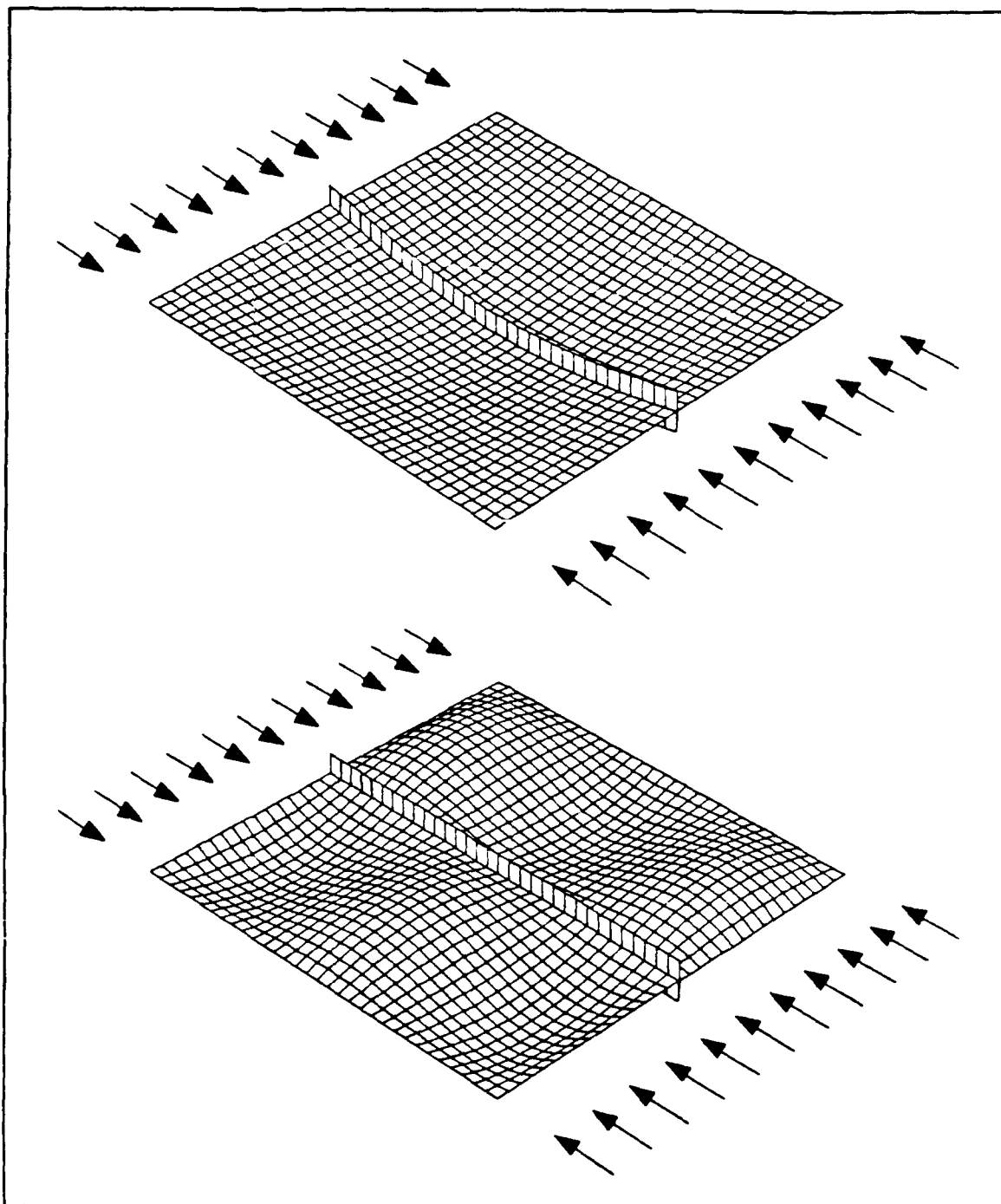


Figure 6. Buckling Shapes for Case 1 with $p = 0.0002822$: For Case 1, total volume $\Theta = 0.04$, with ply angle orientation of $(0^\circ_{beam}/90^\circ/0^\circ)_{sym}$. Represented above are the buckling shapes of the simultaneous overall plate buckling modes.

2. Case 2: $\Theta = 0.04$ and Ply Orientation $(0^\circ_{beam} / 0^\circ / 90^\circ)_{sym}$

For this configuration, only one optimum solution is identified. It is listed in Table 2 below. The same results are presented graphically in Figures 7 and 8. This turns out to be the best possible configuration of those tested. Note that here all four modes buckle simultaneously.

Table 2. RESULTS: $\Theta = 0.04$, PLY ANGLE $(0^\circ_{beam} / 0^\circ / 90^\circ)_{sym}$

t_1	t_2	b	h	p	Buckling Modes
0.00103	0.01385	0.06960	0.07350	0.0003949	1,2,3,4

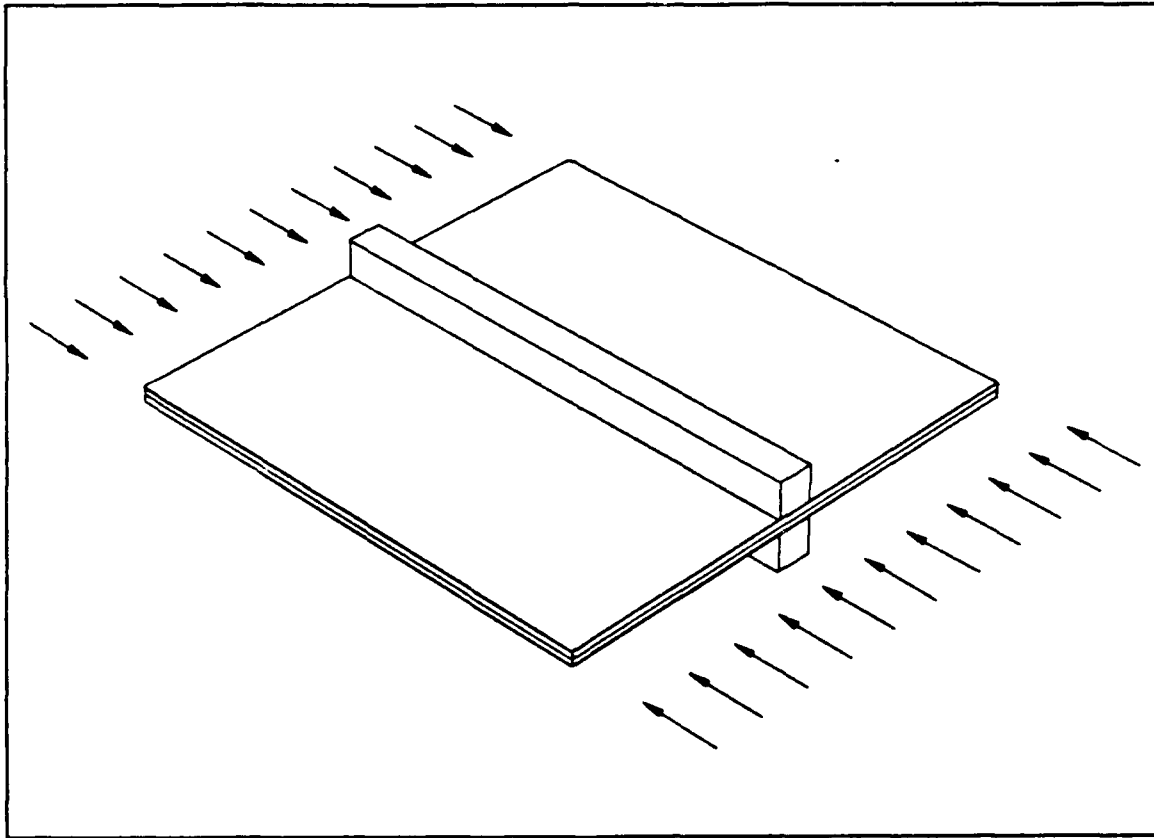


Figure 7. Geometry for Case 2 with $p = 0.0003949$: For Case 2, total volume $\Theta = 0.04$, with ply angle orientation $(0^\circ_{beam} / 0^\circ / 90^\circ)_{sym}$ (to scale)

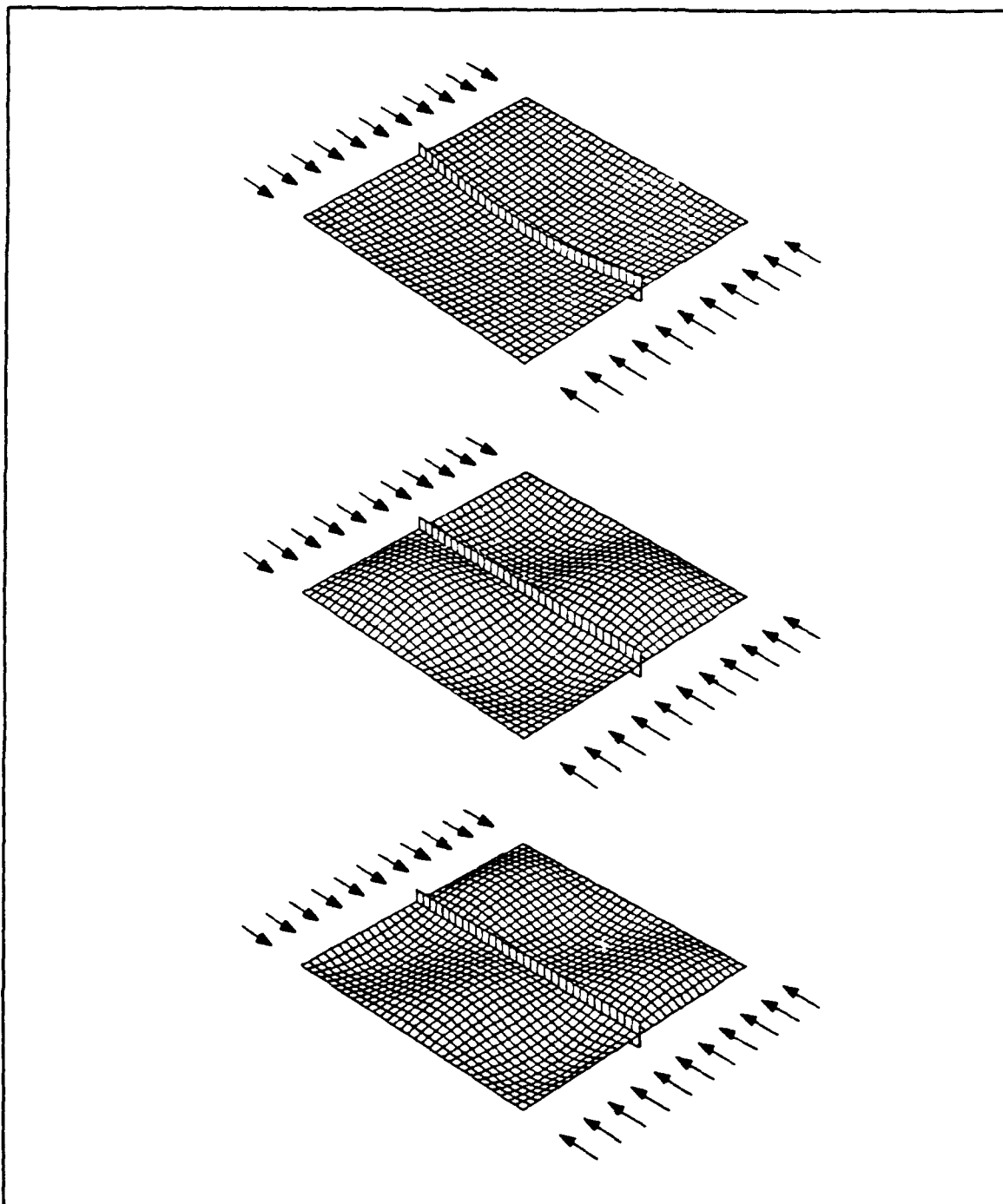


Figure 8. Buckling Shapes for Case 2 with $p = 0.0003949$: For Case 2, total volume $\Theta = 0.04$, with ply angle orientation of $(0^\circ_{\text{bottom}} / 0^\circ / 90^\circ)_{\text{sym}}$. Represented above are the buckling shapes of the simultaneous overall plate buckling modes.

3. Case 3: $\Theta = 0.04$ and Ply Orientation $(90^\circ_{beam} / 90^\circ / 0^\circ)_{sym}$

For this configuration, two different optimum solutions are identified. They are listed in Table 3 below. The same results are presented graphically in Figures 9-12.

Table 3. RESULTS: $\Theta = 0.04$, PLY ANGLE $(90^\circ_{beam} / 90^\circ / 0^\circ)_{sym}$

l_1	l_2	b	h	p	Buckling Modes
0.00100	0.01900	0.00100	0.00100	0.0000677	1
0.00100	0.01538	0.02354	0.15323	0.0001804	1,2,4

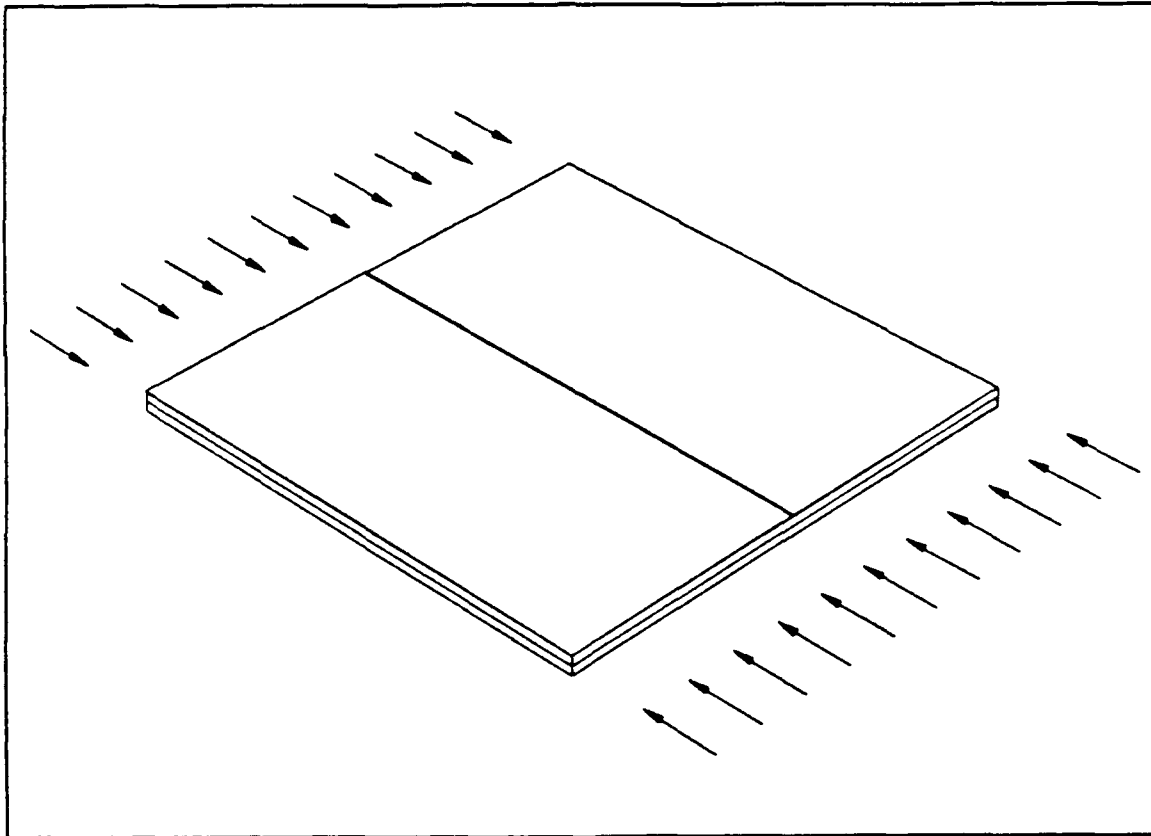


Figure 9. Geometry for Case 3 with $p = 0.0000677$: For Case 3, total volume $\Theta = 0.04$, with ply angle orientation $(90^\circ_{beam} / 90^\circ / 0^\circ)_{sym}$ (to scale)

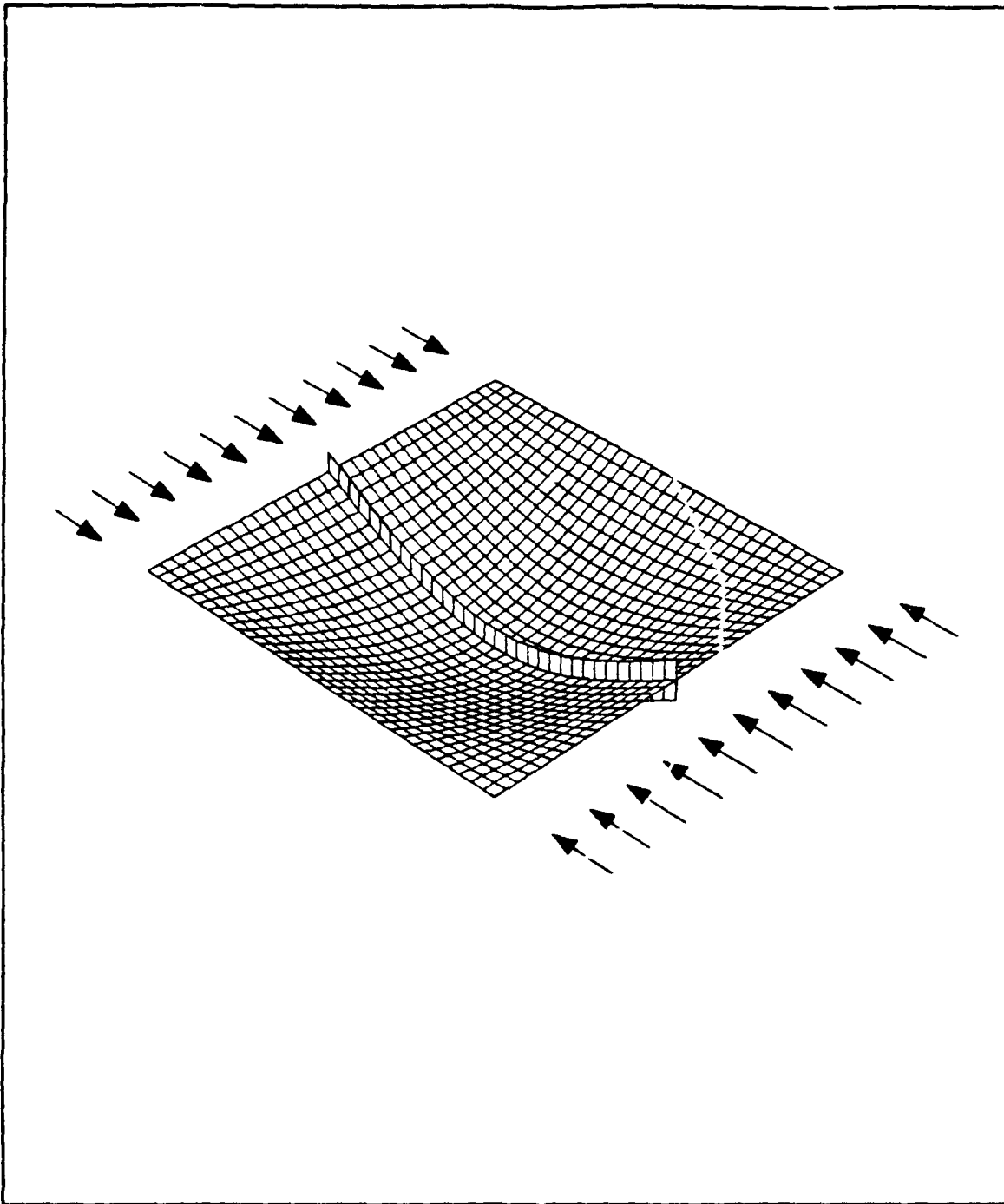


Figure 10. Buckling Shapes for Case 3 with $p = 0.0000677$: For Case 3, total volume $\Theta = 0.04$, with ply angle orientation of $(90^\circ_{\text{beam}} / 90^\circ / 0^\circ)_{\text{sym}}$. Represented above are the buckling shapes of the simultaneous overall plate buckling modes.

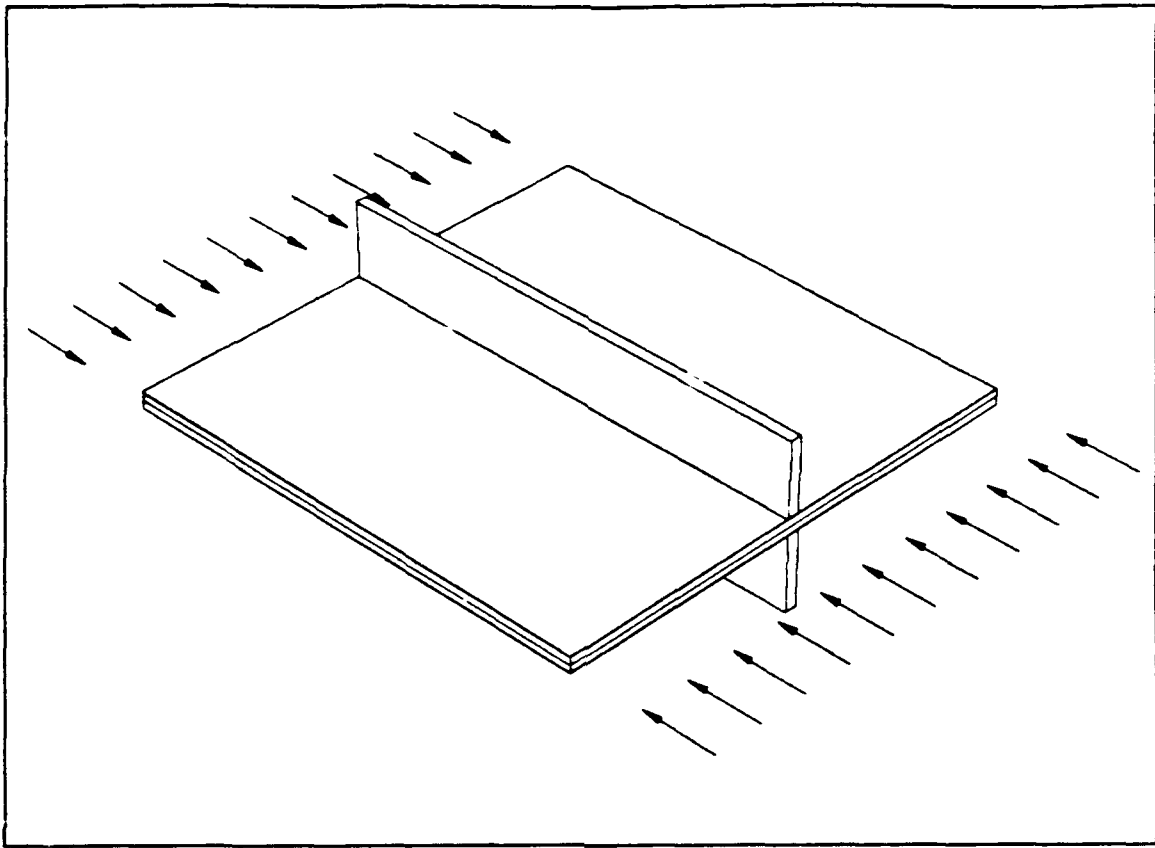


Figure 11. Geometry for Case 3 with $p = 0.0001804$: For Case 3, total volume $\Theta = 0.04$, with ply angle orientation $(90^\circ_{beam} / 90^\circ / 0^\circ)_{sym}$ (to scale)

Of the two optima found, the global optimum occurs when three buckling modes occur simultaneously. No optimum was located that gave simultaneous buckling with all four modes. For this case, the stiffener fibers are in the 90° orientation so the stiffener adds much less strength to the plate than when the stiffener fibers are in the 0° orientation. Thus more of the total volume must be placed into the t_2 (0°) lamina. Because of the volume of material in the t_2 lamina and the stiffener, there is an insufficient volume of material to allow the t_1 (90°) lamina to increase from the lower limit. Because of this, it is impossible to obtain simultaneous buckling with all four modes.

For the local optima case where $p = 0.0000677$, the stiffened plate is trying to reduce itself down to a single lamina with 0° fiber orientation. From this configuration, any incremental increase in the stiffener size causes a decrease in buckling load. By ini-

tially increasing the stiffener size, the load share carried by the stiffener, p_s , increases with the increase in the cross sectional area, s_s . The initial increase in p_s is greater than the increase in stiffness caused by the increase in s_s , therefore, the buckling load initially decreases creating the local optimum.

24.

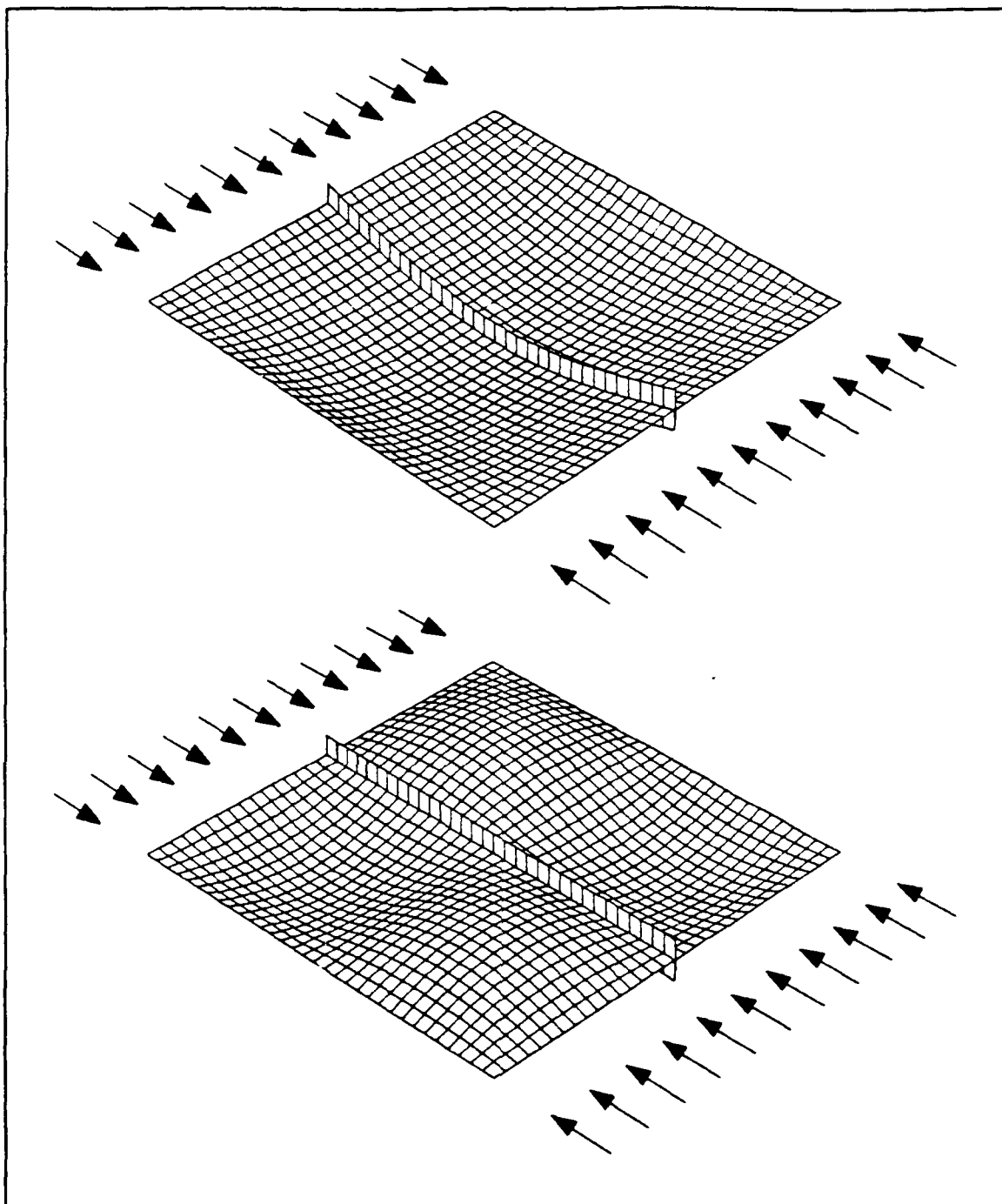


Figure 12. Buckling Shapes for Case 3 with $p = 0.0001804$: For Case 3, total volume $\Theta = 0.04$, with ply angle orientation of $(90^\circ_{beam} / 90^\circ / 0^\circ)_{sym}$. Represented above are the buckling shapes of the simultaneous overall plate buckling modes.

4. Case 4: $\Theta = 0.04$ and Ply Orientation $(90^\circ_{beam} / 0^\circ / 90^\circ)_{sym}$

For this configuration, three different optimum solutions are identified. They are listed in Table 4 below. The same results are presented graphically in Figures 13-18.

Table 4. RESULTS: $\Theta = 0.04$, PLY ANGLE $(90^\circ_{beam} / 0^\circ / 90^\circ)_{sym}$

t_1	t_2	b	h	p	Buckling Modes
0.01900	0.00100	0.00100	0.00100	0.0000677	1
0.01636	0.00100	0.01845	0.14210	0.0001345	1,2,4
0.00778	0.00816	0.02830	0.14310	0.0001702	1,2,3,4

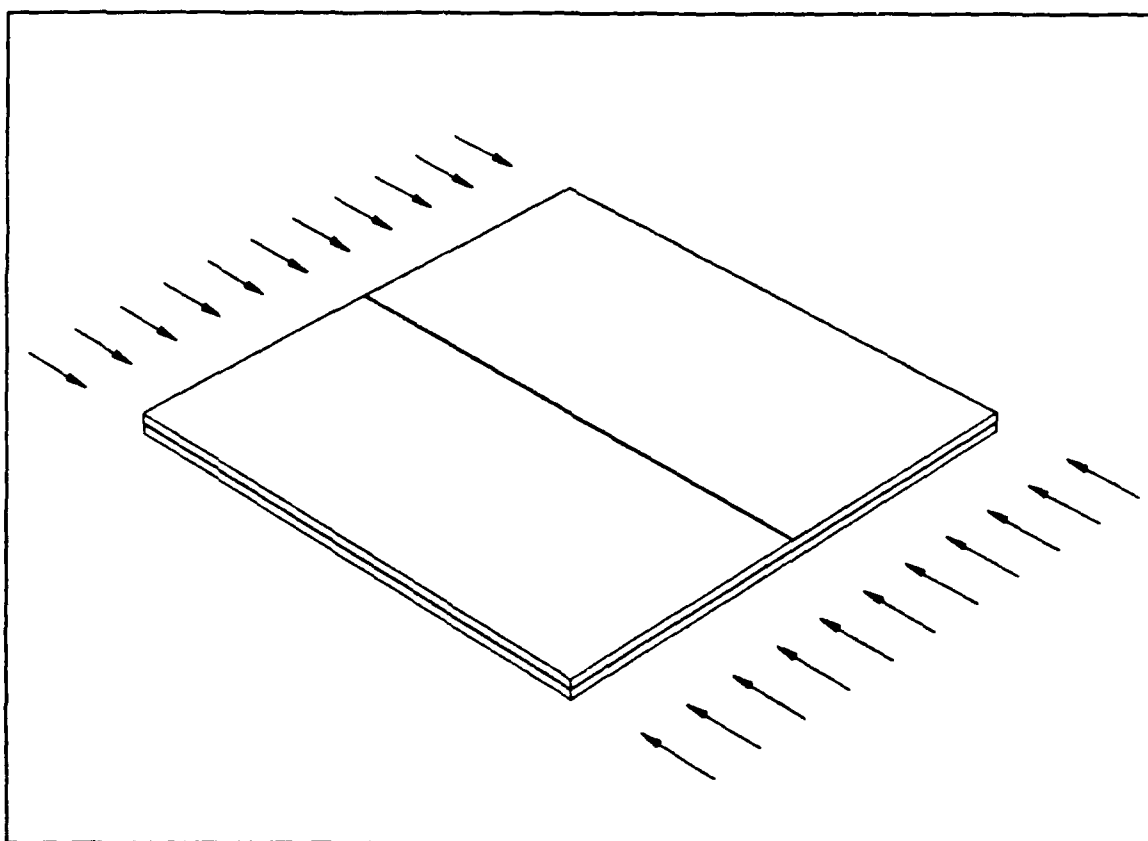


Figure 13. Geometry for Case 4 with $p = 0.0000677$: For Case 4, total volume $\Theta = 0.04$, with ply angle orientation $(90^\circ_{beam} / 0^\circ / 90^\circ)_{sym}$ (to scale)

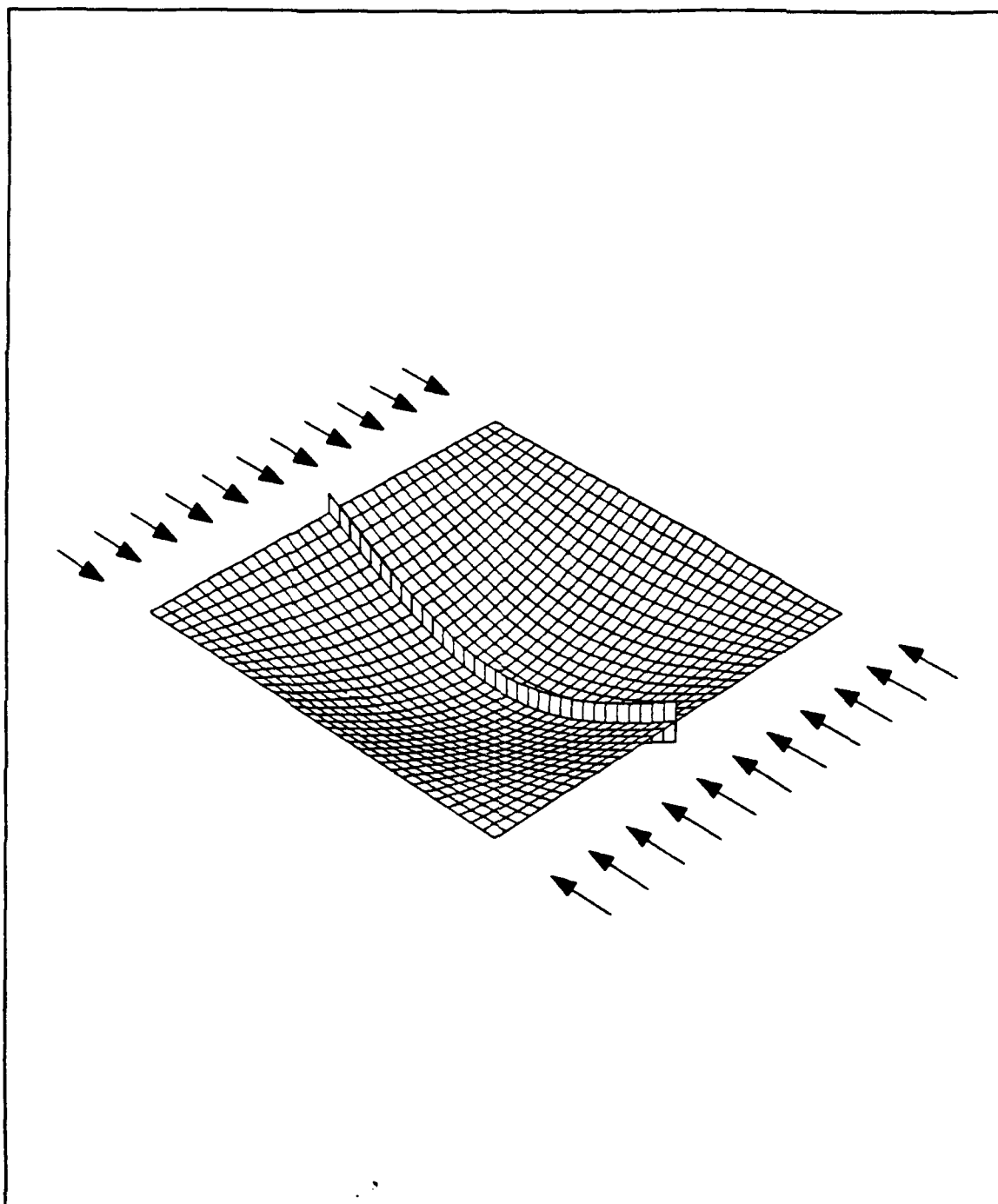


Figure 14. Buckling Shapes for Case 4 with $p = 0.0000677$: For Case 4, total volume $\Theta = 0.04$, with ply angle orientation of $(90^\circ_{beam} / 0^\circ / 90^\circ)_{sym}$. Represented above are the buckling shapes of the simultaneous overall plate buckling modes.

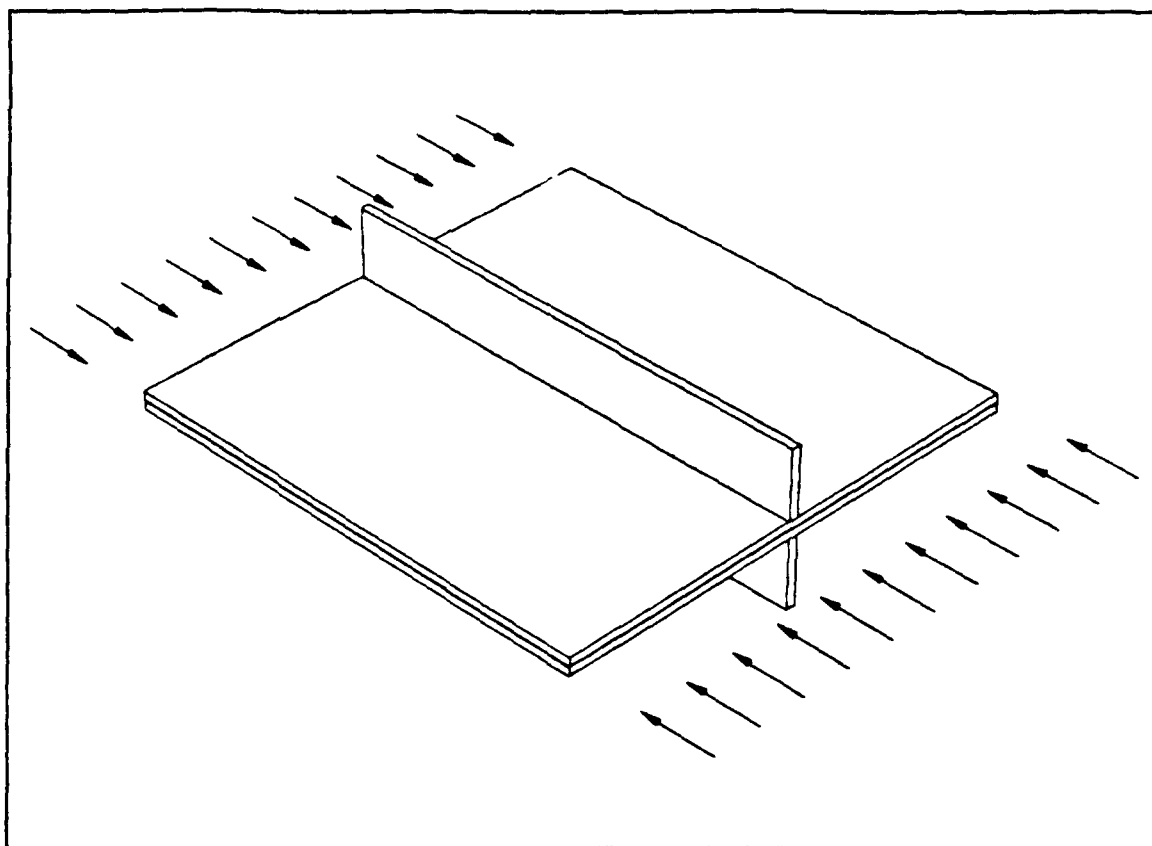


Figure 15. Geometry for Case 4 with $p = 0.0001345$: For Case 4, total volume $\Theta = 0.04$, with ply angle orientation $(90^\circ_{beam} / 0^\circ / 90^\circ)_{sym}$ (to scale)

For this case, the global optimum occurs when all four buckling modes occur simultaneously. However, this global optimum is less than the global optimum of Case 3. It appears as though the inner lamina (t_2) is the preferred location for the 0° fibers.

The configuration which gives $p = 0.0001345$ corresponds closely to the Case 3 global optimum. The only difference is that more 0° fiber orientation volume is required when it is located at the outer layer (t_1). The local optimum, $p = 0.0000677$, corresponds exactly to the Case 3 local optimum with the same load value. Here the same reasons apply for the existence of this local optimum.

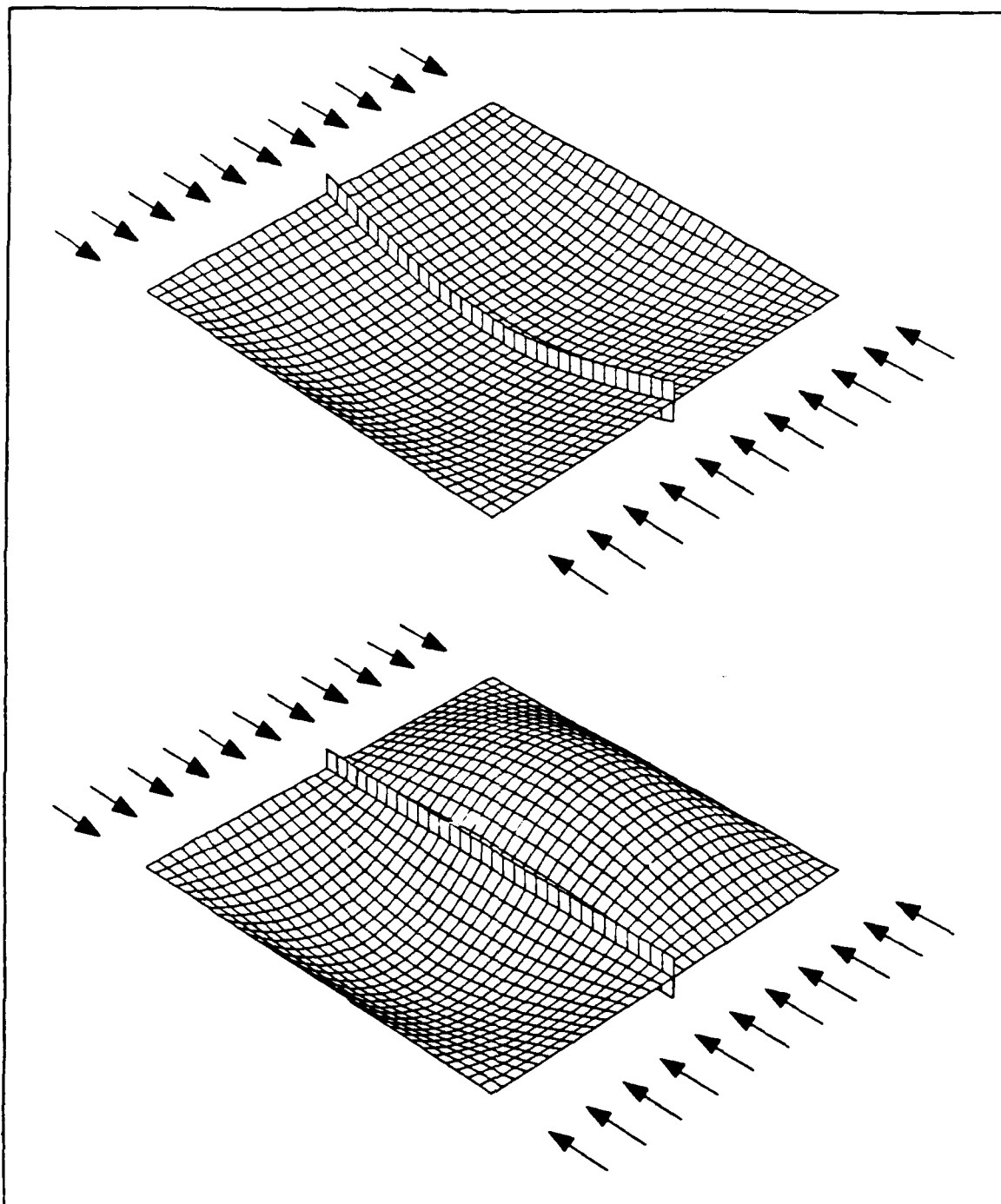


Figure 16. Buckling Shapes for Case 4 with $p = 0.0001345$: For Case 4, total volume $\Theta = 0.04$, with ply angle orientation of $(90^\circ_{beam} / 0^\circ / 90^\circ)_{sym}$. Represented above are the buckling shapes of the simultaneous overall plate buckling modes.

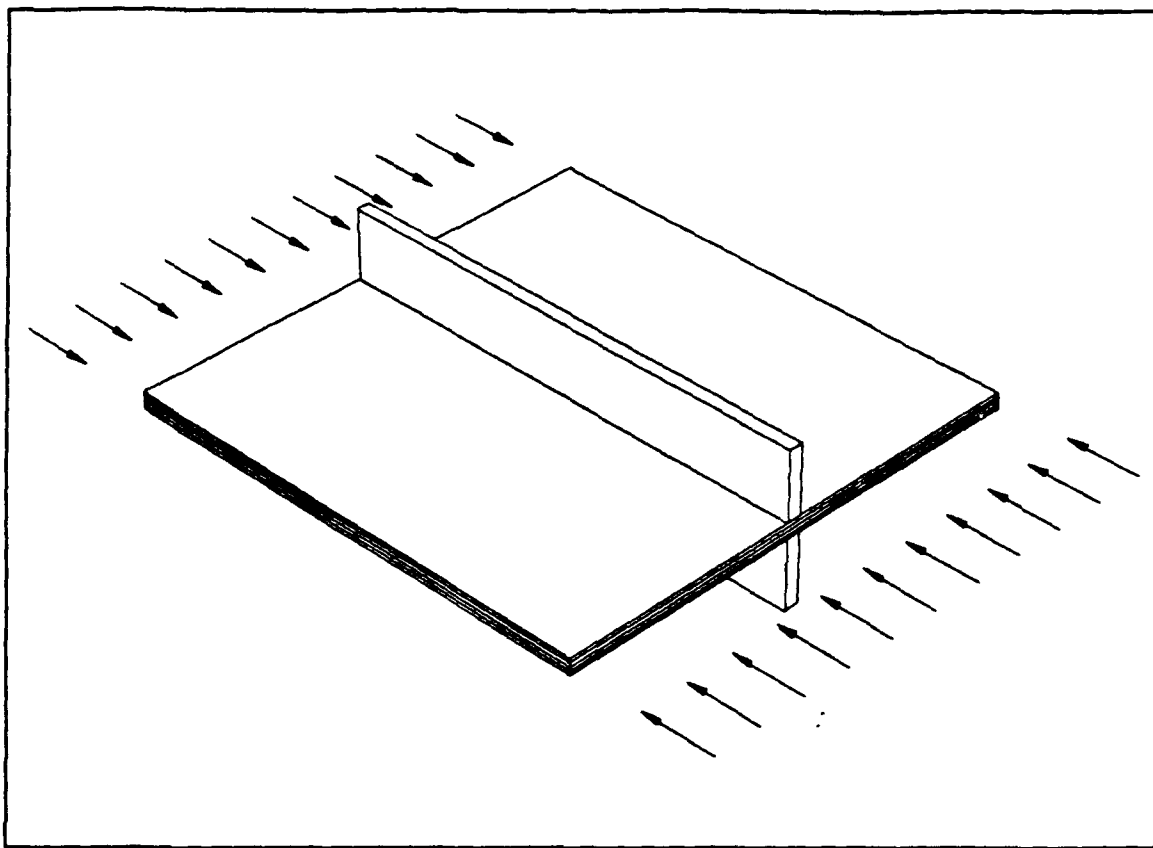


Figure 17. Geometry for Case 4 with $p = 0.0001702$: For Case 4, total volume $\Theta = 0.04$, with ply angle orientation $(90^\circ_{beam} / 0^\circ / 90^\circ)_{sym}$ (to scale)

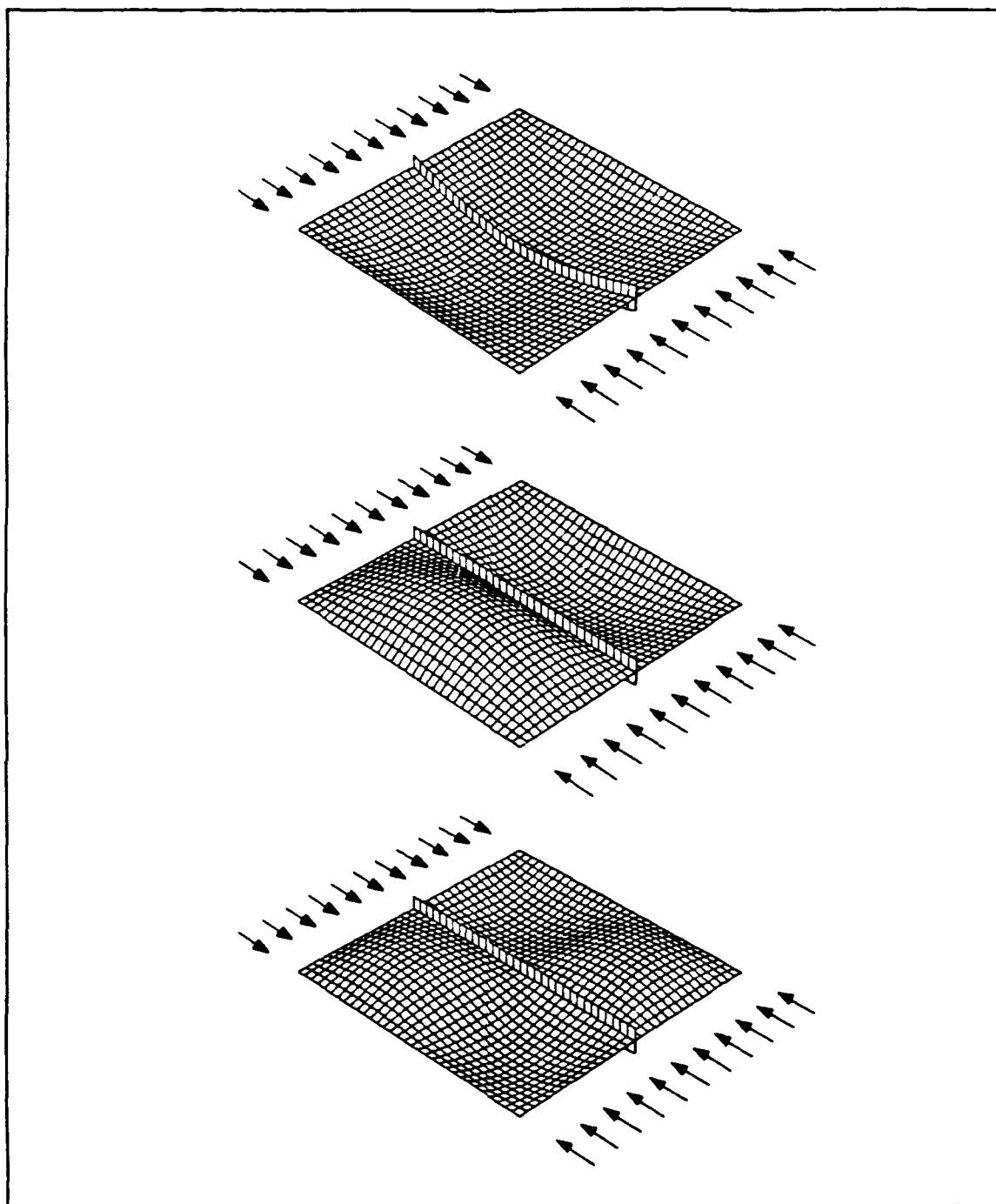


Figure 18. Buckling Shapes for Case 4 with $p = 0.0001702$: For Case 4, total volume $\Theta = 0.04$, with ply angle orientation of $(90^\circ_{beam}/0^\circ/90^\circ)_{sym}$. Represented above are the buckling shapes of the simultaneous overall plate buckling modes.

5. Case 5: $\Theta = 0.015$ and Ply Orientation $(0^\circ_{beam} / 90^\circ / 0^\circ)_{sym}$

For this configuration, two optimum solutions are identified. They are listed in Table 5 below. The same results are presented graphically in Figures 19-22.

Table 5. RESULTS: $\Theta = 0.015$, PLY ANGLE $(0^\circ_{beam} / 90^\circ / 0^\circ)_{sym}$

t_1	t_2	b	h	p	Buckling Modes
0.00298	0.00411	0.01008	0.04029	0.0000156	1,2,3,4
0.00576	0.00100	0.02720	0.02720	0.0000124	1

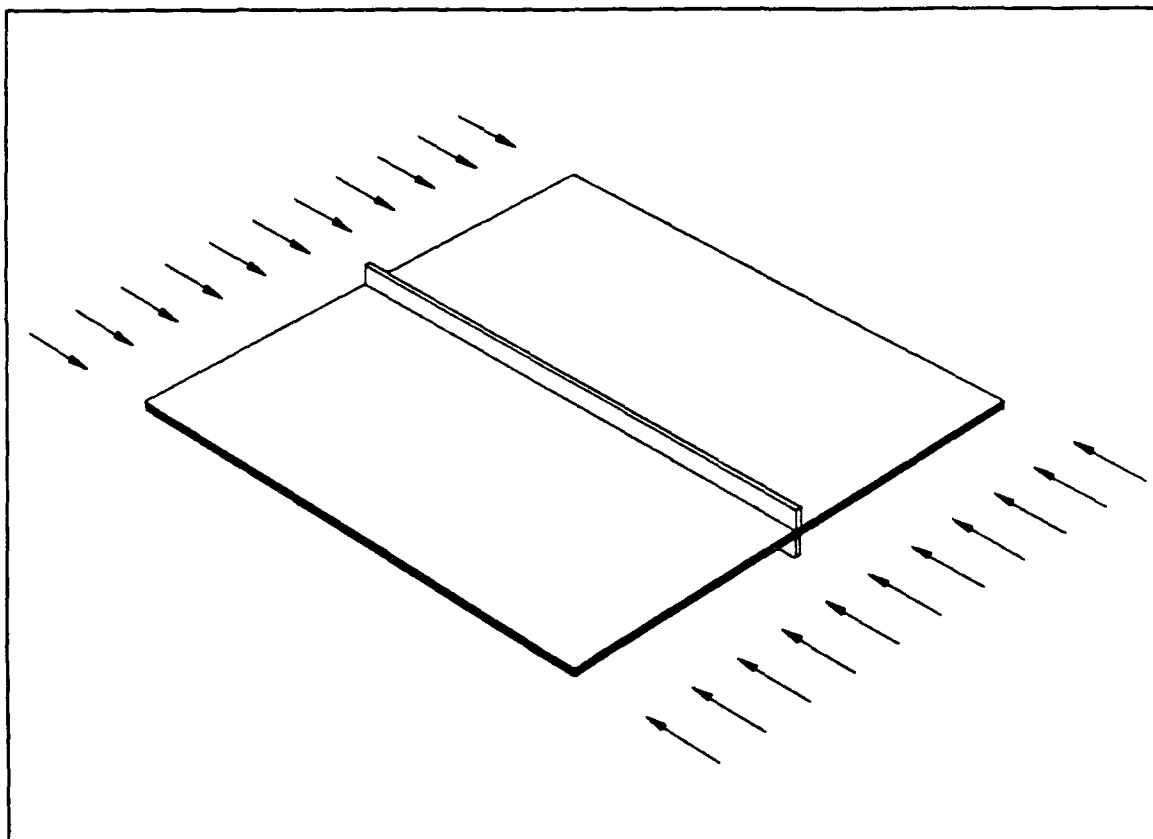


Figure 19. Geometry for Case 5 with $p = 0.0000156$: For Case 5, total volume $\Theta = 0.015$, with ply angle orientation $(0^\circ_{beam} / 90^\circ / 0^\circ)_{sym}$ (to scale)

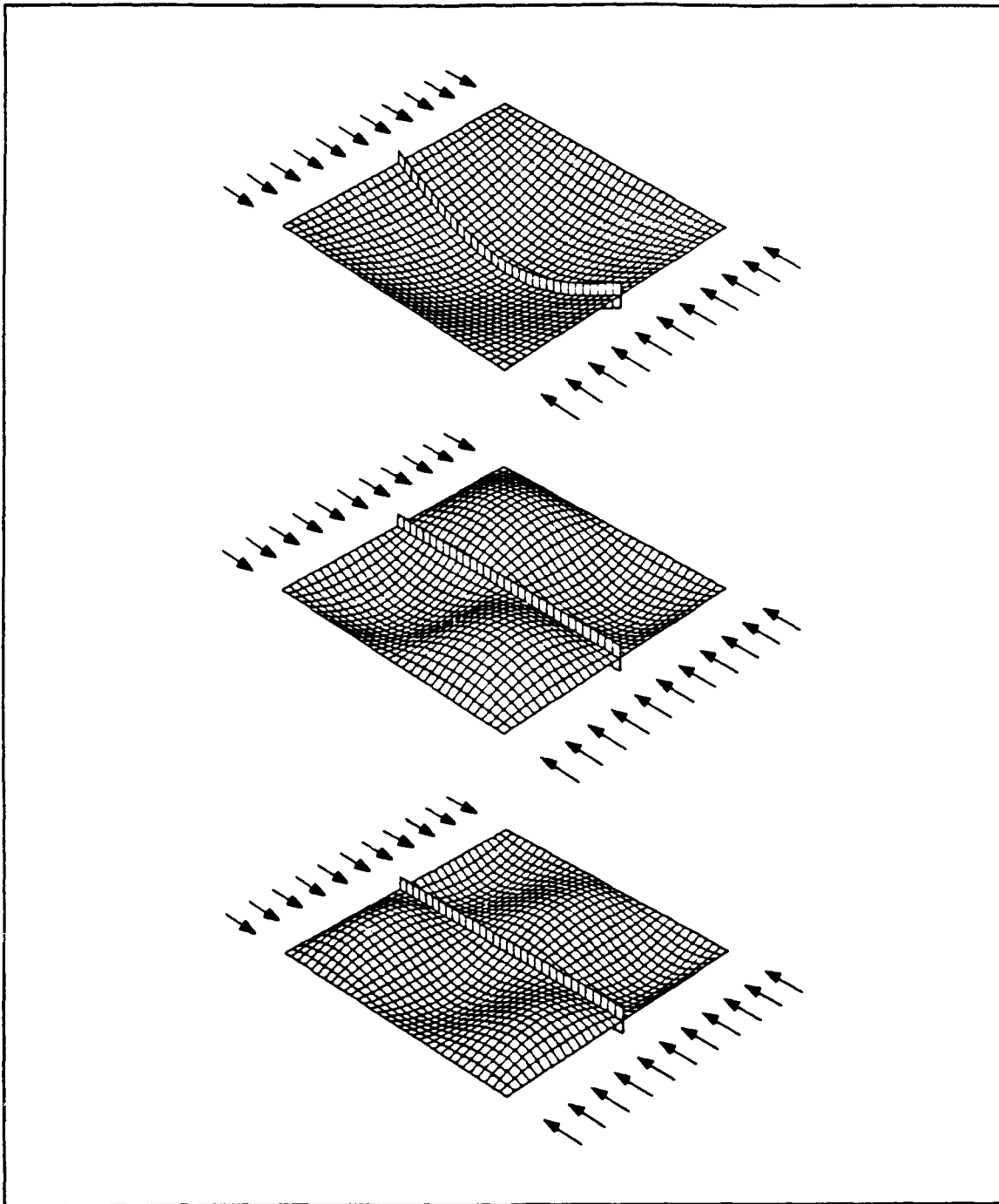


Figure 20. Buckling Shapes for Case 5 with $p = 0.0000156$: For Case 5, total volume $\Theta = 0.015$, with ply angle orientation of $(0^\circ_{beam}/90^\circ/0^\circ)_{sym}$. Represented above are the buckling shapes of the simultaneous overall plate buckling modes.

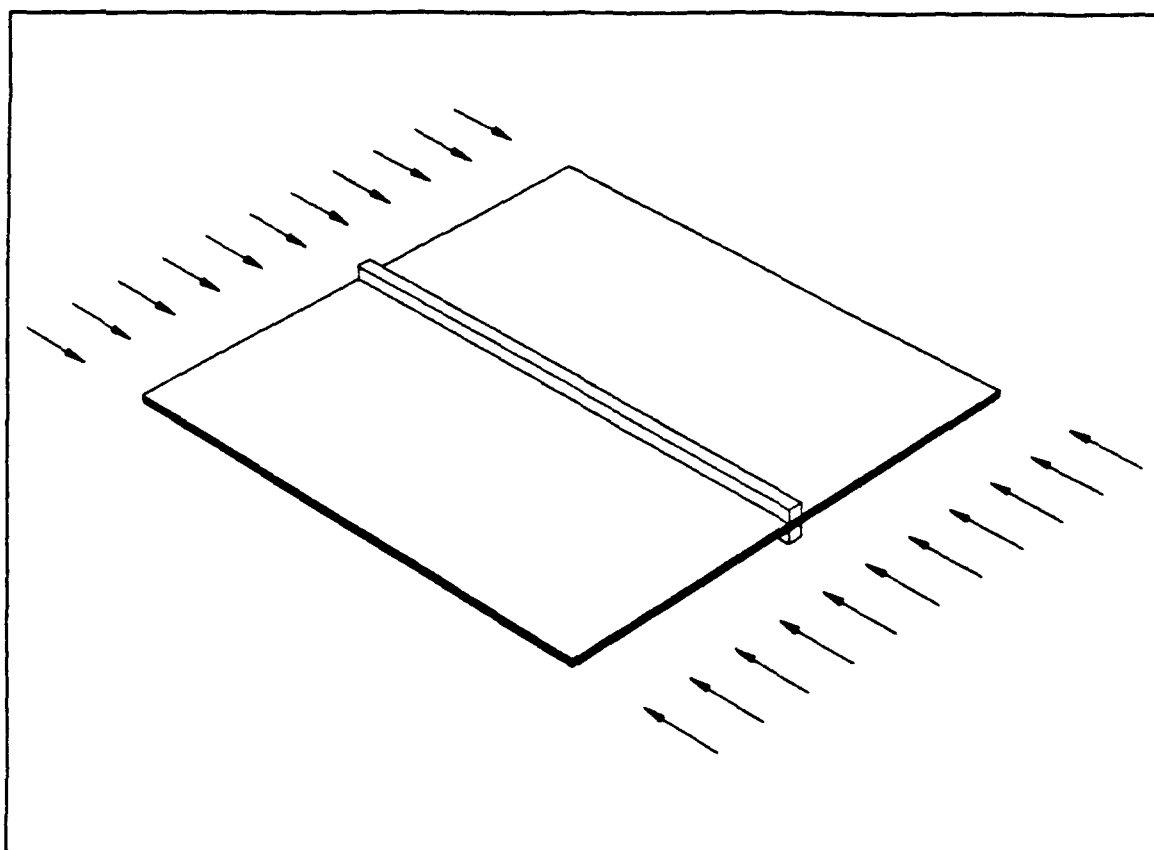


Figure 21. Geometry for Case 5 with $p = 0.0000124$: For Case 5, total volume $\Theta = 0.015$, with ply angle orientation $(0^\circ_{beam} / 90^\circ / 0^\circ)_{sym}$ (to scale)

Here the global optimum is found when the four buckling modes occur simultaneously. This global optimum corresponds to the global optimum found in Case 1. This follows since Case 5 is the same as Case 1, except for the smaller volume of material available. The local optimum found with $p = 0.0000124$ is not a uniquely determined solution. The total stiffener volume is uniquely defined but not the individual dimensions of the stiffener height and width. This occurs because the first buckling mode (the only active mode in this case) does not cause any flexure of the stiffener. The active buckling shape only twists the stiffener so that only its volume and not its cross sectional shape is important to the overall buckling stiffness.

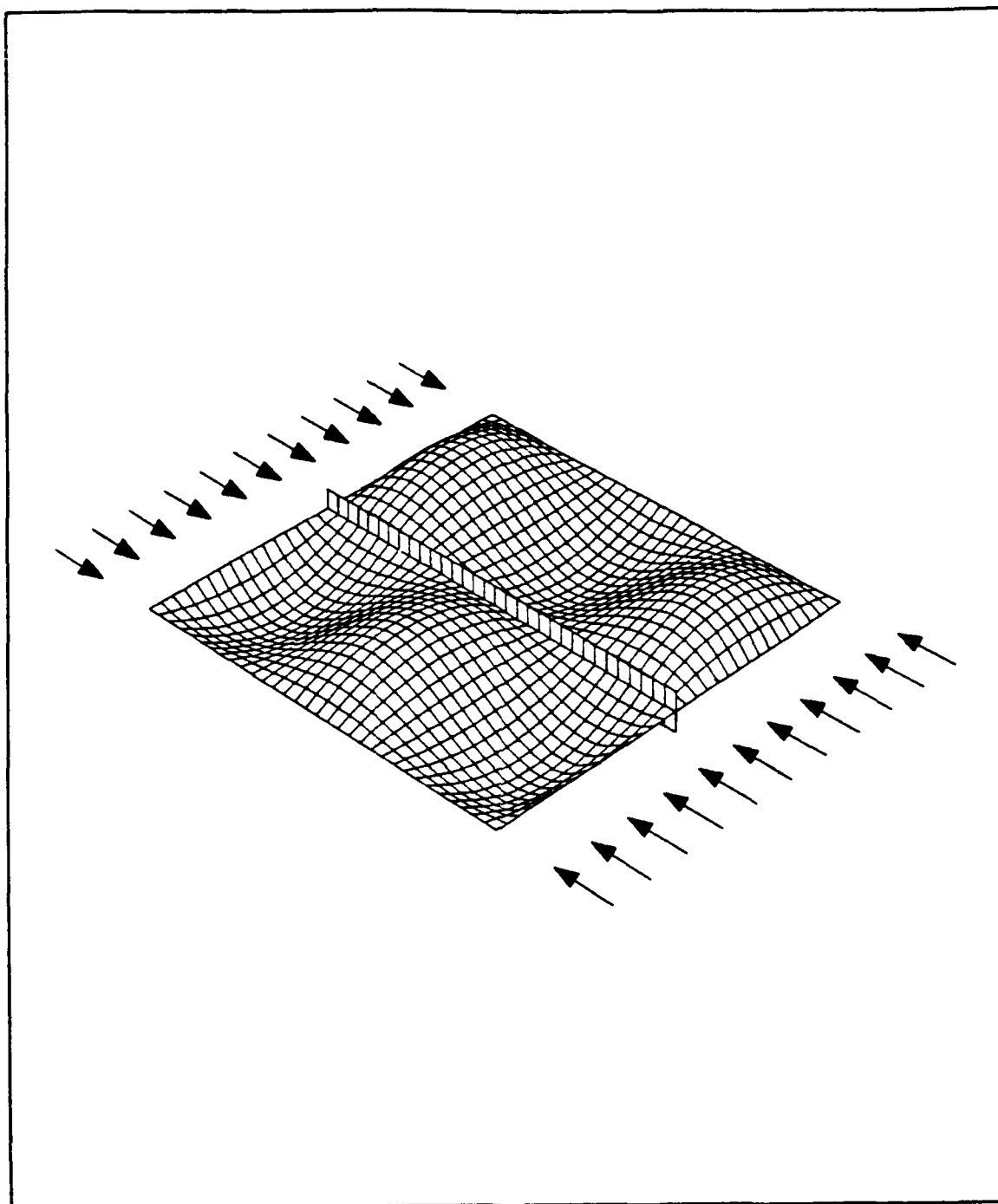


Figure 22. Buckling Shapes for Case 5 with $p = 0.0000124$: For Case 5, total volume $\Theta = 0.015$, with ply angle orientation of $(0^\circ_{beam}/90^\circ/0^\circ)_{sym}$. Represented above are the buckling shapes of the simultaneous overall plate buckling modes.

6. Case 6: $\Theta = 0.015$ and Ply Orientation $(0^\circ_{\text{beam}} / 0^\circ / 90^\circ)_{\text{sym}}$

For this configuration, only one optimum solution is identified. It is listed in Table 6 below. The same results are presented graphically in Figures 23-24. This case is similar to Case 2 except here there is insufficient material available to produce simultaneous buckling of all four modes.

Table 6. RESULTS: $\Theta = 0.015$, PLY ANGLE $(0^\circ_{\text{beam}} / 0^\circ / 90^\circ)_{\text{sym}}$

t_1	t_2	b	h	p	Buckling Modes
0.00100	0.00577	0.01814	0.03986	0.0000179	1

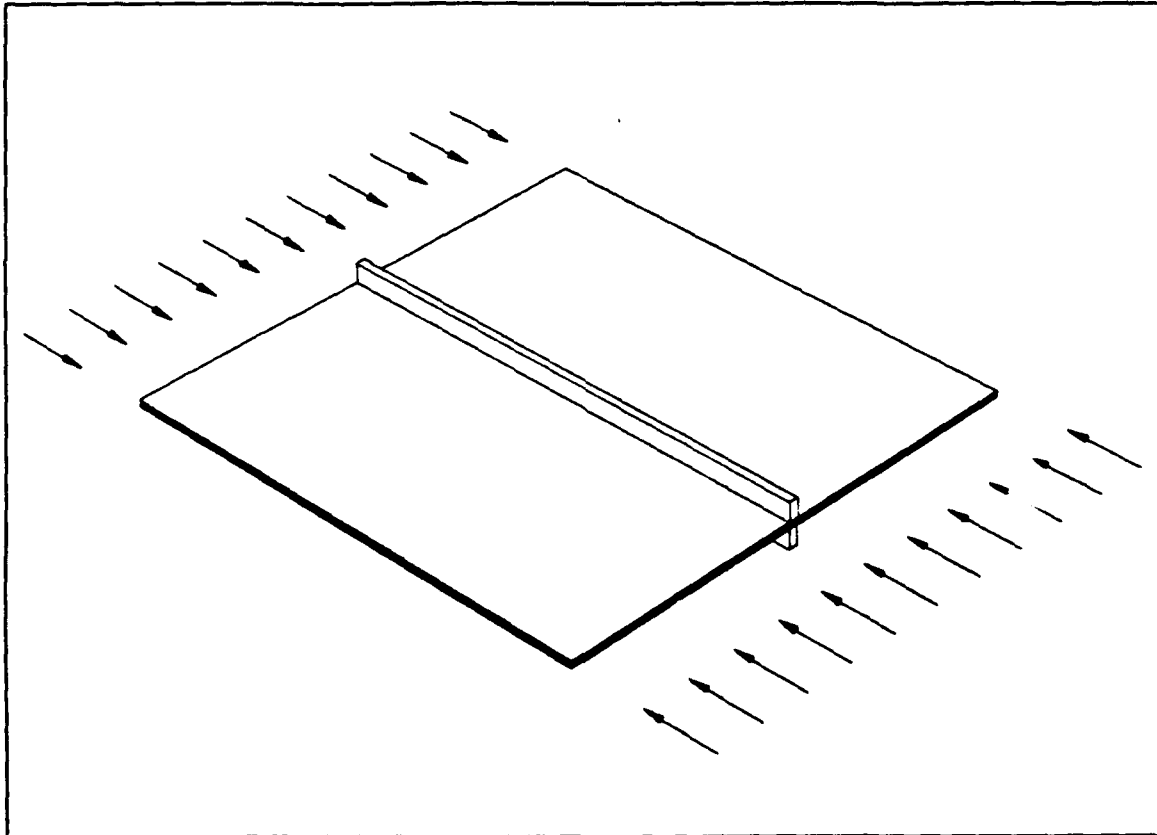


Figure 23. Geometry for Case 6 with $p = 0.0000179$: For Case 6, total volume $\Theta = 0.015$, with ply angle orientation $(0^\circ_{\text{beam}} / 0^\circ / 90^\circ)_{\text{sym}}$ (to scale)

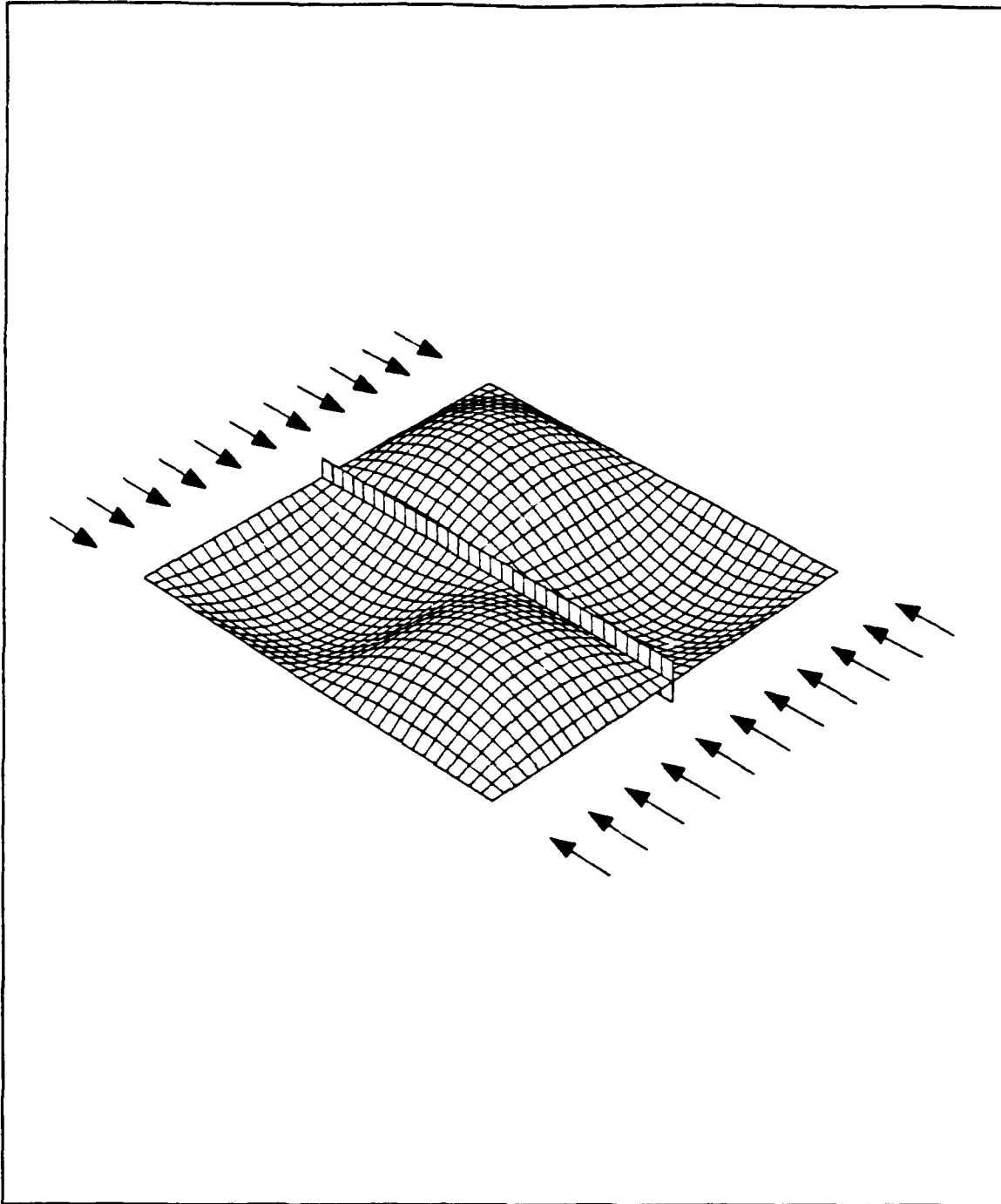


Figure 24. Buckling Shapes for Case 6 with $p = 0.0000179$: For Case 6, total volume $\Theta = 0.015$, with ply angle orientation of $(0^\circ_{beam} / 0^\circ / 90^\circ)_{sym}$. Represented above are the buckling shapes of the simultaneous overall plate buckling modes.

7. Case 7: $\Theta = 0.015$ and Ply Orientation $(90^\circ_{beam} / 90^\circ / 0^\circ)_{sym}$

For this configuration, two different optimum solutions are identified. They are listed in Table 7 below. The same results are presented graphically in Figures 25-28.

Table 7. RESULTS: $\Theta = 0.015$, PLY ANGLE $(90^\circ_{beam} / 90^\circ / 0^\circ)_{sym}$

t_1	t_2	b	h	p	Buckling Modes
0.00100	0.00650	0.00100	0.00100	0.0000036	1
0.00100	0.00584	0.00669	0.09761	0.0000130	1,2,4

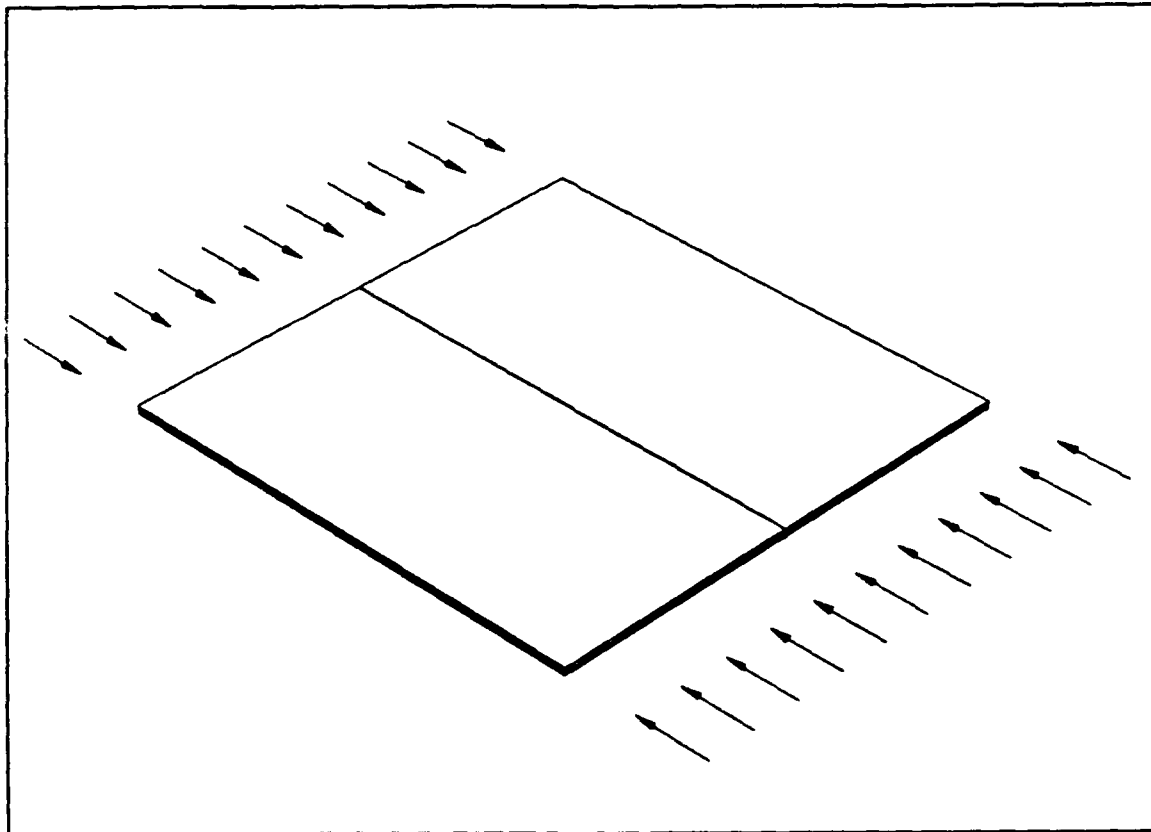


Figure 25. Geometry for Case 7 with $p = 0.0000036$: For Case 7, total volume $\Theta = 0.015$, with ply angle orientation $(90^\circ_{beam} / 90^\circ / 0^\circ)_{sym}$ (to scale)

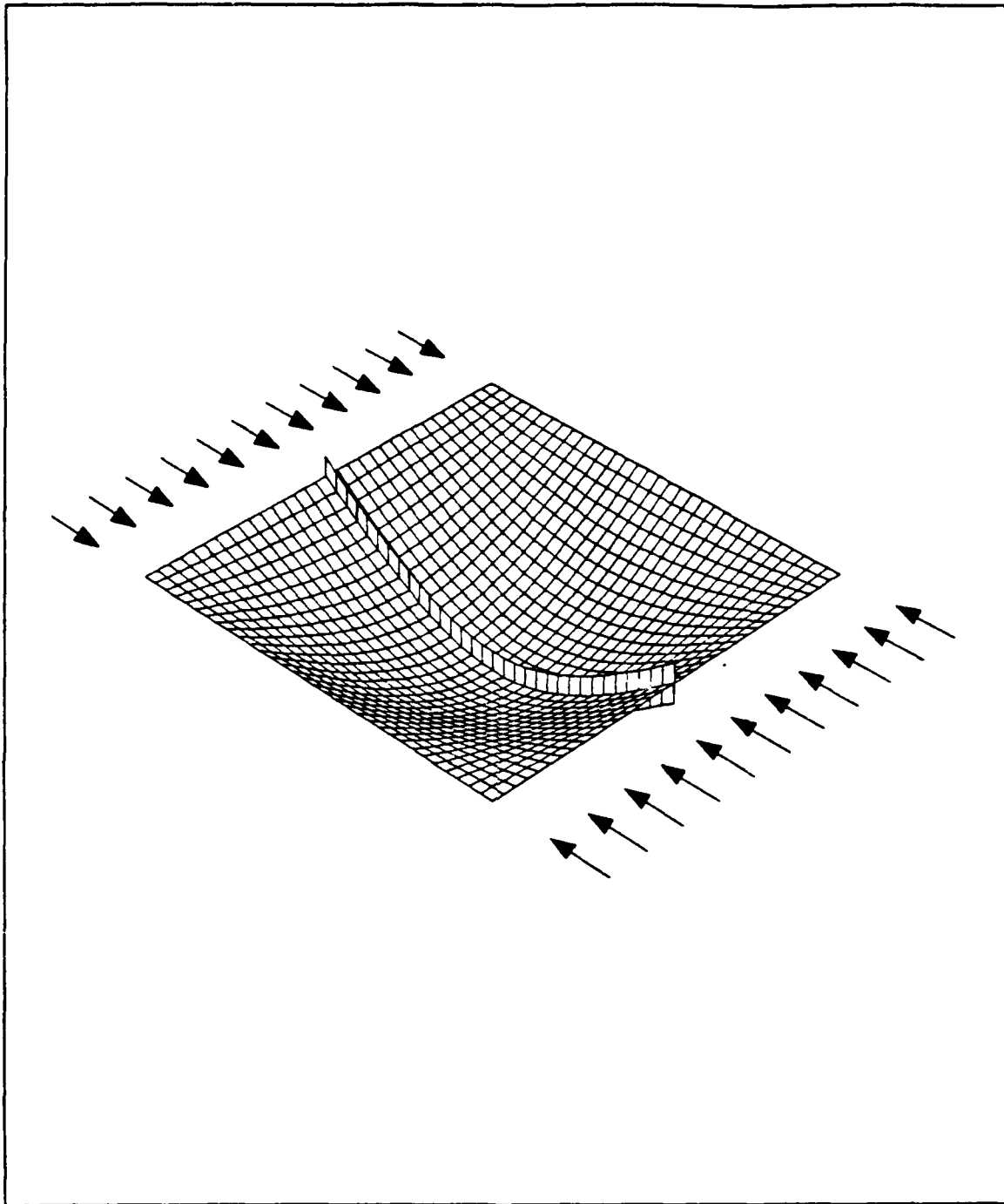


Figure 26. Buckling Shapes for Case 7 with $p = 0.0000036$: For Case 7, total volume $\Theta = 0.015$, with ply angle orientation of $(90^\circ_{beam} / 90^\circ / 0^\circ)_{sym}$. Represented above are the buckling shapes of the simultaneous overall plate buckling modes.

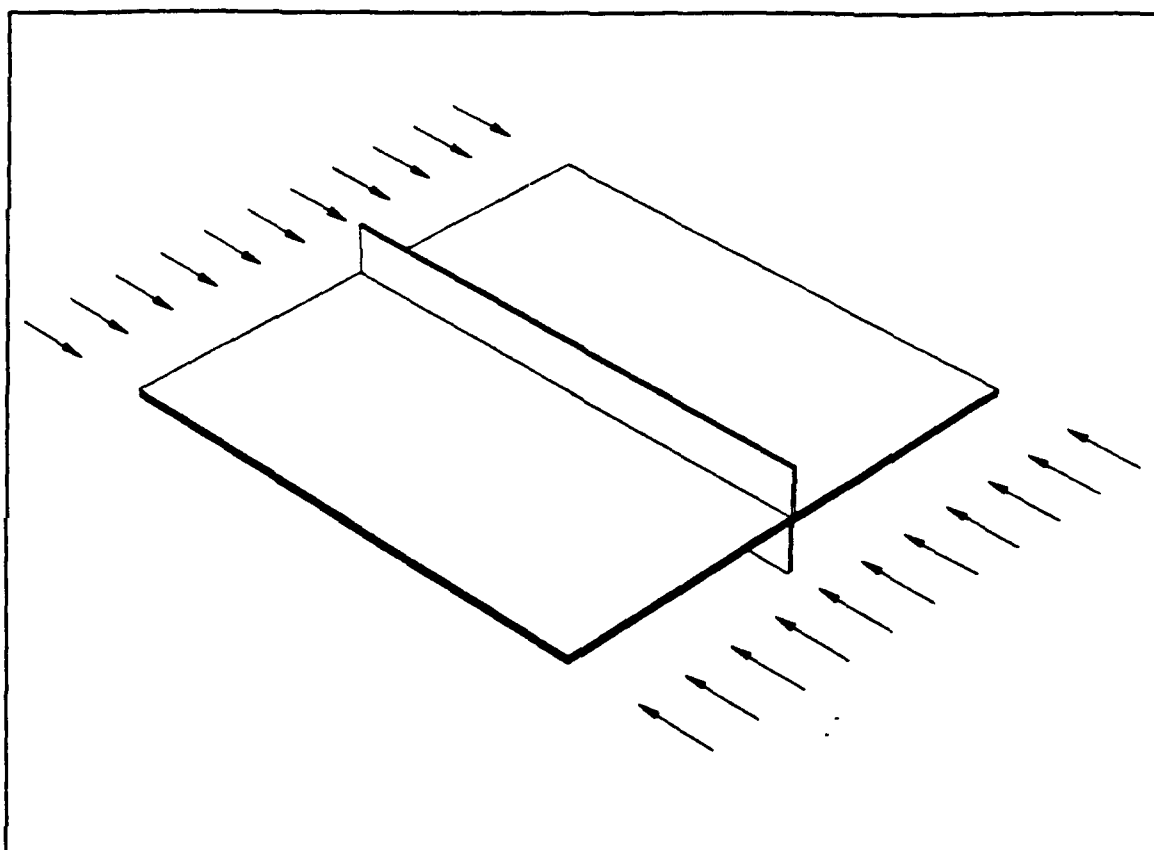


Figure 27. Geometry for Case 7 with $p = 0.0000130$: For Case 7, total volume $\Theta = 0.015$, with ply angle orientation $(90^\circ_{beam} / 90^\circ / 0^\circ)_{sym}$ (to scale)

The optima of Case 7 are closely related to the optima of Case 3. The only difference in the two cases is the total volume of material available. Here the same relative magnitude between the two different optima are present with the global optima again being the configuration with three buckling modes occurring simultaneously. As in Case 3, here too, there is insufficient material available to obtain the case where all four buckling modes occur simultaneously.

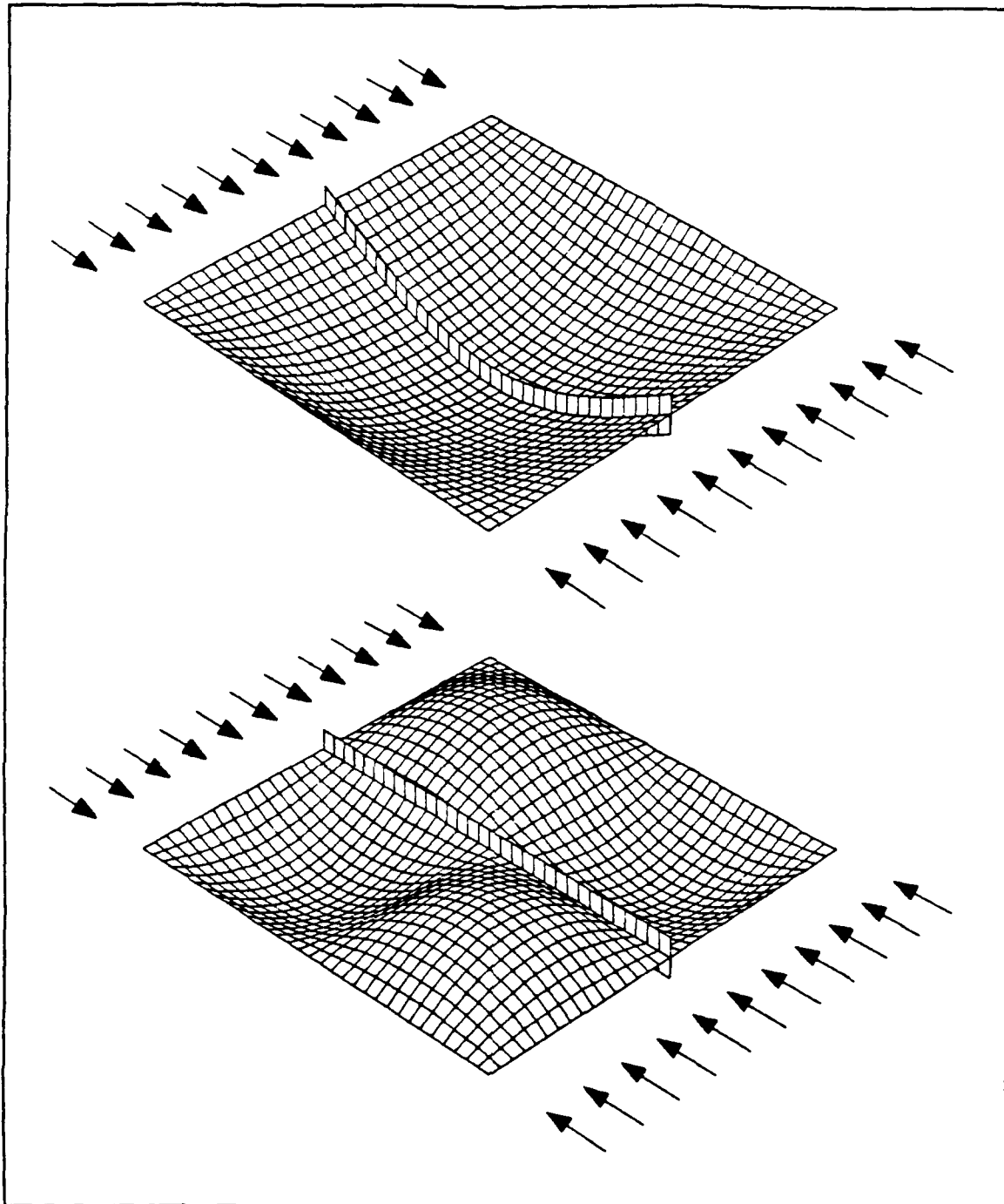


Figure 28. Buckling Shapes for Case 7 with $p = 0.0000130$: For Case 7, total volume $\Theta = 0.015$, with ply angle orientation of $(90^\circ_{beam} / 90^\circ / 0^\circ)_{sym}$. Represented above are the buckling shapes of the simultaneous overall plate buckling modes.

8. Case 8: $\Theta = 0.015$ and Ply Orientation $(90^\circ_{beam} / 0^\circ / 90^\circ)_{sym}$

For this configuration, two different optimum solutions are identified. They are listed in Table 8 below. The same results are presented graphically in Figures 29-32.

Table 8. RESULTS: $\Theta = 0.015$, PLY ANGLE $(90^\circ_{beam} / 0^\circ / 90^\circ)_{sym}$

t_1	t_2	b	h	p	Buckling Modes
0.00650	0.00100	0.00100	0.00100	0.0000036	1
0.00329	0.00345	0.00802	0.09386	0.0000125	1,2,3,4

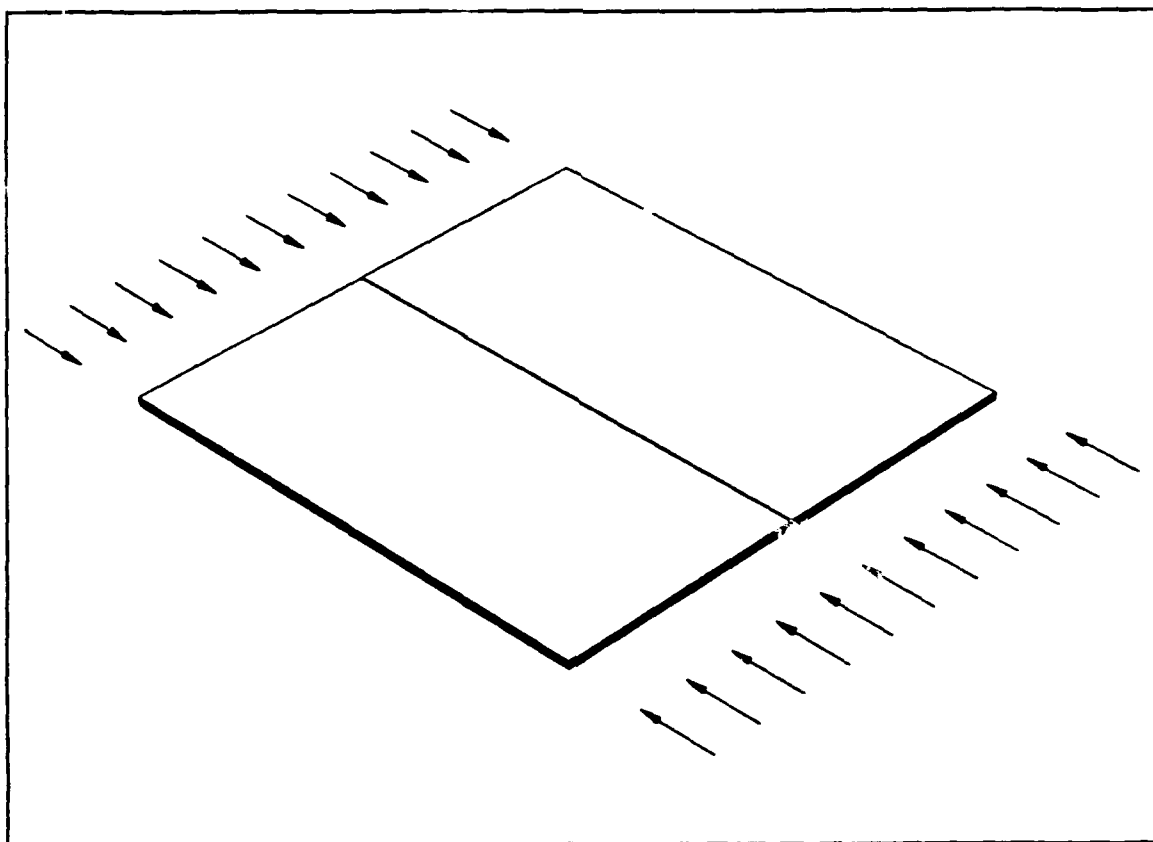


Figure 29. Geometry for Case 8 with $p = 0.0000036$: For Case 8, total volume $\Theta = 0.015$, with ply angle orientation $(90^\circ_{beam} / 0^\circ / 90^\circ)_{sym}$ (to scale)

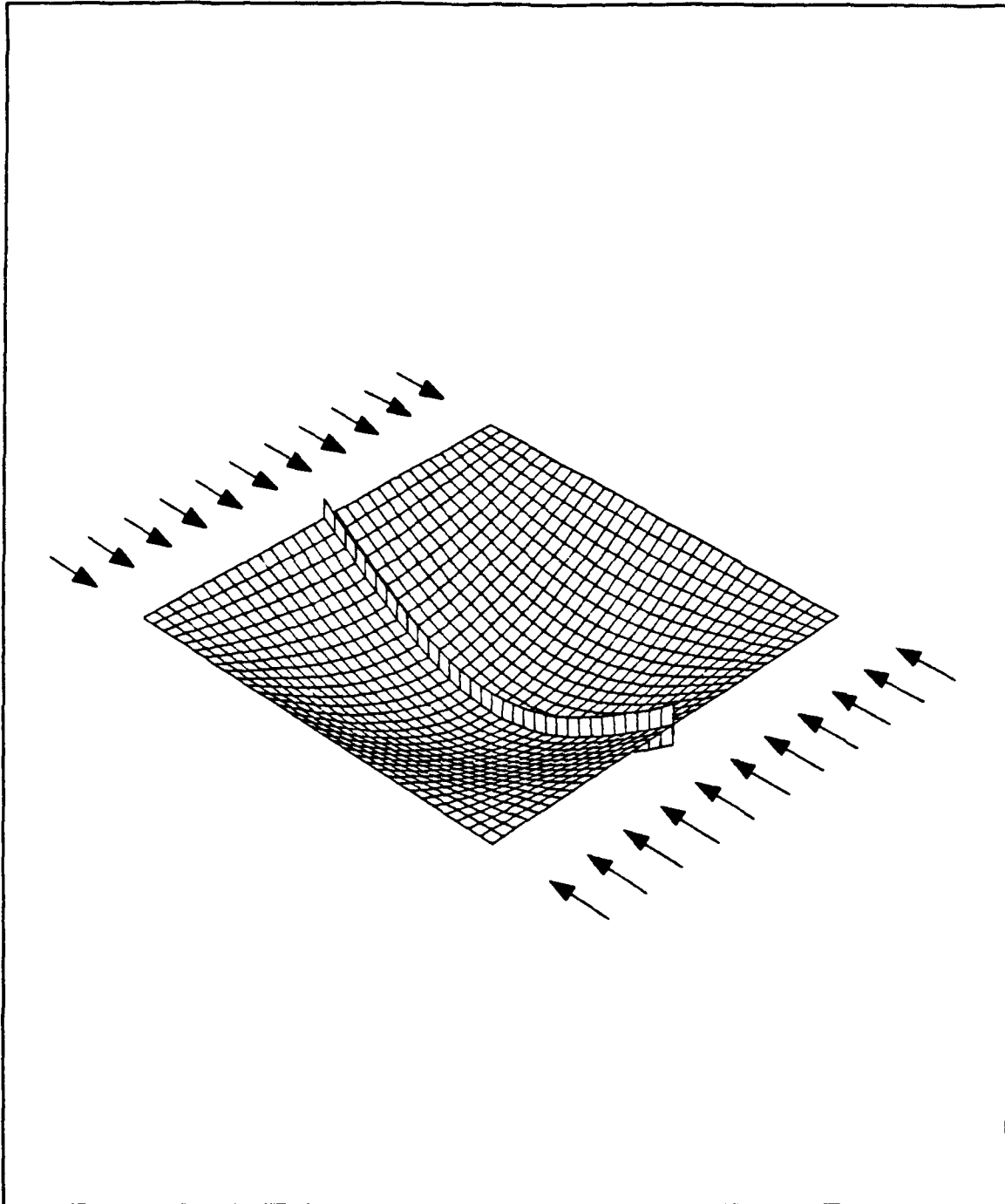


Figure 30. Buckling Shapes for Case 8 with $p = 0.0000036$: For Case 8, total volume $\Theta \approx 0.015$, with ply angle orientation of $(90^\circ_{beam} / 0^\circ / 90^\circ)_{sym}$. Represented above are the buckling shapes of the simultaneous overall plate buckling modes.

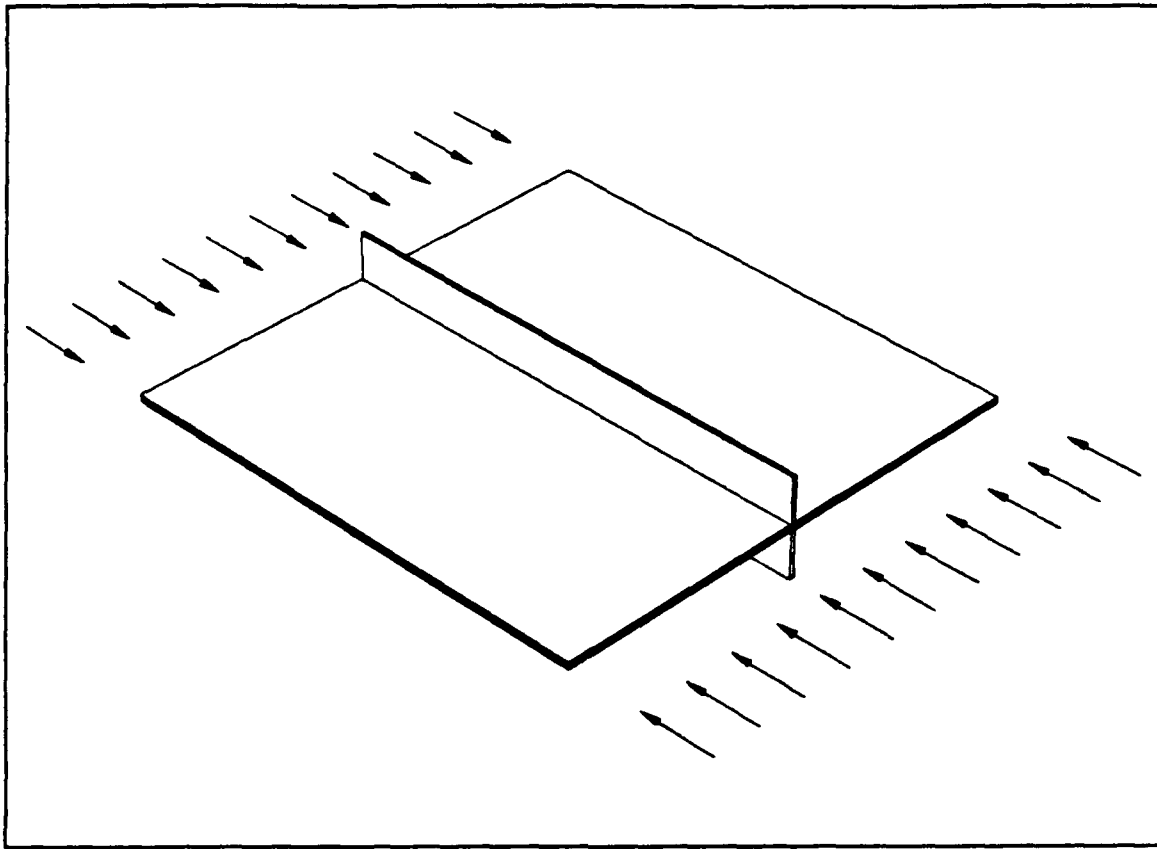


Figure 31. Geometry for Case 8 with $p = 0.0000125$: For Case 8, total volume $\Theta = 0.015$, with ply angle orientation $(90^\circ_{beam} / 0^\circ / 90^\circ)_{sym}$ (to scale)

As in Case 4, the global optimum solution for Case 8 occurs when all four buckling modes occur simultaneously. Also, there is a similar local optimum to that of Case 4, which has only one active buckling mode. This case is present for the same reasons as given in Case 3. One difference between Case 8 and Case 4 is that no local optimum in which three buckling modes occur simultaneously could be found for Case 8 as was found in Case 4.

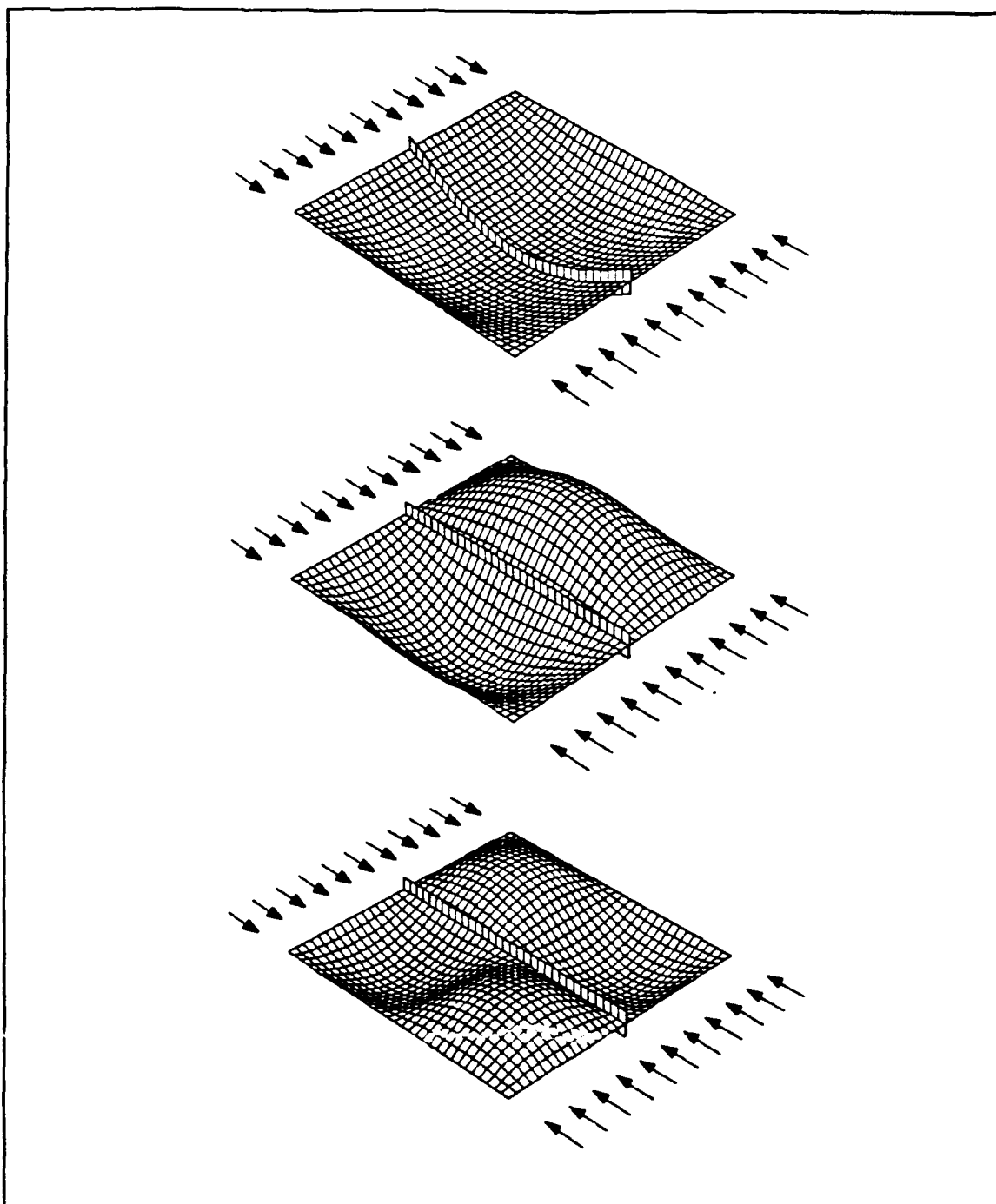


Figure 32. Buckling Shapes for Case 8 with $p = 0.0000125$: For Case 8, total volume $\Theta = 0.015$, with ply angle orientation of $(90^\circ_{beam} / 0^\circ / 90^\circ)_{sym}$. Represented above are the buckling shapes of the simultaneous overall plate buckling modes.

B. OPTIMIZATION EFFICIENCY

To compare the efficiencies of the three optimization routines, two separate criteria are used. These criteria are: the total execution time required to converge to an optimum solution; and the ability of an optimizer to converge to a solution when the initial guess is far from the solution (i.e. globally convergent). In order to compare the relative efficiencies of the three optimization methods, the exact same problem is solved with each of the optimization schemes. For each run, the same initial guess is used and the actual execution time is measured. These results are presented in Table 9 below.

Table 9. RUN TIMES: $\Theta = 0.04$, PLY ANGLE ($0^\circ_{BEAM} / 90^\circ / 0^\circ_{SYM}$)

Opti- mization Program	Initial Guess					Exe- cution Time in CPU seconds
	t_1	t_2	b	h	p	
	0.01000	0.00100	0.10000	0.10000	0.0001000	
	Output					
	t_1	t_2	b	h	p	
IMSL	0.01521	0.00100	0.05794	0.06526	0.0000282	35.8
DOT 1	0.01526	0.00100	0.05831	0.06510	0.0000287	72.9
DOT 2	0.01521	0.00100	0.05795	0.06525	0.0000282	132.4

From these results, it can be seen that for this specific design problem, the IMSL routine is clearly the most efficient in terms of the execution time. The relative speed of convergence for the IMSL routine is due to the high degree of nonlinearity in the design problem. Because the IMSL routine uses sequential quadratic programming as its search algorithm, which is based on a second order derivative, it allows each iteration in the optimum search to be more profitable than those of the DOT algorithms. Both the DOT methods (MFD and SLP) have search directions that are based on first order derivatives. Although the search direction calculation for both DOT methods is simpler, it is not as profitable in each iteration in the optimum search as that of the IMSL method. Thus, more iterations are required for optimum solution convergence with the DOT methods. The savings made in the calculation time for each search direction in the DOT code is not nearly enough to make up for the additional calculation time required for the extra iterations in the optimization. Therefore, due to the highly nonlinear nature of this problem, the IMSL routine is the most efficient in terms of execution time.

The second measure of the optimizer's efficiency is its ability to be globally convergent. That is, to converge to some solution from almost any starting point [Ref. 32: p. 5]. Since the location and number of optima are unknown at the start of the optimization process, the initial guesses are scattered throughout the design space in an attempt to identify all possible optima. Because the IMSL routine is based on a second order search, it is better suited to converge when the initial guess is relatively far away from an optima. Both the DOT methods were unable to converge to an optima on many runs when the initial guess was relatively far from any optima. Qualitatively, the IMSL routine produced actual optimum convergence ten fold more often than either of the DOT methods. Therefore, from the standpoint of globally convergent efficiency, the IMSL routine is clearly superior for this specific nonlinear optimization problem.

V. CONCLUSIONS

Many times it is difficult to draw general conclusions for design problems. This case is no exception, however, there are three main areas where specific conclusions for this particular design problem can be drawn. These areas are: the general character of the design problem; the best configuration of the investigated stacking sequences; and the relative efficiencies of the three optimization routines used.

The first general conclusion drawn is the character of the design problem for the maximum buckling load of the stiffened composite plate. The design optimization problem turns out to be a highly nonlinear problem. For almost all cases investigated, there were multiple optimum solutions indicating a nonlinear solution to the design optimization problem. Some cases had as many as three different optima. Even the case where only one optimum solution is identified cannot be assumed to be an indication of a linear problem. This must be viewed as the only solution identified and not as the only solution that exists. Additionally, these solutions were all located in a limited design space. One would expect even more optima to be found by increasing the size of the design space. Finally, the order of the governing partial differential equation would lead one to assume a highly nonlinear problem without examining the results. The results merely confirm this assumption.

The second area of general conclusions is that of the best design configuration. For both total volume constraints ($\Theta = 0.04$ and 0.015) examined, the best stacking configuration was the $(0^\circ_{beam} / 0^\circ / 90^\circ)_{sym}$ used in cases 2 and 6. The use of the 0°_{beam} stiffener fiber orientation was always superior to the 90°_{beam} stiffener fiber orientation regardless of the laminae ply orientation. This led to the conclusion that the 0°_{beam} stiffener fiber orientation is the most important factor in the design optimization. The laminae fiber orientation of $(0^\circ/90^\circ)_{sym}$ was best when used with the 90°_{beam} stiffener fiber orientation. However, when used with the 0°_{beam} stiffener fiber orientation, the $(90^\circ/0^\circ)_{sym}$ laminae fiber orientation was best. This indicates that for best results, the inner lamina (t_2 layer) should have its fiber orientation perpendicular to that of the stiffener fiber orientation.

The third area of general conclusions is the relative efficiencies of the three optimization routines used. Because of the highly nonlinear nature of this specific design optimization problem, the IMSL subroutine DNCONG proved to be the most efficient, both in terms of convergence speed and in its ability to be globally convergent (i.e.

converge to an optimum from almost any starting point). Because the IMSL routine is based on a second order search direction, it is better suited to optimize the highly nonlinear design problem. In contrast to this, both of the DOT methods have search directions that are based on first order search directions that make them ill-suited for such a highly nonlinear optimization problem.

It is important to note that the conclusions of this research are specific to the specific design optimization problem investigated. Generalizations of these results to other problems must be examined closely due to the nonlinear nature of the problem. Any design optimization problem of a nonlinear system must be closely scrutinized by the designer to ensure that all important aspects of the design are considered. Computer-aided design optimization can be a very powerful tool for a designer, however, caution must be exercised to ensure that a local optimum design is not selected as the best possible design without investigating the entire design space for other optima.

CCCCCCCCCCCC

CCCCCCCC

CCCCC

C

C

C

1

C

```

C === OBTAIN DERIVATIVES OF P WRT T
C
      DO 1305 J=1, NREQ
        WK(J) = EGVC(J,1)
1305  CONTINUE
      LC = 45
      CALL BNDMUL(BANDG,WK,NBAND1,NREQ,WK2,LC)
      DGD(1) = 0.DO
      DO 1320 J=1, NREQ
        DGD(1) = DGD(1) + WK(J)*WK2(J)
1320  CONTINUE
      IF(IDMOD.GE.1) THEN
        DO 1307 J=1, NREQ
          WK1(J) = EGVC(J,2)
1307  CONTINUE
        LC = 45
        CALL BNDMUL(BANDG,WK1,NBAND1,NREQ,WK2,LC)
        DGD(2) = 0.DO
        DO 2320 J=1, NREQ
          DGD(2) = DGD(2) + WK1(J)*WK2(J)
2320  CONTINUE
C
C ***
C      FOR 3RD EIGENVECTOR
C
      CALL BNDMUL(BANDG,EGVC(1,3),NBAND1,NREQ,WK2,LC)
      DGD(3) = 0.DO
      DO 4320 J=1, NREQ
        DGD(3) = DGD(3) + EGVC(J,3)*WK2(J)
4320  CONTINUE
      END IF
C
C
C
      DEL = 1.0D-05
      DO 380 IV=1, NLYR2
        IF(IV.EQ.NLYR1) THEN
          BBM = BBM + DEL
        ELSE IF(IV.EQ.NLYR2) THEN
          HBM = HBM + DEL
        ELSE
          HT(IV) = HT(IV) + DEL
        END IF
      CALL PROPTY
      CALL ELESTF
      CALL ASSEMB
C
C ---
C      GET DK
C
      DO 300 J=1, NREQ
        DO 280 K=1, NBAND1
          BANDKR(K,J) = (BANDKR(K,J) - EGVL(1,1)*BANDG(K,J)
            - DBANDK(K,J))/DEL
280    CONTINUE
300    CONTINUE
C

```

```

C --- GET U*DK*U
C
    LC = 45
    CALL BNDMUL(BANDKR,WK,NBAND1,NREQ,WK2,LC)
    DTHK(IV,1) = 0.DO
    DO 320 J=1, NREQ
        DTHK(IV,1) = DTHK(IV,1) + WK(J)*WK2(J)
320    CONTINUE
    DTHK(IV,1) = DTHK(IV,1)/DGD(1)
C
C --- GET U*DK*U
C
    IF(IDMOD.GE.1) THEN
        LC = 45
        CALL BNDMUL(BANDKR,WK1,NBAND1,NREQ,WK2,LC)
        DTHK(IV,2) = 0.DO
        DO 3320 J=1, NREQ
            DTHK(IV,2) = DTHK(IV,2) + WK1(J)*WK2(J)
3320    CONTINUE
        DTHK(IV,2) = DTHK(IV,2)/DGD(2)
C
        CALL BNDMUL(BANDKR,EGVC(1,3),NBAND1,NREQ,WK2,LC)
        DTHK(IV,3) = 0.DO
        DO 5320 J=1, NREQ
            DTHK(IV,3) = DTHK(IV,3) + EGVC(J,3)*WK2(J)
5320    CONTINUE
        DTHK(IV,3) = DTHK(IV,3)/DGD(3)
    END IF
C
C --- ORIGINAL HT
C
    IF(IV.EQ.NLYR1) THEN
        BBM = BBM - DEL
    ELSE IF(IV.EQ.NLYR2) THEN
        HBM = HBM - DEL
    ELSE
        HT(IV) = HT(IV) - DEL
    END IF
380    CONTINUE
C
    DO 4694 I=1,NLYR2
        DO 4694 J=1,3
            DTHK(I,J) = VNORMAL*DTHK(I,J)
4694    CONTINUE
C
    DO 1111 I=1,3
        EGVL(I,1) = EGVL(I,1)*VNORMAL
1111    CONTINUE
C
    RETURN
    END
C
C
C
C
C

```

```

C
C
SUBROUTINE INPUTB
C
C
IMPLICIT REAL*8(A-H,O-Z)
COMMON/PROPT0/ THETA, ALEN, BLEN
COMMON/PROPT1/ E1(15), E2(15), G12(15), PO12(15), ANGL(15), Z(16)
2      ,NOD(150,4), NX, NY, NSDF, LSDF(150)
COMMON/PROPT4/ HT(15), AAA, BBB, NLYR, NLYR1, NLYR2, NLYR3
COMMON/BEAM/ E1B, E2B, G12B, PO12B, BBM, HBM
C
C READ IN GEOMETRIC PARAMETERS AND PHYSICAL PROPERTIES
C
READ(5,*) ALEN, BLEN
READ(5,*) NLYR,THETA
NLYR1 = NLYR + 1
NLYR2 = NLYR + 2
NLYR3 = NLYR + 3
DO 150 I=1, NLYR
    READ(5,*) E1(I), E2(I), G12(I), PO12(I), ANGL(I)
150 CONTINUE
READ(5,*) NX, NY
READ(5,*) E1B, E2B, G12B, PO12B
RETURN
C
C
C
SUBROUTINE INPUTC
C
C
IMPLICIT REAL*8(A-H,O-Z)
EXTERNAL GRMESH
COMMON/PROPT0/ THETA, ALEN, BLEN
COMMON/PROPT1/ E1(15), E2(15), G12(15), PO12(15), ANGL(15), Z(16)
*      , NOD(150,4), NX, NY, NSDF, LSDF(150)
COMMON/PROPT3/ EBEAM, ABEAM, BMINER, EPLT, APLT, THICK, NODB(18,2)
COMMON/PROPT4/ HT(15), AAA, BBB, NLYR, NLYR1, NLYR2, NLYR3
COMMON/EIG/NBAND, NREQ, NEQ
COMMON/EIG2/ EGVC(150,5), EGVC0(150,5), EGVL(5,4), EGVL0(5,4),
*      DTHK(50,5), DGD(5), EGVCB(150,5), IDMOD
COMMON/BEAM/ E1B, E2B, G12B, PO12B, BBM, HBM
C
Z(1) = 0.00
DO 150 I=1, NLYR
    Z(I+1) = Z(I) + HT(I)
150 CONTINUE
THICK = Z(NLYR1)*2.000
APLT = BLEN*THICK
C
NEL = NX*NY
CALL GRMESH(NNM,NEM)
C *** BEAM CONNECTIVITY MATRIX ***
C
NX1 = NX + 1
NY1 = NY + 1

```

```

      NODO = NY/2*NX1 + 1
      DO 124 I=1, NX
        NODN = NODO + 1
        NODB(I,1) = NODO
        NODB(I,2) = NODN
        NODO = NODN
124    CONTINUE
C
C *** BOUNDARY CONDITIONS OF SIMPLE SUPPORT ***
C
      NSDF = 12 + 4*(NX-1) + 4*(NY-1)
      N = 0
      DO 400 K=1, NY1
        DO 300 J=1, NX1
          IF(K.NE.1.AND.K.NE.NY1) THEN
            IF(J.NE.1.AND.J.NE.NX1) THEN
              GO TO 300
            ELSE
              DO 200 I=1, 2
                N = N + 1
                LSDF(N) = 4*((K-1)*NX1 + J - 1) + I
200          CONTINUE
              END IF
            ELSE
              IF(J.NE.1.AND.J.NE.NX1) THEN
                DO 250 I=1, 3, 2
                  N = N + 1
                  LSDF(N) = 4*((K-1)*NX1 + J - 1) + I
250          CONTINUE
                ELSE
                  DO 270 I=1, 3
                    N = N + 1
                    LSDF(N) = 4*((K-1)*NX1 + J - 1) + I
270          CONTINUE
                END IF
              END IF
            CONTINUE
          300    CONTINUE
        400    CONTINUE
C
      AAA = ALN/NX
      BBB = BLN/NY
      NEQ = 4*(NX+1)*(NY+1)
      NREQ = NEQ - NSDF
C
C --- CLEAR EGVCB
C
      DO 722 I=1, 3
        DO 721 J=1, NREQ
          EGVCB(J,I) = 0.D0
721    CONTINUE
722    CONTINUE
      RETURN
C
C
C
C

```

```

C
C
C SUBROUTINE PROPTY
C
C IMPLICIT REAL*8(A-H,O-Z)
COMMON/PROPT4/ HT(15), AAA, BBB, NLYR, NLYR1, NLYR2, NLYR3
COMMON/PROPT1/ E1(15), E2(15), G12(15), PO12(15), ANGL(15), Z(16)
*      , NOD(150,4), NX, NY, NSDF, LSDF(150)
COMMON/PROPT2/ DM(3,3)
COMMON/PROPT3/ EBEAM, ABEAM, BMINER, EPLT, APLT, THICK, NODB(18,2)
COMMON/BEAM/ E1B, E2B, G12B, PO12B, BBM, HBM
DIMENSION DANGL(15)

C
Z(1) = 0.D0
DO 5 I=1, NLYR
  Z(I+1) = Z(I) + HT(I)
5 CONTINUE
C
DO 10 I=1, 3
  DO 10 J=1, 3
    DM(I,J)=0.0
10 CONTINUE
AM11 = 0.D0
AM12 = 0.D0
AM13 = 0.D0
AM22 = 0.D0
AM23 = 0.D0
AM33 = 0.D0

C
C *** DO-LOOP FOR NUMBER OF LAYERS
C
DO 30 I=1,NLYR
C
C *** CALCULATION OF THE REDUCED STIFFNESSES
C
PO21=E2(I)*PO12(I)/E1(I)
BPO=1.0-PO12(I)*PO21
Q11=E1(I)/BPO
Q12=PO12(I)*E2(I)/BPO
Q22=E2(I)/BPO
Q66=G12(I)

C
C *** CALCULATION OF THE TRANSFORMED REDUCED STIFFNESSES
C
DANGL(I)=3.141592D0*ANGL(I)/180.D0
SC=DSIN(DANGL(I))*DCOS(DANGL(I))
S2=(DSIN(DANGL(I)))**2
C2=(DCOS(DANGL(I)))**2
C
QB11=Q11*C2*C2+2.0*(Q12+2.0*Q66)*SC*SC+Q22*S2*S2
QB22=Q11*S2*S2+2.0*(Q12+2.0*Q66)*SC*SC+Q22*C2*C2
QB12=(Q11+Q22-4.0*Q66)*SC*SC+Q12*(S2*S2+C2*C2)
QB16=(Q11-Q12-2.0*Q66)*SC*C2+(Q12-Q22+2.0*Q66)*SC*S2
QB26=(Q11-Q12-2.0*Q66)*SC*S2+(Q12-Q22+2.0*Q66)*SC*C2

```



```

        DIMENSION BK(16,3), WK1616(16,16), WK163(16,3), WK316(3,16),
*          WK33(3,3), DV(6)
C
      DATA GAUSS4/.0694318D0,0.3300095D0,0.6699905D0,0.9305681D0/
      DATA GAUSS3/.1127017D0,0.5D0,0.88729833D0/
      DATA WT4/0.1739274D0,0.3260725D0,0.3260725D0,0.1739274D0/
      DATA WT3/0.2777777D0,0.4444444D0,0.2777777D0/
C
C *** INTERPOLATION FUNCTIONS AND THEIR DERIVATIVES ***
C
      FN1(P) = 1.D0 - 3.D0*P*P + 2.D0*P*P*P
      FN2(P) = (1.D0 - 2.D0*P + P*P)*P
      FN3(P) = (3.D0 - 2.D0*P)*P*P
      FN4(P) = P*P*(1.D0 - P)
C
      DFN1(P) = P*(-6.D0 + 6.D0*P)
      DFN2(P) = 1.D0 - 4.D0*P + 3.D0*P*P
      DFN3(P) = 6.D0*P*(1.D0 - P)
      DFN4(P) = P*(2.D0 - 3.D0*P)
C
      DDFN1(P) = -6.D0 + 12.D0*P
      DDFN2(P) = -4.D0 + 6.D0*P
      DDFN3(P) = 6.D0 - 12.D0*P
      DDFN4(P) = 2.D0 - 6.D0*P
C
C *** COMPONENT OF D MATRIX
C
      DV(1) = DM(1,1)
      DV(2) = DM(1,2)
      DV(3) = DM(1,3)
      DV(4) = DM(2,2)
      DV(5) = DM(2,3)
      DV(6) = DM(3,3)
C
C
C
C *** INITIALIZE THE ELEMENT MATRICES AND VECTORS
C
      DO 20 J=1, 16
        DO 20 I=1, 16
          EG(I,J) = 0.D0
          EKT(I,J) = 0.D0
20    CONTINUE
C
      DO 30 K=1, 6
        DO 30 J=1, 16
          DO 30 I=1, 16
            EK(I,J,K) = 0.D0
30    CONTINUE
C
C *** NUMERICAL INTEGRATION BY GAUSS QUADRATURE
C
      DO 500 NI=1,3
        XI=GAUSS3(NI)
        DXF1 = DFN1(XI)
        DXF2 = DFN2(XI)

```

```

DXF3 = DFN3(XI)
DXF4 = DFN4(XI)
DO 500 NJ=1,4
    ETA=GAUSS4(NJ)
    EF1 = FN1(ETA)
    EF2 = FN2(ETA)
    EF3 = FN3(ETA)
    EF4 = FN4(ETA)
C
    BG(1) = DXF1*EF1/AAA
    BG(2) = DXF1*EF2*BBB/AAA
    BG(3) = -DXF2*EF1
    BG(4) = DXF2*EF2*BBB
C
    BG(5) = DXF3*EF1/AAA
    BG(6) = DXF3*EF2*BBB/AAA
    BG(7) = DXF4*EF1
    BG(8) = -DXF4*EF2*BBB
C
    BG(9) = DXF3*EF3/AAA
    BG(10) = -DXF3*EF4*BBB/AAA
    BG(11) = DXF4*EF3
    BG(12) = DXF4*EF4*BBB
C
    BG(13) = DXF1*EF3/AAA
    BG(14) = -DXF1*EF4*BBB/AAA
    BG(15) = -DXF2*EF3
    BG(16) = -DXF2*EF4*BBB
C
    DO 250 J=1, 16
        DO 250 I=1, 16
            EG(I,J) = EG(I,J) + WT3(NI)*WT4(NJ)*BG(I)*BG(J)
250    CONTINUE
C
    500 CONTINUE
C
    *** MULTIPLY THE LOAD FACTOR ***
C
    FACTOR = EPLT*THICK/(EPLT*APLT + EBEAM*ABEAM)*AAA*BBB
    DO 555 J=1, 16
        DO 555 I=1, 16
            EG(I,J) = EG(I,J)*FACTOR
555    CONTINUE
C
C
    DO 600 NI=1, 4
        XI=GAUSS4(NI)
        XF1 = FN1(XI)
        XF2 = FN2(XI)
        XF3 = FN3(XI)
        XF4 = FN4(XI)
        DXF1 = DFN1(XI)
        DXF2 = DFN2(XI)
        DXF3 = DFN3(XI)
        DXF4 = DFN4(XI)
        DDXF1 = DDFN1(XI)

```

```

DDXF2 = DDFN2(XI)
DDXF3 = DDFN3(XI)
DDXF4 = DDFN4(XI)
DO 600 NJ=1, 4
  ETA=GAUSS4(NJ)
  EF1 = FN1(ETA)
  EF2 = FN2(ETA)
  EF3 = FN3(ETA)
  EF4 = FN4(ETA)
  DEF1 = DFN1(ETA)
  DEF2 = DFN2(ETA)
  DEF3 = DFN3(ETA)
  DEF4 = DFN4(ETA)
  DDEF1 = DDFN1(ETA)
  DDEF2 = DDFN2(ETA)
  DDEF3 = DDFN3(ETA)
  DDEF4 = DDFN4(ETA)

```

C

```

BK(1,1) = DDXF1*EF1/AAA/AAA
BK(2,1) = DDXF1*EF2*BBB/AAA/AAA
BK(3,1) = -DDXF2*EF1/AAA
BK(4,1) = DDXF2*EF2*BBB/AAA

```

C

```

BK(5,1) = DDXF3*EF1/AAA/AAA
BK(6,1) = DDXF3*EF2*BBB/AAA/AAA
BK(7,1) = DDXF4*EF1/AAA
BK(8,1) = -DDXF4*EF2*BBB/AAA

```

C

```

BK(9,1) = DDXF3*EF3/AAA/AAA
BK(10,1) = -DDXF3*EF4*BBB/AAA/AAA
BK(11,1) = DDXF4*EF3/AAA
BK(12,1) = DDXF4*EF4*BBB/AAA

```

C

```

BK(13,1) = DDXF1*EF3/AAA/AAA
BK(14,1) = -DDXF1*EF4*BBB/AAA/AAA
BK(15,1) = -DDXF2*EF3/AAA
BK(16,1) = -DDXF2*EF4*BBB/AAA

```

C

```

BK( 1,2) = XF1*DDEF1/BBB/BBB
BK( 2,2) = XF1*DDEF2/BBB
BK( 3,2) = -XF2*DDEF1*AAA/BBB/BBB
BK( 4,2) = XF2*DDEF2*AAA/BBB

```

C

```

BK( 5,2) = XF3*DDEF1/BBB/BBB
BK( 6,2) = XF3*DDEF2/BBB
BK( 7,2) = XF4*DDEF1*AAA/BBB/BBB
BK( 8,2) = -XF4*DDEF2*AAA/BBB

```

C

```

BK( 9,2) = XF3*DDEF3/BBB/BBB
BK(10,2) = -XF3*DDEF4/BBB
BK(11,2) = XF4*DDEF3*AAA/BBB/BBB
BK(12,2) = XF4*DDEF4*AAA/BBB

```

C

```

BK(13,2) = XF1*DDEF3/BBB/BBB
BK(14,2) = -XF1*DDEF4/BBB
BK(15,2) = -XF2*DDEF3*AAA/BBB/BBB

```

```

C      BK(16,2) = -XF2*DDEF4*AAA/BBB

C      BK( 1,3) =  2.DO*DXF1*DEF1/AAA/BBB
      BK( 2,3) =  2.DO*DXF1*DEF2/AAA
      BK( 3,3) = -2.DO*DXF2*DEF1/BBB
      BK( 4,3) =  2.DO*DXF2*DEF2

C      BK( 5,3) =  2.DO*DXF3*DEF1/AAA/BBB
      BK( 6,3) =  2.DO*DXF3*DEF2/AAA
      BK( 7,3) =  2.DO*DXF4*DEF1/BBB
      BK( 8,3) = -2.DO*DXF4*DEF2

C      BK( 9,3) =  2.DO*DXF3*DEF3/AAA/BBB
      BK(10,3) = -2.DO*DXF3*DEF4/AAA
      BK(11,3) =  2.DO*DXF4*DEF3/BBB
      BK(12,3) =  2.DO*DXF4*DEF4

C      BK(13,3) =  2.DO*DXF1*DEF3/AAA/BBB
      BK(14,3) = -2.DO*DXF1*DEF4/AAA
      BK(15,3) = -2.DO*DXF2*DEF3/BBB
      BK(16,3) = -2.DO*DXF2*DEF4

C
C ***
C      GET TRANSPOSE OF BK

      DO 570 I=1, 3
        DO 570 J=1, 16
          WK316(I,J) = BK(J,I)
570      CONTINUE
C
      DO 580 KK=1, 6
        DO 560 JL=1, 3
          DO 560 IL=1, 3
            WK33(IL,JL) = 0.DO
560      CONTINUE
            IF(KK.EQ.1) THEN
              WK33(1,1) = 1.DO
            ELSE IF(KK.EQ.2) THEN
              WK33(1,2) = 1.DO
              WK33(2,1) = 1.DO
            ELSE IF(KK.EQ.3) THEN
              WK33(1,3) = 1.DO
              WK33(3,1) = 1.DO
            ELSE IF(KK.EQ.4) THEN
              WK33(2,2) = 1.DO
            ELSE IF(KK.EQ.5) THEN
              WK33(2,3) = 1.DO
              WK33(3,2) = 1.DO
            ELSE IF(KK.EQ.6) THEN
              WK33(3,3) = 1.DO
            END IF
            CALL MULTP2(BK,WK33,16,3,3,WK163)
            CALL MULTP2(WK163,WK316,16,3,16,WK1616)

C
C ***
C      MULTIPLY WIGHT FC. AND SUM UP FOR ELEMENT STIFF. MATRIX

      DO 550 J=1, 16

```

```

DO 550 I=1, 16
    EK(I,J,KK) = EK(I,J,KK) + WT4(NI)*WT4(NJ)*WK1616(I,J)
550    CONTINUE
580    CONTINUE
C
600    CONTINUE
C
C *** ASSEMBLE FOR ELEMENT STIFFNESS MATRIX
C
DO 620 I=1, 6
    DO 615 J=1, 16
        DO 615 K=1, 16
            EK(K,J,I) = EK(K,J,I)*AAA*BBB
615    CONTINUE
        DO 620 J=1, 16
            DO 620 K=1, 16
                EKT(K,J) = EKT(K,J) + DV(I)*EK(K,J,I)
620    CONTINUE
C
EI = EBEAM*BMINER
ARSTF(1,1) = EI*12.DO/AAA**3
ARSTF(1,2) = -EI*6.DO/AAA**2
ARSTF(1,3) = -ARSTF(1,1)
ARSTF(1,4) = ARSTF(1,2)
ARSTF(2,2) = EI*4.DO/AAA
ARSTF(2,3) = -ARSTF(1,2)
ARSTF(2,4) = EI*2.DO/AAA
ARSTF(3,3) = ARSTF(1,1)
ARSTF(3,4) = -ARSTF(1,2)
ARSTF(4,4) = ARSTF(2,2)
C
ARSTF(2,1) = ARSTF(1,2)
ARSTF(3,1) = ARSTF(1,3)
ARSTF(3,2) = ARSTF(2,3)
ARSTF(4,1) = ARSTF(1,4)
ARSTF(4,2) = ARSTF(2,4)
ARSTF(4,3) = ARSTF(3,4)
C
C
FACTOR = EBEAM*ABEAM/(EPLT*APLT + EBEAM*ABEAM)
ARGEM(1,1) = FACTOR*1.2DO/AAA
ARGEM(1,2) = -FACTOR*0.1DO
ARGEM(1,3) = -ARGEM(1,1)
ARGEM(1,4) = ARGEM(1,2)
ARGEM(2,2) = FACTOR*2.DO/15.DO*AAA
ARGEM(2,3) = -ARGEM(1,2)
ARGEM(2,4) = -FACTOR*AAA/30.DO
ARGEM(3,3) = ARGEM(1,1)
ARGEM(3,4) = -ARGEM(1,2)
ARGEM(4,4) = ARGEM(2,2)
C
ARGEM(2,1) = ARGEM(1,2)
ARGEM(3,1) = ARGEM(1,3)
ARGEM(3,2) = ARGEM(2,3)
ARGEM(4,1) = ARGEM(1,4)
ARGEM(4,2) = ARGEM(2,4)

```

```

      ARGEM(4,3) = ARGEM(3,4)
C
      RETURN
      END
C
C
C
C
      SUBROUTINE ASSEMB
C
C
C
C
      THIS SUBROUTINE ASSEMBLES THE ELEMENT STIFFNESS, ELEMENT GEOM.
      STIFFNESS MATRIX TO OBTAIN THE GLOBAL MATRIX
C
C
C
      IMPLICIT REAL*8(A-H,O-Z)
      COMMON/ELEMNT/ EK(16,16,6), EKT(16,16), EG(16,16)
      COMMON/ELEMB/ ARSTF(4,4), ARGEM(4,4)
      COMMON/PROPT1/ E1(15), E2(15), G12(15), PO12(15), ANGL(15), Z(16)
      *      , NOD(150,4), NX, NY, NSDF, LSDF(150)
      COMMON/PROPT3/ EBEAM, ABEAM, BMINER, EPLT, APLT, THICK, NODB(18,2)
      COMMON/TOTAL / GK(150,150),GG(150,150)
      COMMON/BAND/ BANDK(45,150), BANDKR(45,150), BANDG(45,150)
      COMMON/EIG/NBAND, NREQ, NEQ
      DIMENSION NK(4)
C
C *** CLEAR ARRAY
C
      DO 50 I=1, NEQ
        DO 50 J=1, NEQ
          GK(J,I) = 0.D0
          GG(J,I) = 0.D0
50    CONTINUE
C
      NEL = NX*NY
      DO 100 N=1, NEL
C
        DO 100 I=1, 4
          NR=(NOD(N,I)-1)*4
          DO 100 II=1, 4
            NR=NR+1
            L=(I-1)*4+II
            DO 200 J=1, 4
              NCL=(NOD(N,J)-1)*4
              DO 200 JJ=1, 4
                M=(J-1)*4+JJ
                NC=NCL+JJ
                GK(NR,NC)=GK(NR,NC)+EKT(L,M)
                GG(NR,NC)=GG(NR,NC)+EG(L,M)
200          CONTINUE
100    CONTINUE
C
C *** IMPOSITION OF THE BEAM ELEMENT MATRIX ***
C
      DO 250 I=1, NX
        NOD1 = 4*(NODB(I,1)-1)

```



```

COMMON/PROPT1/ E1(15), E2(15), G12(15), PO12(15), ANGL(15), Z(16)
*      , NOD(150,4), NX, NY, NSDF, LSDF(150)
COMMON/PROPT3/ EBEAM, ABEAM, BMINER, EPLT, APLT, THICK, NODB(18,2)
COMMON/PROPT4/ HT(15), AAA, BBB, NLYR, NLYR1, NLYR2, NLYR3
COMMON/TOTAL / GK(150,150),GG(150,150)
COMMON/BAND/ BANDK(45,150), BANDKR(45,150), BANDG(45,150)
COMMON/EIG/NBAND, NREQ, NEQ
COMMON/EIG2/ EGVC(150,5), EGVC0(150,5), EGV(5,4), EGVLO(5,4),
*      DTHK(50,5), DGD(5), EGVCB(150,5), IDMOD
COMMON/NORMAL/ VNORMAL

C      DIMENSION WORK(22500), IND(3)
      EQUIVALENCE (GG(1,1), WORK(1))
      EXTERNAL OP, IOVECT

C
C *** FACTOR THE BANDED STIFFNESS MATRIX ***
C (LINPACK SUBROUTINE "DPBFA")
C
      LDA = 45
      CALL DPBFA(BANDK, LDA, NREQ, NBAND, INFO)
      IF(INFO.NE.0) STOP

C
C *** INPUT FOR SUB-SPACE ITERATION ***
C
      NVAL = 3
      NFIG = 10
      NPERM = 0
      NMVAL = 3
      NMVEC = 150
      NBLOCK = NREQ/6
      IF(NBLOCK.GE.8) NBLOCK = 8
      MAXOP = NREQ
      MAXJ = 150
      NREQ2 = 2*NREQ

C
C *** CLEAR THE WORK SPACE
C
      NV = IABS(NVAL)
      NWORK1 = 2*NREQ*NBLOCK + MAXJ*(NBLOCK+NV+2) + 2*NBLOCK**2 + 3*NV
      NWORK2 = N*NBLOCK
      NWORK3 = MAXJ*(2*NBLOCK+3) + 2*NV + 6 + (2*NBLOCK+2)*(NBLOCK+1)
      IF(NWORK2.GT.NWORK3) NWORK3 = NWORK2
      NWORK = NWORK1 + NWORK3

C
C --- INITIAL VALUE OF THE EIGENVECTORS
C
      NPR7 = NV
      IF(NBLOCK.LE.NV) NPR7 = NBLOCK
      DO 608 I=1, NPR7
        DO 607 J=1, NREQ
          WORK((I-1)*NREQ+J) = EGVCB(J,I)
607      CONTINUE
608      CONTINUE
C
      DO 1 I=1, NREQ
        WORK(I) = 0.D-05

```



```

COMMON/EIG/NBAND, NREQ, NEQ
C
DO 999 L=1, M
    DO 105 J=1, N
        PBAR(J) = P(J,L)
105    CONTINUE
C
C *** OBTAIN PBAR(N,M) USING THE SUBROUTINE "DPBSL2" ***
C
    CALL DPBSL2(BANDK,45,NREQ,NBAND,PBAR(1))
C
C *** BANDED GEOMETRIC STIFFNESS MATRIX TIMES PBAR ***
C
    NBAND1 = NBAND + 1
    LC = 45
    CALL BNDMUL(BANDG,PBAR,NBAND1,NREQ,Q(1,L),LC)
C
C *** OBTAIN Q(N,M) USING THE SUBROUTINE "DPBSL1" ***
C
    CALL DPBSL1(BANDK,45,NREQ,NBAND,Q(1,L))
999    CONTINUE
    RETURN
    END
C
C
C
SUBROUTINE IOVECT(N,M,Q,J,K)
C
C
    IMPLICIT REAL*8(A-H,O-Z)
    COMMON/TOTAL / GK(150,150),GG(150,150)
    DIMENSION Q(N,M)
    IF(K.EQ.1) GO TO 30
    DO 20 L=1, M
        L1 = J-M+L
        DO 10 I=1, N
            GK(I,L1) = Q(I,L)
10        CONTINUE
20    CONTINUE
    RETURN
C
30    DO 50 L=1, M
        L1 = J-M+L
        DO 40 I=1, N
            Q(I,L) = GK(I,L1)
40    CONTINUE
50    CONTINUE
    RETURN
    END
C
C
C
SUBROUTINE BNDMUL(BAND,WK,NBAND1,NREQ,WK2,LC)
C
C
    IMPLICIT REAL*8(A-H,O-Z)

```

```

      DOUBLE PRECISION BAND(LC,*), WK(*), WK2(*)
      NBAND = NBAND1 - 1
      DO 4200 I=1, NREQ
        SUM = 0.DO
        DO 4150 J=1, NBAND1
          IPR = I - NBAND1 + J
          IF(IPR.LE.0) GO TO 4150
          SUM = SUM + BAND(J,I)*WK(IPR)
4150      CONTINUE
        DO 4160 K=1, NBAND
          IPR = I + K
          IF(IPR.GT.NREQ) GO TO 4160
          SUM = SUM + BAND(NBAND1-K,IPR)*WK(IPR)
4160      CONTINUE
        WK2(I) = SUM
4200      CONTINUE
      RETURN
      END

```

C
C
C
C

SUBROUTINE GRMESH(NNM,NEM)

C
C
C
C
C
C
C

THIS SOUBROUTINE GENERATES THE BOOLEAN CONNECTIVITY MATRIX

C
C
C
C
C

```

      IMPLICIT REAL*8(A-H,O-Z)
      COMMON/PROPT1/ E1(15), E2(15), G12(15), PO12(15), ANGL(15), Z(16)
      *              , NOD(150,4), NX, NY, NSDF, LSDF(150)

```

C

```

      NX1 = NX + 1
      NY1 = NY + 1
      NXX1=NXX+1
      NYY1=NYY+1
      NEM = NX*NY
      NNM = NX1*NY1

```

C

```

      NOD(1,1) = 1
      NOD(1,2) = 2
      NOD(1,3) = NX1 + 2
      NOD(1,4) = NX1 + 1
      IF(NY.EQ.1) GO TO 230
      M=1
      DO 220 N=2, NY
        L = (N-1)*NX + 1
        DO 210 I=1, 4
          NOD(L,I) = NOD(M,I) + NX1
210      CONTINUE
        M=L
220      CONTINUE
230      IF(NX.EQ.1) GO TO 270
      DO 260 NI=2, NX
        DO 240 I=1, 4

```

```

      NOD(NI,I) = NOD(NI-1,I) + 1
240  CONTINUE
      M=NI
      DO 260 NJ=2, NY
        L = (NJ-1)*NX + NI
        DO 250 J=1, 4
          NOD(L,J) = NOD(M,J) + NX1
250  CONTINUE
      M=L
260  CONTINUE
270  RETURN
      END

```

APPENDIX B. OPTIMIZATION PROBLEM CODE LISTING USING IMSL

```

C
C
C      PROGRAM MAINIM
C
C
C
C      VARIABLE DECLARATIONS
C
C      IMPLICIT REAL*8(A-H,O-Z)
C      DOUBLEPRECISION XLB(18), XUB(18), XGUESS(18), T(18)
C      PARAMETER (IBTYPE=0, IPRINT=3, M=5, MAXITN=100, ME=1)
C      EXTERNAL FCN, GRAD, INPUTB, LIMITS, GUESS, DNCONG
C
C      COMMON BLOCKS
C
C      COMMON/ELEMNT/ EK(16,16,6), EKT(16,16), EG(16,16)
C      COMMON/ELEMNB/ ARSTF(4,4), ARGEM(4,4)
C      COMMON/PROPT0/ THETA, ALEN, BLEN
C      COMMON/PROPT1/ E1(15), E2(15), G12(15), PO12(15), ANGL(15), Z(16),
2      NOD(150,4), NX, NY, NSDF, LSDF(150)
C      COMMON/PROPT2/ DM(3,3)
C      COMMON/PROPT3/ EBEAM, ABEAM, BMINER, EPLT, APLT, THICK, NODB(18,2)
C      COMMON/PROPT4/ HT(15), AAA, BBB, NLYR, NLYR1, NLYR2, NLYR3
C      COMMON/TOTAL/ GK(150,150), GG(150,150)
C      COMMON/BAND/ BANDK(45,150), BANDKR(45,150), BANDG(45,150)
C      COMMON/EIG/ NBAND, NREQ, NEQ
C      COMMON/EIG2/ EGVC(150,5), EGVCO(150,5), EGV(5,4), EGVLO(5,4),
2      DTHK(50,5), DGD(5), EGVCB(150,5), IDMOD
C      COMMON/FSAVE/ VVV2(100)
C      COMMON/BEAM/ E1B, E2B, G12B, PO12B, BBM, HBM
C      COMMON/BEAM2/ DBTHK(50), PBEAM
C      COMMON/BIMO/ VECRAT(5,5), V99, INDVC(5)
C      COMMON/LEVY/ SD11, SD12, SD22, SD66, ALPM, ALPMS, PEM, OMEGA
C      COMMON/NORMAL/ VNORMAL
C
C      VNORMAL IS SCALING FACTOR FOR T(NLYR3) TO INCREASE ACCURACY
C
C      VNORMAL = 1.0D 03
C
C      CALL INPUTB
C      N = NLYR + 3
C      CALL LIMITS (XLB, XUB)
C      CALL GUESS (XGUESS)
C      CALL DNCONG (FCN, GRAD, M, ME, N, XGUESS, IBTYPE, XLB, XUB,
2      IPRINT, MAXITN, T, PMAX)
C      END
C
C
C

```

```

C
C
C SUBROUTINE FCN (M, ME, N, T, ACTIVE, P, G)
C
C
C   IMPLICIT REAL*8(A-H,O-Z)
C   LOGICAL ACTIVE(*)
C   DOUBLEPRECISION G(*), T(*)
C   EXTERNAL INPUTC, EIGANL4, LEVYS
C
C   COMMON BLOCKS *****
C
C   COMMON/ELEMNT/ EK(16,16,6), EKT(16,16), EG(16,16)
C   COMMON/ELEMB/ ARSTF(4,4), ARGEM(4,4)
C   COMMON/PROPT0/ THETA, ALN, BLEN
C   COMMON/PROPT1/ E1(15), E2(15), G12(15), PO12(15), ANGL(15), Z(16),
2   NOD(150,4), NX, NY, NSDF, LSDF(150)
C   COMMON/PROPT2/ DM(3,3)
C   COMMON/PROPT3/ EBEAM, ABEAM, BMINER, EPLT, APLT, THICK, NODB(18,2)
C   COMMON/PROPT4/ E(15), AAA, BBB, NLYR, NLYR1, NLYR2, NLYR3
C   COMMON/TOTAL/ GK(150,150), GG(150,150)
C   COMMON/BAND/ BANDK(45,150), BANDKR(45,150), BANDG(45,150)
C   COMMON/EIG/ NBAND, NREQ, NEQ
C   COMMON/EIG2/ EGVC(150,5), EGVC0(150,5), EGVL(5,4), EGVL0(5,4),
2   DTHK(50,5), DGD(5), EGVCB(150,5), IDMOD
C   COMMON/BEAM/ E1B, E2B, G12B, PO12B, BBM, HBM
C   COMMON/BEAM2/ DBTHK(50), PBEAM
C
C   UPDATE VALUES OF HT(*), BBM, AND HBM
C
C   DO 100 I=1,NLYR
C     HT(I) = T(I)
100 CONTINUE
C   BBM = T(NLYR1)
C   HBM = T(NLYR2)
C
C   CALCULATE VALUES OF P1, P2, P3, AND PBEAM FOR CURRENT VALUES OF
C   HT(*), BBM, AND HBM
C
C   CALL INPUTC
C   CALL EIGANL4
C   CALL LEVYS
C   P1 = EGVL(1,1)
C   P2 = EGVL(2,1)
C   P3 = EGVL(3,1)
C
C   FUNCTION DEFINITION
C
C   P = -T(NLYR3)
C
C   CALCULATE CONSTRAINT VALUES FOR CURRENT VALUES OF HT(*), BBM, & HBM
C
C   IF (ACTIVE(1)) G(1) = APLT + ABEAM - THETA
C   IF (ACTIVE(2)) G(2) = P1 - T(NLYR3)
C   IF (ACTIVE(3)) G(3) = .999*P2 - T(NLYR3)
C   IF (ACTIVE(4)) G(4) = .998*P3 - T(NLYR3)

```

```

      IF (ACTIVE(5)) G(5) = PBEAM - T(NLYR3)
C
      RETURN
C
C
C
      SUBROUTINE GUESS (XGUESS)
C
C
      IMPLICIT REAL*8(A-H,O-Z)
      DOUBLEPRECISION XGUESS(18)
      COMMON/PROPT4/ HT(15), AAA, BBB, NLYR, NLYR1, NLYR2, NLYR3
      COMMON/NORMAL/ VNORMAL
C
C
      READ IN XGUESS VALUES
C
      DO 200 I=1,NLYR3
        READ(8,*) XGUESS(I)
200  CONTINUE
C
      SCALE T(NLYR3) GUESS FOR ADDITIONAL ACCURACY
C
      XGUESS(NLYR3)=XGUESS(NLYR3)*VNORMAL
C
      RETURN
C
C
C
C
      SUBROUTINE LIMITS (XLB, XUB)
C
C
      IMPLICIT REAL*8(A-H,O-Z)
      COMMON/PROPT0/ THETA, ALEN, BLEN
      COMMON/PROPT4/ HT(15), AAA, BBB, NLYR, NLYR1, NLYR2, NLYR3
      DOUBLEPRECISION XLB(18), XUB(18)
C
C
      SET LOWER LIMITS FOR DESIGN VARIABLES, T(*)
C
      DO 100 I=1,NLYR
        XLB(I) = 1.0D-03
100  CONTINUE
        XLB(NLYR1) = 1.0D-03
        XLB(NLYR2) = 1.0D-03
        XLB(NLYR3) = 1.0D-06
C
C
      SET UPPER LIMITS FOR DESIGN VARIABLES, HT(*)
C
      DO 200 I=1,NLYR
        XUB(I) = 2.0D-01
200  CONTINUE
        XUB(NLYR1) = 2.0D-01
        XUB(NLYR2) = 2.0D-01
        XUB(NLYR3) = 1.0D 06
C
      RETURN

```


APPENDIX C. OPTIMIZATION PROBLEM CODE LISTING USING DOT

```

C _____
C
C   PROGRAM MNDOT
C _____
C
C   VARIABLE DECLARATIONS
C
      IMPLICIT REAL*8(A-H,O-Z)
      DOUBLEPRECISION XLB(18), XUB(18), XGUESS(18), T(18), DG(6,18),
2      G(6), AA(18,6), WK(2000), RPRM(20)
      DIMENSION IPRM(20), IWK(1000)
      EXTERNAL FCNDOT, INPUTB, LIMITS, GUESS, DOT
C
C   COMMON BLOCKS
C
      COMMON/ELEMNT/ EK(16,16,6), EKT(16,16), EG(16,16)
      COMMON/ELEMNB/ ARSTF(4,4), ARGEM(4,4)
      COMMON/PROPT0/ THETA, ALEN, BLEN
      COMMON/PROPT1/ E1(15), E2(15), G12(15), PO12(15), ANGL(15), Z(16),
2      NOD(150,4), NX, NY, NSDF, LSDF(150)
      COMMON/PROPT2/ DM(3,3)
      COMMON/PROPT3/ EBEAM, ABEAM, BMINER, EPLT, APLT, THICK, NODB(18,2)
      COMMON/PROPT4/ HT(15), AAA, BBB, NLYR, NLYR1, NLYR2, NLYR3
      COMMON/TOTAL/ GK(150,150), GG(150,150)
      COMMON/BAND/ BANDK(45,150), BANDKR(45,150), BANDG(45,150)
      COMMON/EIG/ NBAND, NREQ, NEQ
      COMMON/EIG2/ EGVC(150,5), EGVC0(150,5), EGVL(5,4), EGVL0(5,4),
2      DTHK(50,5), DGD(5), EGVCB(150,5), IDMOD
      COMMON/FSAVE/ VVV2(100)
      COMMON/BEAM/ E1B, E2B, G12B, PO12B, BBM, HBM
      COMMON/BEAM2/ DBTHK(50), PBEAM
      COMMON/BIMO/ VECRAT(5,5), V99, INDVC(5)
      COMMON/LEVY/ SD11, SD12, SD22, SD66, ALPM, ALPMS, PEM, OMEGA
      COMMON/NORMAL/ VNORMAL, SCALTH
C
C   VNORMAL IS SCALING FACTOR FOR T(NLYR3) TO INCREASE ACCURACY
C
      VNORMAL = 1.0D+02
C
C   DEFINE WORK SPACE REQUIREMENTS
C
      NRWK = 2000
      NRIWK = 1000
C
C   ZERO RPRM AND IPRM
C
      DO 50 I=1,20
        RPRM(I) = 0.0D0

```

```

        IPRM(I) = 0
50    CONTINUE
C
C    READ IN PROBLEM DATA AND VALUES OF T(*), XLB(*), AND XUB(*)
C
        CALL INPUTB
        CALL LIMITS (XLB, XUB)
        CALL GUESS (XGUESS)
        DO 100 I=1,NLYR3
            T(I) = XGUESS(I)
100    CONTINUE
C
C    SPECIFY THAT GRADIENTS ARE TO BE PROVIDED
C    SET PARAMETER IPRM(1) = 1
C
        IPRM(1) = 1
C
C    DEFINE METHOD, NDV, NCON, IPRINT, MINMAX
C    METHOD = 1 FOR MFD
C    METHOD = 2 FOR SLP
C
        METHOD =
        NDV = NLYR3
        NCON = 5
        IPRINT = 5
        MINMAX = 0
C
C    READY TO OPTIMIZE
C
        INFO = 0
200    CALL DOT (INFO,METHOD,IPRINT,NDV,NCON,T,XLB,XUB,P,MINMAX,G,
2        RPRM,IPRM,WK,NRWK,IWK,NRIWK)
C
C    PROVIDE GRADIENTS IF DOT REQUESTS THEM
C
        IF(INFO.EQ.2) GO TO 300
C
C    EXIT IF CONVERGENCE IS OBTAINED
C
        IF(INFO.EQ.0) GO TO 1000
C
C    EVALUATE OBJECTIVE FUNCTION AND CONSTRAINTS
C
        CALL FCNDOT (T, P, G)
        GO TO 200
C
C    GRADIENT EVALUATION
C
300    CONTINUE
C
C    CALCULATE FUNCTION GRADIENT WRT DESIGN VARIABLES AT POINT HT(*)
C
        DO 400 I=1,NLYR2
            WK(I) = 0.0D0
400    CONTINUE

```

```

      WK(NLYR3) = -1.0D0
C
C IF NUMBER OF ACTIVE CONSTRAINTS EQUAL ZERO RETURN TO DOT
C
      NGT = IPRM(20)
      IF(NGT.EQ.0) GO TO 200
C
C CALCULATE CONSTRAINT GRADIENTS WRT DESIGN VARIABLES AT POINT HT(*)
C
      DO 510 I=1,NLYR2
        DG(1,I) = -DTHK(I,1)
510      CONTINUE
        DG(1,NLYR3) = 1.0D0
C
      DO 520 I=1,NLYR2
        DG(2,I) = -DTHK(I,2) * 0.999D0
520      CONTINUE
        DG(2,NLYR3) = 1.0D0
C
      DO 530 I=1,NLYR2
        DG(3,I) = -DTHK(I,3) * 0.998D0
530      CONTINUE
        DG(3,NLYR3) = 1.0D0
C
      DO 540 I=1,NLYR2
        DG(4,I) = -DBTHK(I)
540      CONTINUE
        DG(4,NLYR3) = 1.0D0
C
      DO 550 I=1,NLYR
        DG(5,I) = 2.0D0 * BLEN/THETA
550      CONTINUE
        DG(5,NLYR1) = 2.0D0 * T(NLYR2)/THETA
        DG(5,NLYR2) = 2.0D0 * T(NLYR1)/THETA
        DG(5,NLYR3) = 0.0D0
C
C STORE ACTIVE GRADIENT INFORMATION IN ARRAY WK(*)
C
      DO 600 K=1,NGT
        J = IWK(K)
        AA(1,K) = DG(J,1)
        AA(2,K) = DG(J,2)
        AA(3,K) = DG(J,3)
        AA(4,K) = DG(J,4)
        AA(5,K) = DG(J,5)
600      CONTINUE
        N1 = NDV
        DO 800 K=1,NGT
          DO 700 I=1,NDV
            WK(I+N1) = AA(I,K)
          700      CONTINUE
          N1 = N1 + NDV
600      CONTINUE
        GO TO 200
1000 CONTINUE

```

```

      END
C
C
C SUBROUTINE FCNDOT (T, P, G)
C
C
C   IMPLICIT REAL*8(A-H,O-Z)
C   DOUBLEPRECISION G(*), T(*)
C   EXTERNAL INPUTC, EIGANL4, LEVYS
C
C   COMMON BLOCKS *****
C
C   COMMON/ELEMNT/ EK(16,16,6), EKT(16,16), EG(16,16)
C   COMMON/ELEMB/ ARSTF(4,4), ARGEM(4,4)
C   COMMON/PROPT0/ THETA, ALEN, BLEN
C   COMMON/PROPT1/ E1(15), E2(15), G12(15), PO12(15), ANGL(15), Z(16),
2     NOD(150,4), NX, NY, NSDF, LSDF(150)
C   COMMON/PROPT2/ DM(3,3)
C   COMMON/PROPT3/ EBEAM, ABEAM, BMINER, EPLT, APLT, THICK, NODB(18,2)
C   COMMON/PROPT4/ HT(15), AAA, BBB, NLYR, NLYR1, NLYR2, NLYR3
C   COMMON/TOTAL/ GK(150,150), GG(150,150)
C   COMMON/BAND/ BANDK(45,150), BANDKR(45,150), BANDG(45,150)
C   COMMON/EIG/ NBAND, NREQ, NEQ
C   COMMON/EIG2/ EGVC(150,5), EGVC0(150,5), EGVL(5,4), EGVL0(5,4),
2     DTHK(50,5), DGD(5), EGVCB(150,5), IDMOD
C   COMMON/BEAM/ E1B, E2B, G12B, PO12B, BBM, HBM
C   COMMON/BEAM2/ DBTHK(50), PBEAM
C   COMMON/NORMAL/ VNORMAL, SCALTH
C
C   UPDATE VALUES OF HT(*), BBM, AND HBM
C
C   DO 100 I=1,NLYR
C     HT(I) = T(I)
100  CONTINUE
C   BBM = T(NLYR1)
C   HBM = T(NLYR2)
C
C   CALCULATE VALUES OF P1, P2, P3, AND PBEAM FOR CURRENT VALUES OF
C   HT(*), BBM, AND HBM
C
C   CALL INPUTC
C   CALL EIGANL4
C   CALL LEVYS
C   P1 = EGVL(1,1)
C   P2 = EGVL(2,1)
C   P3 = EGVL(3,1)
C
C   CALCULATE FUNCTION VALUE FOR CURRENT VALUES OF HT(*), BBM, & HBM
C
C   P = -T(NLYR3)
C
C   CALCULATE CONSTRAINT VALUES FOR CURRENT VALUES OF HT(*), BBM, & HBM
C
C   G(1) = (T(NLYR3)-P1)
C   G(2) = (T(NLYR3)-0.999D0*P2)
C   G(3) = (T(NLYR3)-0.998D0*P3)

```

```

      G(4) = (T(NLYR3)-PBEAM)
      G(5) = (APLT + ABEAM)/THETA - 1.0D0
C
      RETURN
C
C
C
      SUBROUTINE GUESS (XGUESS)
C
C
      IMPLICIT REAL*8(A-H,O-Z)
      DOUBLEPRECISION XGUESS(18)
      COMMON/PROPT4/ HT(15), AAA, BBB, NLYR, NLYR1, NLYR2, NLYR3
      COMMON/NORMAL/ VNORMAL
C
C  READ IN XGUESS VALUES
C
      DO 200 I=1,NLYR3
        READ(8,*) XGUESS(I)
200  CONTINUE
C
C  SCALE T(NLYR3) GUESS FOR ADDITIONAL ACCURACY
C
      XGUESS(NLYR3)=XGUESS(NLYR3)*VNORMAL
C
      RETURN
C
C
C
      SUBROUTINE LIMITS (XLB, XUB)
C
C
      IMPLICIT REAL*8(A-H,O-Z)
      COMMON/PROPT0/ THETA, ALEN, BLEN
      COMMON/PROPT4/ HT(15), AAA, BBB, NLYR, NLYR1, NLYR2, NLYR3
      DOUBLEPRECISION XLB(18), XUB(18)
C
C  SET LOWER LIMITS FOR DESIGN VARIABLES, T(*)
C
      DO 100 I=1,NLYR
        XLB(I) = 1.0D-03
100  CONTINUE
      XLB(NLYR1) = 1.0D-03
      XLB(NLYR2) = 1.0D-03
      XLB(NLYR3) = 1.0D-06
C
C  SET UPPER LIMITS FOR DESIGN VARIABLES, HT(*)
C
      DO 200 I=1,NLYR
        XUB(I) = 2.0D-01
200  CONTINUE
      XUB(NLYR1) = 2.0D-01
      XUB(NLYR2) = 2.0D-01
      XUB(NLYR3) = 1.0D 06
C
      RETURN

```

LIST OF REFERENCES

1. Schmit, L.A. Jr. and Ramanathan, R.K., "Multilevel Approach to Minimum Weight Design Including Buckling Constraints," *AIAA Journal*, 16 (1978): 97-104.
2. Bendsoe, Martin P., "On Obtaining a Solution to Optimization Problems for Solid, Elastic Plates by Restriction of the Design Space," *Journal of Structural Mechanics*, 11 (1983/4): 501-521.
3. Cheng, K.T. and Olhoff, N., "An Investigation Concerning Optimal Design of Solid Elastic Plates," *Int. J. Solids Struct.*, 17 (1981): 305-323.
4. Rozvany, George. I.N., Olhoff, N., Cheng, K.T. and Taylor, J.E., "On the Solid Plate Paradox in Structural Optimization," *Journal of Structural Mechanics*, 10 (1982): 1-32.
5. Chao, C.C., Koh, S.L. and Sun, C.T., "Optimization of Buckling and Yield Strengths of Laminated Composites," *AIAA Journal*, 13 (1975): 1131-1132.
6. Chen, T.L.C. and Bert, C.B., "Design of Composite-Material Plates for Maximum Uniaxial Compressive Buckling," *Proc. Oklahoma Academy of Science*, 56 (1976): 104-107.
7. Bert, C.W., "Optimal Design of Composite-Material Panels for Business Aircraft," Business Aircraft Meeting of Society of Automotive Engineers, Wichita, Kansas (March 29-April 1, 1977).
8. Bert, C.W., "Optimal Design of Composite-Material Plate to Maximize its Fundamental Frequency," *Journal of Sound and Vibration*, 50 (1977): 229-237.
9. Bert, C.W., "Design of Clamped Composite Plates to Maximize Fundamental Frequency," *Journal of Mechanical Design*, 100 (1978): 274-278.

10. Hirano, Y., "Optimum Design of Laminated Plates Under Axial Compression," *AIAA Journal*, 17 (1979): 1017-1019.
11. Fukanaga, H. and Hirano, Y., "Stability Optimization of Laminated Composite Plates under In-Plane Loads," *Proc. ICCM-IV*, Tokyo, 1 (1982): 565-572.
12. Tauchert, T.R. and Adibhatla, S., "Design of Laminated Plates for Maximum Stiffness," *Journal of Composite Materials*, 18 (1984): 58-69.
13. Tauchert, T.R. and Adibhatla, S., "Design of Laminated Plates for Maximum Bending Strength," *Engineering Optimization*, 8 (1985): 253-263.
14. Adali, S., "Optimization of Fibre Reinforced Composite Laminates Subject to Fatigue Loading," *Proc. of 3rd Int. Conf. on Composite Structures*, Scotland, (September 9-11, 1985).
15. Pedersen, P., "Minimum Flexibility of Non-Harmonic Loaded Plates," *Mechanical Characterization of Fibre Composite Materials*, ed. Pyrz, R., Aalborg University, Denmark, (1986): 182-196.
16. Miki, M., "Optimum Design of Fibrous Laminated Composite Plates Subject to Axial Compression," *Proc. 3rd Japan-US Composite Material Conference*, Tokyo, (1986): 673-680.
17. Miki, M. and Tonomura, K., "Optimum Design of Hybrid Fibrous Laminated Composite Plates Subject to Axial Compression," *Proc. 4th International Conference on Composite Structures*, Paisley, Scotland, 1 (1987): 1.367-1.377.
18. Schmit, L.A., Jr. and Farshi, B., "Optimum Design of Laminated Fibre Composite Plates," *International Journal for Numerical Methods in Engineering*, 11 (1977): 623-640.
19. Starnes, J.H., Jr. and Haftka, R.T., "Preliminary Design of Composite Wings for Buckling, Strength, and Displacement Constraints," *Journal of Aircraft*, 16 (1978): 564-570.

20. Rao, S.S. and Singh, K., "Optimum Design of Laminates with Natural Frequency Constraints," *Journal of Sound and Vibration*, 67 (1972): 101-112.
21. Anderson, M.S., Stroud, W.J., Durling, B.J. and Hennessy, K.W., "PASCO: Structural Panel Analysis and Sizing Code Users Manual," NASA TM-80182 (1981).
22. Jones, Robert M., *Mechanics of Composite Materials*, Scripta Book Company, Washington, D.C., 1975.
23. Shin, Philip Y. and Haftka, Raphael T., "Optimal Design of Stiffened Laminated Plates Using a Homotopy Method," paper to be presented at the 32nd SDM Conference, Baltimore, MD, April 8-10, 1991.
24. Scott, D.S. and Parlett, B.N., "LASO2," *NETLIB*, Argonne National Lab., Argonne, IL, 1983.
25. Golub, G.H., Underwood, R. and Wilkinson, J.H., "The Lanczos Algorithm for the Symmetric $Ax = \lambda Bx$ Problem," *Report STAN-CS-72-270*, Department of Computer Science, Stanford University, Stanford, CA, 1972.
26. Gallagher, Richard H., *Finite Element Analysis Fundamentals*, Prentice-Hall, Inc., Englewood Cliffs, NJ, 1975.
27. Yang, T.Y., *Finite Element Structural Analysis*, Prentice-Hall, Inc., Englewood Cliffs, NJ, 1986.
28. Timoshenko, S. and Woinowsky-Krieger, S., *Theory of Plates and Shells*, McGraw-Hill Book Company, New York, NY, 1959.
29. Shin, Yung S., Haftka, Raphael T., Watson, Layne T. and Plant, Raymond H., "Design of Laminated Plates for Maximum Buckling Load," *Journal of Composite Materials*, 23 (April 1989): 348-369.

30. Schittkowski, K., "NLPQL: A FORTRAN Subroutine Solving Constrained Non-linear Programming Problems," Edited by Clyde L. Monma, *Annals of Operational Research*, 5 (1985, 6): 485-500.
31. Vanderplaats, G.N. and Hansen, S.R., *DOT User Manual*, VMA Engineering, Goleta, CA, 1989.
32. Dennis, J.E., Jr. and Schnabel, Robert B., *Numerical Methods for Unconstrained Optimization and Nonlinear Equations*, Prentice-Hall, Inc., Englewood Cliffs, NJ, 1983.

INITIAL DISTRIBUTION LIST

		No. Copies
1.	Defense Technical Information Center Cameron Station Alexandria, VA 22304-6145	2
2.	Library, Code 52 Naval Postgraduate School Monterey, CA 93943-5002	2
3.	Superintendent Naval Postgraduate School Attn: Professor A.J. Healey, Code ME Hy Department of Mechanical Engineering Monterey, CA 93932-5004	1
4.	Superintendent Naval Postgraduate School Attn: Professor P.Y. Shin, Code ME Sp Department of Mechanical Engineering Monterey, CA 93932-5004	3
5.	Superintendent Naval Postgraduate School Attn: Curricular Officer, Code 34 Monterey, CA 93932-5004	1
6.	David Taylor Research Center Ship Structures and Protection Department Attn: Dr. J.C. Adamchak Bethesda, MD 20084	1
7.	Mark R. Achenbach 305 Northcrest Collinsville, IL 62234	2